

- I. Structural Analysis Using  $^{15}\text{N}$  NMR Spectroscopy
- II. An Investigation of the Interaction of Grignard Reagents with Mesityl Ketones

Thesis by  
Amy Abe

In Partial Fulfillment of the Requirements  
for the Degree of  
Doctor of Philosophy

California Institute of Technology  
Pasadena, California

1979

(Submitted March 5, 1979)

to Dad

## ACKNOWLEDGMENT

I would like to thank Professor John D. Roberts for the ideas, freedom, and encouragement he provided during the course of this research. Many rewarding discussions with members of the Roberts group are gratefully acknowledged. Special thanks are due to Dr. Glenn Sullivan, Dr. Will Vine, Dr. Mike Squillacote, Tom Perkins, Tom Dunn, Irv Moskovitz, and Elizabeth Fischer for assistance in deciphering terms such as "nmr spectrometer" and "spectra."

Support was received from the Institute in the form of Graduate Research and Teaching Assistantships and an Earle C. Anthony Fellowship and from an NIH Predoctoral Traineeship (1974-1976). This assistance has been greatly appreciated.

## ABSTRACT

PART I. Structural Analysis Using  $^{15}\text{N}$  NMR Spectroscopy

The proton-coupled, natural-abundance  $^{15}\text{N}$  NMR spectra of three series of compounds were examined with emphasis on obtaining conformational, structural and configurational data.

Amino acids and peptides. Chemical shifts of aliphatic amino acids and glycyl dipeptides followed typical  $\alpha$ ,  $\beta$ , and  $\gamma$ -substituent effects. Vicinal  $^{15}\text{N}_{\alpha}$ ,  $\text{H}_{\beta}$  coupling constants were obtained for seven amino acids and Gly-X dipeptides which possess either a single or three equivalent  $\beta$ -protons. Average vicinal couplings were obtained for amino acids with diastereotopic  $\beta$ -protons. Conformational preferences for the rotamers about the  $\text{C}_{\alpha}$ - $\text{C}_{\beta}$  bond of threonine and allothreonine were found by extending the traditional Pachler analysis to allow for interaction among substituents through treating both population and torsion angle as variables. Hydrogen-bond formation between the hydroxyl and the carboxylate was favored over that between the hydroxyl and nitrogen for both amino acids.

Biotin. The proton on the  $\text{N1}'$  nitrogen of biotin exchanges more readily with solvent than that on the sterically-hindered  $\text{N3}'$  nitrogen. The order of exchange was established through correlation of the nitrogen NMR resonances with the ureido proton resonances by variable single-frequency decoupling of the ureido protons and through assignment of the proton spectrum by homonuclear-decoupling experiments. Assignment of the nitrogen resonances in biotin ( $\text{N1}' = 285.6$  ppm and  $\text{N3}' = 294.7$  ppm) and desthiobiotin ( $\text{N1}' = 279.3$  ppm

and  $N3' = 285.0$  ppm) was achieved with the aid of single-frequency, proton-decoupled nitrogen resonances with partial NOE.

Oximes. The large difference between two-bond  $^{15}\text{N}$ ,  $H_{\alpha}$  coupling constants for the E- and Z-isomers of the oximes allows the configurations of aldoximes to be assigned from geminal couplings obtained from the  $^{15}\text{N}$  NMR spectra and also the configuration of O-alkylaldoximes from nitrogen spectra in which the protons on the alkyl group are selectively decoupled.

PART II. An Investigation of the Interaction of Grignard Reagents with Mesityl Ketones.

The reaction of acetomesitylene with benzyl Grignard reagent was reinvestigated because of uncertainty in the mechanism and site of addition of the benzyl moiety. The addition product was identified as mesitylmethylbenzylcarbinol as is consistent with a "normal" addition to the ketone proceeding through an initial ketone-Grignard reagent complex.

## TABLE OF CONTENTS

	<u>Page</u>
LIST OF TABLES . . . . .	viii
LIST OF FIGURES . . . . .	x
PART I. Structural Analysis Using $^{15}\text{N}$ NMR Spectroscopy . . .	1
CHAPTER I. Introduction . . . . .	2
References . . . . .	4
CHAPTER II. Amino Acids and Peptides. . . . .	6
Introduction. . . . .	6
Experimental . . . . .	7
Materials. . . . .	7
NMR Spectra . . . . .	7
Results and Discussion. . . . .	10
Chemical shifts and structure . . . . .	10
Coupling constants and conformation . . . . .	24
Conclusion. . . . .	33
Appendices	
A. Amino acid abbreviations . . . . .	35
B. Absolute configuration diastereomeric amino acids. . . . .	36
C. A model for the rotamer populations of $\delta$ -methyllleucine. . . . .	37
D. A model for the rotamer populations of threonine and allothreonine. . . . .	42
References . . . . .	52

## TABLE OF CONTENTS (continued)

	<u>Page</u>
CHAPTER III. Biotin . . . . .	56
Introduction . . . . .	56
Experimental . . . . .	58
Materials . . . . .	58
NMR Spectra . . . . .	58
Results . . . . .	60
Desthiobiotin . . . . .	60
Biotin . . . . .	65
<sup>1</sup> H NMR Spectrum . . . . .	65
<sup>15</sup> N NMR Spectrum . . . . .	66
Discussion . . . . .	74
Conclusion . . . . .	81
References . . . . .	82
CHAPTER IV. Oximes . . . . .	85
Introduction . . . . .	85
Experimental . . . . .	87
Results and Discussion . . . . .	89
References . . . . .	97
PART II. An Investigation of the Interaction of Grignard	
Reagents with Mesityl Ketones . . . . .	99
Introduction . . . . .	100
Results and Discussion . . . . .	105
Experimental . . . . .	116
References . . . . .	123
Propositions . . . . .	128

## LIST OF TABLES

	<u>Page</u>
PART I	
CHAPTER II	
Table II.1. $^{15}\text{N}$ NMR chemical shifts of amino and imino acids . . . . .	14
Table II.2. $^{15}\text{N}$ NMR chemical shifts of dipeptides . . . . .	16
Table II.3. Amine coupling constants. . . . .	17
Table II.4. Amide nitrogen coupling constants. . . . .	17
Table II.5. Threonine vicinal coupling constants. . . . .	29
APPENDIX II. C	
Table C.1. Calculated rotamer conformations and populations for $\delta$ -methylleucine . . . . .	39
APPENDIX II. D.	
Table D.1. Calculated rotamer conformations and populations for allothreonine using equation A . . . . .	43
Table D.2. Calculated rotamer conformations and populations for threonine using equation A . . . . .	45
Table D.3. Calculated rotamer conformations and populations for allothreonine using equation B . . . . .	48
Table D.4. Calculated rotamer conformations and populations for threonine using equation B . . . . .	49

## LIST OF TABLES (continued)

	<u>Page</u>
CHAPTER III	
Table III.1. $^{15}\text{N}$ NMR Chemical shifts and coupling constants for biotin and model compounds .	61
CHAPTER IV	
Table IV.1. $^{15}\text{N}$ Chemical shifts and coupling constants	88

## LIST OF FIGURES

	<u>Page</u>
PART I	
CHAPTER II	
Figure II.1. Assignment of the $^{15}\text{N}$ amide resonances of the glycyloleucines . . . . .	9
Figure II.2. Proton coupled $^{15}\text{N}$ NMR spectra of amino acids . . . . .	18
Figure II.3. $^{15}\text{N}$ NMR spectra of glycyglycine amide resonance . . . . .	20
Figure II.4. $^{15}\text{N}$ NMR spectra of glycyloleucine amide resonances. . . . .	22
APPENDIX II. C	
Figure C.1. Computer program for calculating rotamer populations in $\delta$ -methylleucine .	38
Figure C.2. 90 MHz Proton NMR spectra of $\delta$ -methyl- leucine. . . . .	40
APPENDIX II. D	
Figure D.1. Computer program for calculating allothreonine rotamer populations using equation A. . . . .	46
Figure D.2. Computer program for calculating threonine rotamer populations using equation A. . . . .	47

## LIST OF FIGURES (continued)

	<u>Page</u>
Figure D. 3. Computer program for calculating allothreonine rotamer populations using equation B. . . . .	50
Figure D.4. Computer program for calculating threonine rotamer populations using equation B . . . . .	51
CHAPTER III	
Figure III.1. $^{15}\text{N}$ NMR spectra of desthiobiotin in DMSO solution. . . . .	62
Figure III.2. 220 MHz $^1\text{H}$ NMR spectrum of biotin in dimethylsulfoxide- $\text{d}_6$ . . . . .	64
Figure III.3. Biotin H-D exchange experiment . . . . .	68
Figure III.4. Effect of ureido H-D exchange on H4 and H3 resonances . . . . .	69
Figure III.5. Selective proton decoupling to assign biotin ureido resonances . . . . .	70
Figure III.6. Plot of nitrogen residual splittings, $J_r$ , as a function of proton-decoupler position for biotin . . . . .	71
Figure III.7. $^{15}\text{N}$ NMR spectra of biotin in DMSO solution. . . . .	72
Figure III.8. Schemes for urea proton exchange . . . . .	78

## LIST OF FIGURES (continued)

	<u>Page</u>
Figure III. 9. Single-frequency decoupled biotin spectra, with and without gated noise decoupling . . . . .	80
CHAPTER IV	
Figure IV. 1. $^{15}\text{N}$ NMR spectra of <u>O</u> -methyl-benzaldoximes . . . . .	94
Figure IV. 2. Proton-coupled $^{15}\text{N}$ NMR spectrum of formamideoxime. . . . .	96
PART II	
Figure 1. Uv spectrum of transiently colored acetomesitylene reaction mixture at $0^\circ\text{C}$	112
Figure 2. Uv spectrum of the orange pivaloyl-mesitylene reaction mixture. . . . .	114
Figure 3. Esr spectrum of the orange reaction mixture from benzyl Grignard reagent and pivaloylmesitylene. . . . .	115

**PART I**

**Structural analysis using  $^{15}\text{N}$  NMR spectroscopy**

CHAPTER IINTRODUCTION

Nitrogen-15 NMR spectroscopy is a potentially powerful tool for elucidating molecular structure. In addition to chemical-shift data<sup>1</sup> with which nitrogen functional groups can be characterized, nitrogen relaxation rates<sup>2</sup> ( $T_1$  and  $T_2$ ) and coupling constants<sup>3</sup> provide information about configurations and conformations. Numerous studies<sup>1b, 3</sup> have been conducted in which proton-nitrogen coupling constants, derived from <sup>1</sup>H NMR of <sup>15</sup>N-enriched compounds, are correlated with the conformation of molecules in solution. Yet little has been done to utilize the proton-coupling information present in the nitrogen spectrum. Often, the low signal-to-noise ratios in natural-abundance <sup>15</sup>N spectra preclude the possibility of obtaining coupled spectra.<sup>4</sup> If <sup>15</sup>N-enriched compounds were easily available, proton NMR spectroscopy would be the method of choice<sup>6</sup> to observe proton-nitrogen couplings because of the high sensitivity and generally higher resolution possible with proton NMR.

The sensitivity problems associated with proton-coupled nitrogen spectra can be overcome in certain cases with currently available instrumentation and spectroscopic methods. Thus, through use of a high-resolution, large sample capacity spectrometer and gated proton-decoupling techniques,<sup>7</sup> the coupled spectra of nitrogens with directly bonded hydrogens can be obtained with a workable compromise between signal-to-noise ratio and the time required to obtain a spectrum. In

subsequent chapters, the feasibility of obtaining NH coupling constants from natural-abundance  $^{15}\text{N}$  spectra is demonstrated. Structural, configurational and conformational information derived from the coupled spectra is discussed for biotin, oximes, and amino acids and peptides.

Many of the previous NH coupling-constant studies have focused on biologically significant systems, especially peptide conformations.<sup>8</sup> In Chapter Two, after a discussion of amino acid and peptide nitrogen chemical shifts, the use of three-bond NH coupling constants for determining side-chain conformations is critically examined. The geometrical dependence of two-bond NH coupling constants in oximes is well documented from proton NMR investigations.<sup>9</sup> The nitrogen spectra of several oxime derivatives are examined and discussed in Chapter Four. The configuration of these molecules is characterized by NH coupling constants and, to a lesser extent, the nitrogen chemical shifts.

The NMR spectra of biotin and several derivatives are analyzed in Chapter Three. Selective proton-decoupling experiments<sup>10</sup> allow NH couplings in the biotin spectrum to be assigned and utilized for assignment of the nitrogen spectrum.

References

1. (a) M. Witanowski, L. Stefaniak and H. Januszewski in "Nitrogen NMR," M. Witanowski and G. A. Webb, Eds., Plenum Press, London, 1973, Chapter 4; (b) M. Witanowski, L. Stefaniak and G. A. Webb, Ann. Reports NMR Spectroscopy, 7, 117-244 (1977).
2. (a) J. B. Lambert and D. A. Netzol, J. Mag. Res., 20, 575-77 (1975); (b) G. C. Levy, J. J. Dechter and J. Kowalewski, J. Am. Chem. Soc., 100, 2308-14 (1978); (c) G. C. Levy et al., J. Mag. Res., 29, 553-62 (1978) and references therein.
3. T. Axenrod in "Nitrogen NMR," M. Witanowski and G. A. Webb, Eds., Plenum Press, London, 1973, Chapter 5.
4. Fourier-transform difference spectroscopy has recently<sup>5</sup> been used to obtain <sup>15</sup>N-H coupling constants from proton spectra of compounds with natural isotopic abundance levels of <sup>15</sup>N.
5. (a) M. Llinás, W. J. Horsley and M. P. Klein, J. Am. Chem. Soc., 98, 7554-8 (1976); (b) J.-P. Marchal and D. Canet, J. Am. Chem. Soc., 97, 6581-82 (1975); (c) J.-P. Marchal and D. Canet, J. Mag. Res., 31, 23-32 (1978).
6. J. A. Sogn, W. A. Gibbons and E. W. Randall, Biochemistry, 12, 2100-2105 (1973).
7. D. Shaw, "Fourier Transform N.M.R. Spectroscopy," Elsevier Scientific Publishing Company, Amsterdam, 1976, Chapter 9.
8. V. F. Bystrov, Progress NMR Spectroscopy, 10, 41-81 (1976).

References (continued)

9. D. Crépaux and J.-M. Lehn, Org. Mag. Res., 7, 524-6 (1975) and references therein.
10. (a) F. W. Wehrli and T. Wirthlin, "Interpretation of Carbon-13 NMR Spectra," Heyden, London, 1976, Chapter 3; (b) K. Bock and C. Pederson, J. Mag. Res., 25, 227-30 (1977).

CHAPTER IIAMINO ACIDS AND PEPTIDESIntroduction

The  $^{15}\text{N}$  nucleus is fast becoming a valuable probe for NMR studies of amino acids,<sup>1</sup> peptides<sup>2</sup> and proteins.<sup>3</sup>  $^{15}\text{N}$  enrichment of a cofactor<sup>4</sup> or amino acid residue<sup>5</sup> at the active site of an enzyme can permit taking spectra which may yield further information about the catalytic mechanism. The conformations of the amide backbone in peptides in solution have been corroborated by examining one-bond  $^{15}\text{NH}$  coupling constants<sup>6,7</sup> and solvent dependences<sup>7</sup> of the  $^{15}\text{N}$  chemical shifts. The conformations of side-chain groups in peptides<sup>8,9</sup> and amino acids<sup>1d,9-11</sup> can be deduced from three-bond  $\text{NH}_\beta$  coupling constants.

The majority of these conformational studies have utilized  $^{15}\text{N}$ -enriched compounds. In this section, the structural and conformational information available in the  $^{15}\text{N}$  NMR spectra of amino acids and dipeptides with natural-abundance levels of  $^{15}\text{N}$  is investigated.

## Experimental

### Materials

The amino acids, with the exception of  $\delta$ -methylleucine, were purchased. The sources of the diastereomeric amino acids were: DL-threonine (Sigma T-8375, lot 37C-0185), allo-DL-threonine (ICN 100394, lot 3043), DL-isoleucine (MCB LX-235, lot A5H02), iso-leucines (mixture of the four stereoisomers, Sigma I-2627, lot 67C-0452), 4-hydroxy-L-proline (Sigma H-6002, lot 76C-0024) and allo-4-hydroxy-D-proline (Sigma H-5877, lot 64C-5008).

$\delta$ -Methylleucine was obtained from the reaction<sup>12</sup> of aqueous ammonium hydroxide with the  $\alpha$ -bromo acid prepared<sup>13</sup> from 4,4-dimethylpentanoic acid (Saber Laboratories, Inc.). The glyceryl dipeptides resulted from treatment<sup>12</sup> of the N-(chloroacetyl)amino acids<sup>14</sup> with aqueous ammonium hydroxide.

### NMR Spectra

Proton spectra were recorded on Varian EM390 (90 MHz) or A56-60 (60 MHz) spectrometers.

The <sup>13</sup>C and <sup>15</sup>N NMR spectra were recorded on a Bruker WH-180 Fourier-transform quadrature-detection spectrometer operating at 42 kGauss (45.29 MHz for <sup>13</sup>C and 18.25 MHz for <sup>15</sup>N). Saturated aqueous solutions of the amino acids were contained in 25-mm sample tubes with a concentric 5-mm capillary containing 1M H<sup>15</sup>NO<sub>3</sub> in D<sub>2</sub>O for chemical-shift reference and deuterium field-frequency lock. Solution temperatures, measured by inserting a

thermometer in the sample, were between 18 and 24° C. The nitrogen chemical shifts are reported in ppm upfield of 1M nitric acid with a precision of  $\pm 0.1$  ppm. Coupling constants were obtained from spectra with data acquisition times of 4.096 sec resulting in a computer-limited digital-resolution of 0.25 Hz.

The chemical shifts and coupling constants of Gly-Ile and Gly- $\alpha$ Ile were obtained from spectra of the mixture. When Gly-Ile was added to the mixture, a proportionate increase in the downfield amide resonance was seen (Figure II.1) thus allowing the chemical shifts to be assigned. A single resonance was observed for the amine nitrogens.

Three-bond couplings were observed in the  $^{15}\text{N}$  spectra of the amino acid solutions only after paramagnetic metal ions were removed by treatment with Chelex resin. The sodium salt of Chelex-100 (Bio-Rad) was neutralized with excess Ultrapure hydrochloric acid (Alfa), washed and suspended in doubly distilled water. Approximately 1 ml of gravity-packed suspension (pH  $\sim$  6.5) was shaken with 20 ml of amino acid solution and filtered directly into an NMR tube. The resolution of NMR signals of samples which remained in the glass tubes was found to deteriorate with time presumably due to leaching<sup>1d</sup> of metal ions from the glass. The proton-coupled spectra of the carbonyl carbons were particularly susceptible to this problem.

Many of the free-induction decays were treated with an exponential weighting function to increase the signal to noise ratio of the Fourier transformed spectrum. The increase in peak width which results from this process is expressed as "line-broadening".

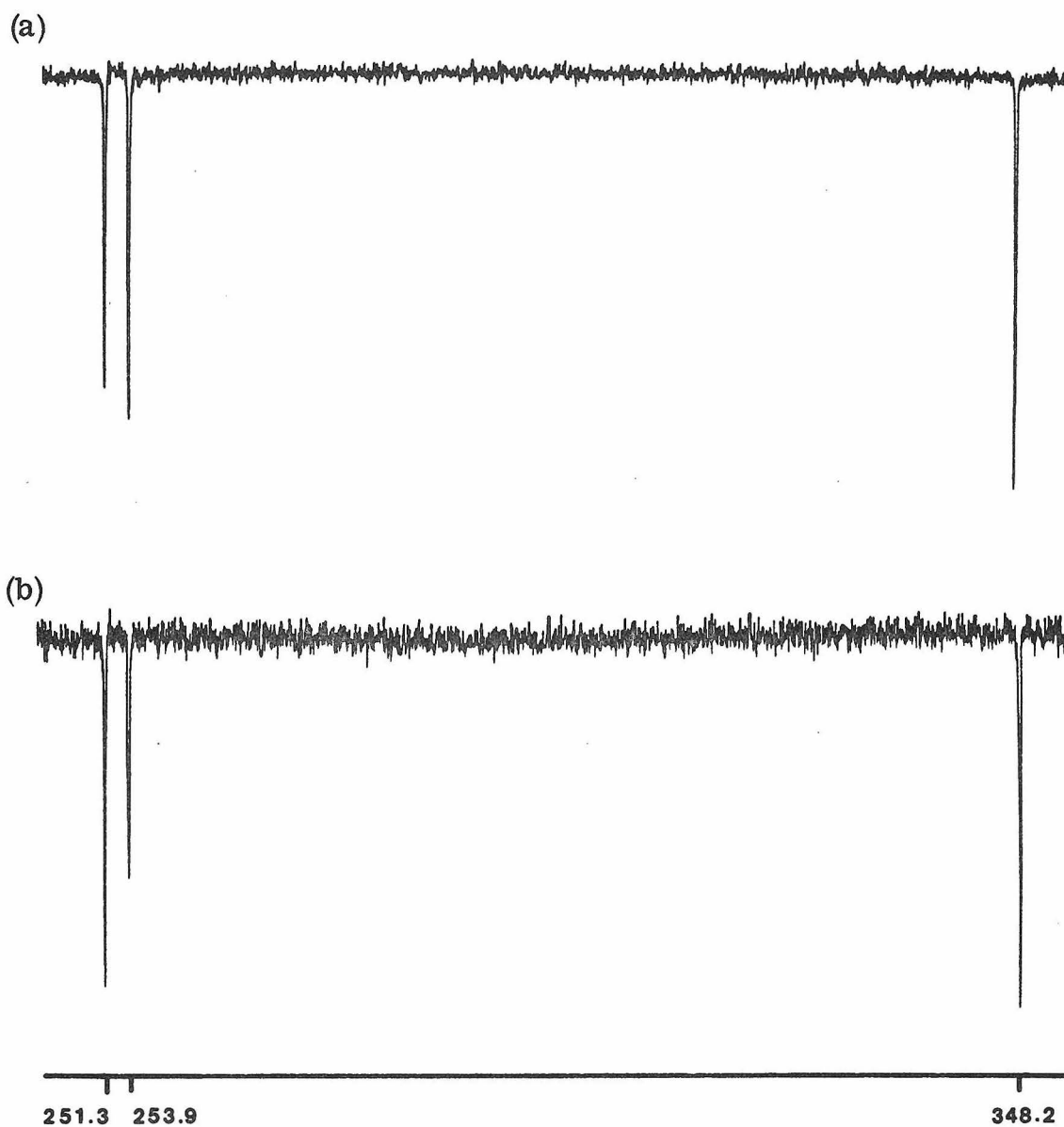
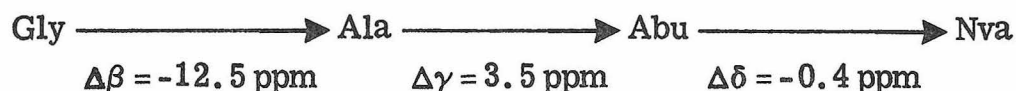


Figure II.1. Assignment of the  $^{15}\text{N}$  amide resonances of the glycyloisoleucines. (a) Spectrum of an aqueous solution of a Gly-Ile, Gly-Ile mixture. (b) Addition of Gly-Ile to the solution results in an enhanced amide resonance at 251.3 ppm.

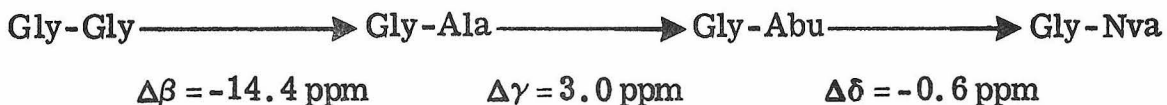
## Results and Discussion

### Chemical shifts and structure

The  $^{15}\text{N}$  chemical shifts of aliphatic amino acids and N-glycyl-dipeptides (Tables II.1 and II.2) in aqueous solution span about 15 ppm. The effect of introducing methyl groups in  $\beta$ ,  $\gamma$ , or  $\delta$  positions relative to the nitrogen is shown for amino acids: <sup>†</sup>



and dipeptide amide resonances:



The substituent parameters for these series parallel each other and are consistent with those previously reported for amino acid ester hydrochlorides, <sup>15</sup> N-formyl and N-acetyl amino acids, <sup>2b</sup> and amines. <sup>16</sup> The  $\Delta\delta$  value is effective for predicting the shifts of amino acids with two aliphatic substituents at the  $\beta$ -carbon but gives poor agreement with the observed shift when an electronegative hydroxyl group is at the  $\beta$ -carbon. While the additivity of the  $\Delta\gamma$  parameter for the dipeptides is not as good as for aliphatic amino acids, certain predictions can be made. The calculated value of the amide  $^{15}\text{N}$  shift of Gly-Val is such as to distinguish it from Gly-Gly

---

<sup>†</sup>See Appendix II.A for amino-acid abbreviations.

	Calculated shift, ppm	Observed shift, ppm
Val	Abu + $\Delta\gamma$ = 339.3	339.0
Ile, aIle	Nva + $\Delta\gamma$ = 338.9	337.4, 340.0
Thr, aThr	Ser + $\Delta\gamma$ = 342.5	340.8, 341.4
Gly-Val	Gly-Abu + $\Delta\gamma$ = 253.1	252.2

(260.4), Gly-Ala (246.0) and Gly-Leu (248.1).<sup>2c</sup>

In general, the chemical shifts of the amino acids in Table II.1 can be classified along the lines defined by the substituent parameters:

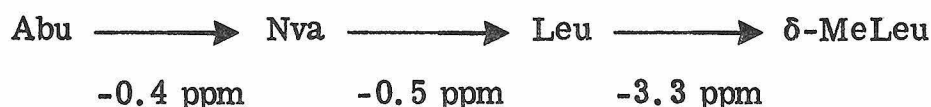
Structural class	Observed shifts, ppm	Representative amino acids
no $\alpha$ -side chain	345.8	Gly
$\beta$ -CH <sub>3</sub>	332	Ala
1 $\gamma$ -carbon	334.9 to 336.2	Leu, Asn, His (pH 4.4), Nva, Phe, Abu, His (pH 7.8)
2 $\gamma$ -carbons	337.4 to 340.0	Ile, Val, aIle

This categorization is the result of small ( $< 1$  ppm)  $\Delta\delta$  substituent effects for replacing a hydrogen on the  $\gamma$ -carbon with an imidazole, phenyl, carboxamide or protonated imidazole group. The non-overlapping chemical shift ranges allow the general structure of amino acids to be identified. However, differentiating residues within each of the structural classes may be difficult due to the small shift variations in each class.

Small differences in <sup>15</sup>N chemical shift are observed between

the diastereomeric<sup>†</sup> isoleucenes (2.6 ppm), threonines (0.6 ppm), and hydroxyprolines (0.1 ppm). While the additivity of substituent parameters would argue for identical chemical shifts, the observed shifts reflect<sup>17</sup> the differences in molecular symmetry and conformation of the diastereomers. Similar effects have been reported<sup>18</sup> for meso- and DL-isomers of di-2-butylamine (0.6 ppm) and di-2-hexylamine (0.4 ppm).

The  $\delta$ -substituent effect was further explored by varying the number of methyl groups at the  $\gamma$ -carbon. While the first two methyl



groups result in quite small shifts, the third produces a substantial downfield shift. The net effect of replacing a  $\gamma$ -proton with a tert-butyl group (*i.e.*, Ala  $\rightarrow$   $\delta$ -MeLeu) is a small 0.7 ppm downfield shift. Similar  $\delta$ -tert-butyl substituent effects have been reported for <sup>13</sup>C NMR chemical shifts. Roberts and coworkers<sup>20</sup> indicate the chemical shifts reflect the effect of introducing a bulky tert-butyl group on the rotamer conformations and populations about the C <sub>$\alpha$</sub> -C <sub>$\beta$</sub>  bond. Preference for the least sterically crowded rotamer was seen.<sup>20a</sup> More recently, Batchelor<sup>19</sup> has proposed that paramagnetic shielding by the electric field associated with fluctuating molecular dipoles could account for the larger  $\Delta\delta$  effect of a third methyl group.

---

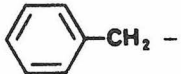
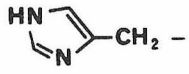
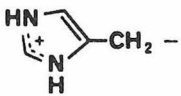
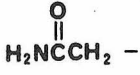
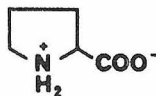
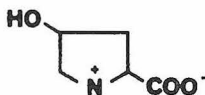
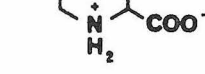
<sup>†</sup>See Appendix II.B for the absolute configurations of the diastereomeric amino acids.

The vicinal proton coupling constants in  $\delta$ -methy lleucine were consistent with rotamer populations having minimal interaction of the tert-butyl group with either the carboxylate or amino substituents. (See Appendix II. C for further details.) Thus both explanations for unusual  $\Delta\delta$  substituent effects in  $^{13}\text{C}$  spectra are applicable to the  $^{15}\text{N}$  case.

Table II.1.  $^{15}\text{N}$  NMR chemical shifts of amino and imino acids

	$\text{R} - \text{CH} \begin{array}{l} \diagup \text{COO}^- \\ \diagdown \text{NH}_3^+ \end{array}$	
	R	$\delta$ , ppm
Glycine	H -	344.8
DL-Alanine	$\text{CH}_3$ -	332.3
DL- $\alpha$ -Aminobutyric acid	$\text{CH}_3\text{CH}_2$ -	335.8
DL-Norvaline	$\text{CH}_3\text{CH}_2\text{CH}_2$ -	335.4
DL-Leucine	$\begin{array}{c} \text{CH}_3 \\ \diagup \\ \text{CH}_3 \end{array} \text{CHCH}_2 -$	334.9
$\delta$ -Methylleucine	$\begin{array}{c} \text{CH}_3 \\   \\ \text{CH}_3\text{CCH}_2 - \\   \\ \text{CH}_3 \end{array}$	331.6
DL-Valine	$\begin{array}{c} \text{CH}_3 \\ \diagup \\ \text{CH}_3 \end{array} \text{CH} -$	339.0
Isoleucine	$\begin{array}{c} \text{CH}_3\text{CH}_2 \\ \diagup \\ \text{CH}_3 \end{array} \text{CH} -$	337.4
Alloisoleucine	$\begin{array}{c} \text{CH}_3 \\ \diagup \\ \text{CH}_3 \end{array} \text{CH} -$	340.0
DL-Serine	$\text{HOCH}_2$ -	339.0
DL-Threonine	$\begin{array}{c} \text{HO} \\ \diagup \\ \text{CH}_3 \end{array} \text{CH} -$	340.8
DL-Allothreonine	$\begin{array}{c} \text{HO} \\ \diagup \\ \text{CH}_3 \end{array} \text{CH} -$	341.4

Table II.1 (continued)

	R	$\delta$ , ppm
DL-Phenylalanine		335.7
L-Histidine, pH 7.8		336.2 <sup>a</sup>
L-Histidine, pH 4.4		335.2 <sup>a</sup>
DL-Asparagine		335.2
Proline		319.9
<u>cis</u> -4-Hydroxyproline		322.8
<u>trans</u> -4-Hydroxyproline		322.9

<sup>a</sup>W. W. Bachovchin and J. D. Roberts, J. Am. Chem. Soc.,  
100, 8041-47 (1978).

Table II.2.  $^{15}\text{N}$  NMR chemical shifts of dipeptides

The diagram shows the chemical structure of a dipeptide. It consists of a protonated amino group ( $\text{H}_3\text{N}^+$ ) attached to a methylene group ( $\text{CH}_2$ ), which is linked to a carbonyl group ( $\text{C}=\text{O}$ ). This carbonyl group is bonded to a nitrogen atom ( $\text{NH}$ ), which is further bonded to a methylene group ( $\text{CH}$ ) attached to an R group and a carboxylate group ( $\text{COO}^-$ ).

	R	NH	$\delta$ , ppm	+ $\text{NH}_3$
Gly-Gly	H -	260.4	348.1	
Gly-Ala	$\text{CH}_3$ -	246.0	348.7	
Gly-Abu	$\text{CH}_2\text{CH}_2$ -	249.0	348.4	
Gly-Nva	$\text{CH}_2\text{CH}_2\text{CH}_2$ -	248.4	348.4	
Gly-Val	$\begin{array}{l} \text{CH}_3 \\ \text{CH}_3 \end{array} > \text{CH}$ -	252.2	346.6	
Gly-Ile	$\begin{array}{l} \text{CH}_2\text{CH}_2 \\ \text{CH}_3 \end{array} > \text{CH}$ -	251.3	348.2	
Gly-aIle	$\begin{array}{l} \text{CH}_2\text{CH}_2 \\ \text{CH}_3 \end{array} > \text{CH}$ -	253.9		

Table II.3. Amine coupling constants

	$^3J_{\text{NH}\beta}$ , Hz		$^3J_{\text{NH}\beta}$ , Hz
Ala	< 3.7	Ser	3.08*
Abu	3.25*	Thr	2.7
Val	2.7	aThr	2.7

\*Average coupling.

Table II.4. Amide nitrogen coupling constants

	$^1J_{\text{NH}}$ , Hz	$^3J_{\text{NH}\beta}$ , Hz
Gly-Gly	92.0	-
Gly-Ala	91.8	3.5
Gly-Val	91.5	3.1
Gly-Ile	91.8	3.8
Gly-aIle	92.4	2.6

Figure II.2. Proton-coupled  $^{15}\text{N}$  NMR spectra of amino acids

Spectra were acquired in a gated decoupling mode with  $83^\circ$  pulse flip angle, 4.1-sec acquisition time and 2.0-sec noise-decoupler-on pulse delay.

- (a) Alanine: 1121 scans, 0.73 Hz line broadening.
- (b)  $\alpha$ -Aminobutyric acid: 2709 scans, 0.24 Hz line broadening.
- (c) Valine: 5388 scans, 0.73 Hz line broadening.
- (d) Serine: 1452 scans, 0.73 Hz line broadening.
- (e) Allothreonine: 4871 scans, 0.73 Hz line broadening.
- (f) Threonine: 1278 scans, 0.24 Hz line broadening.

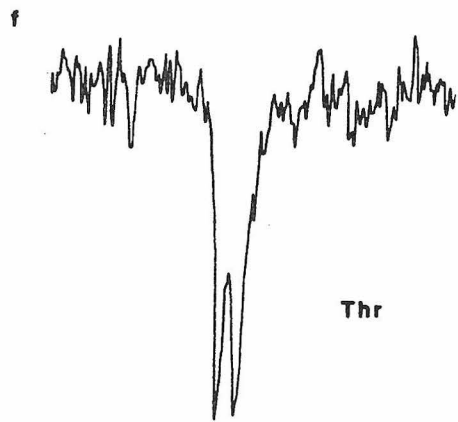
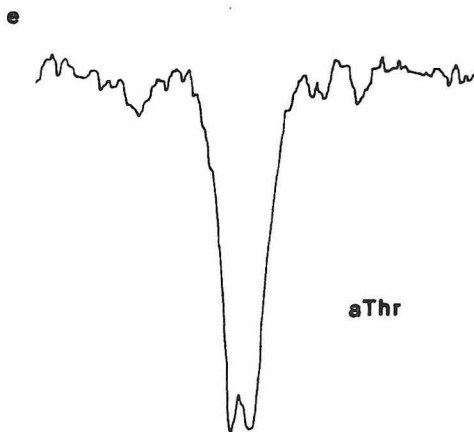
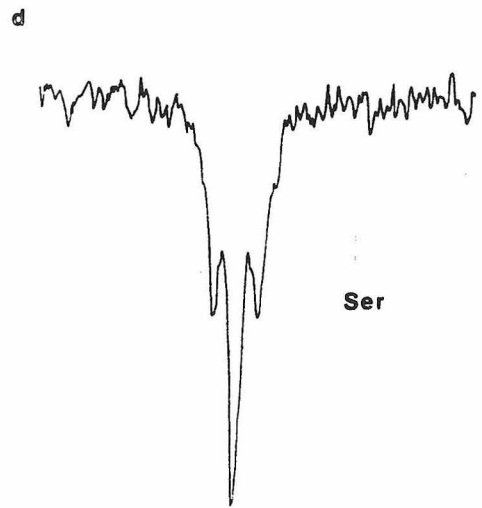
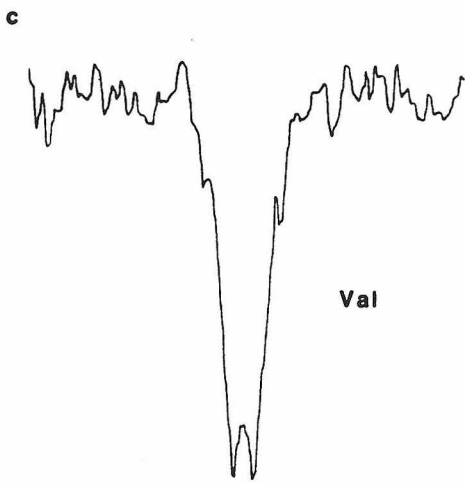
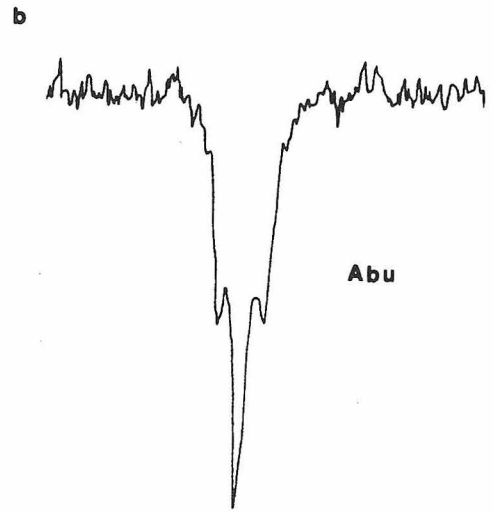
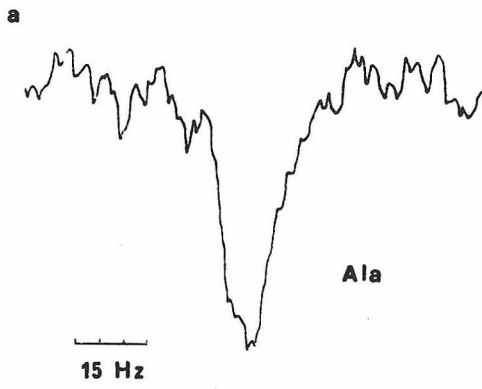
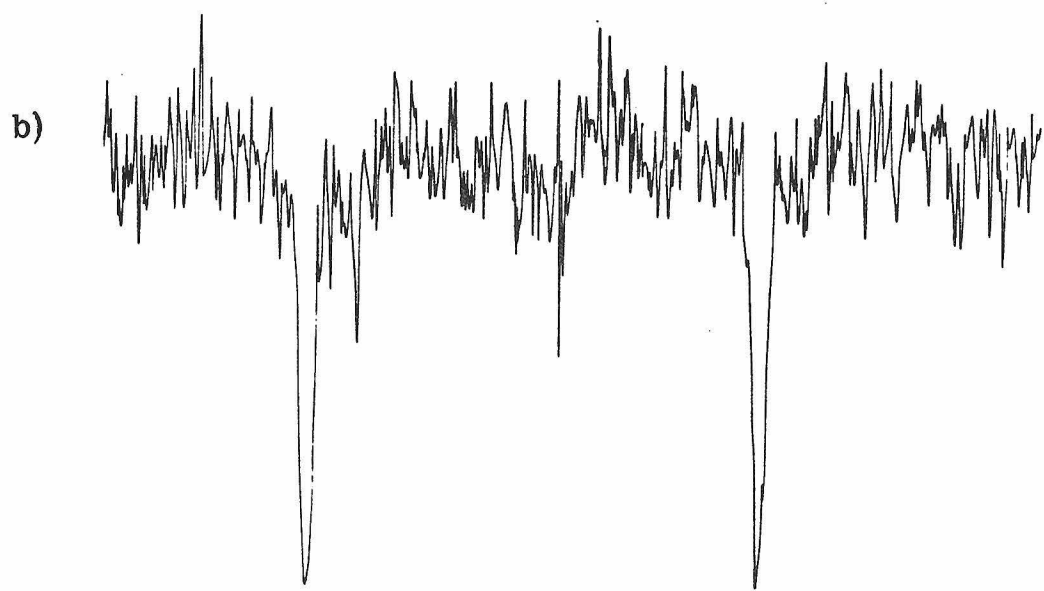
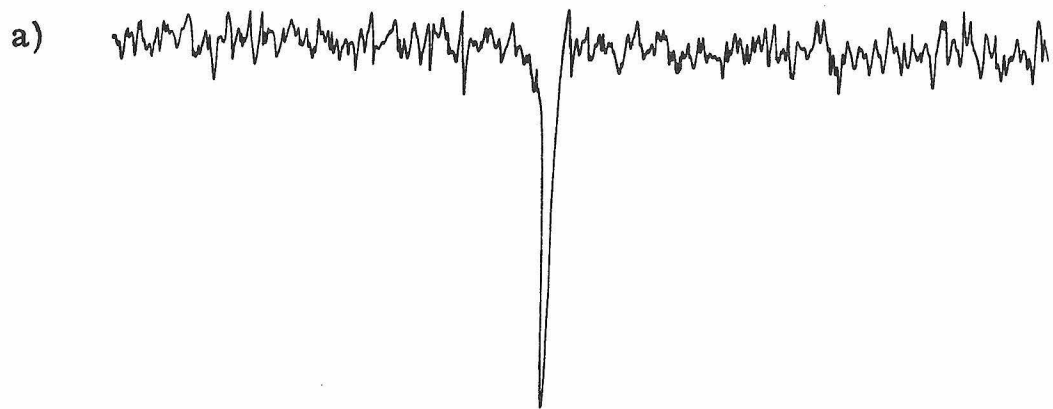


Figure II.3.  $^{15}\text{N}$  NMR spectra of glycylglycine amide resonance.

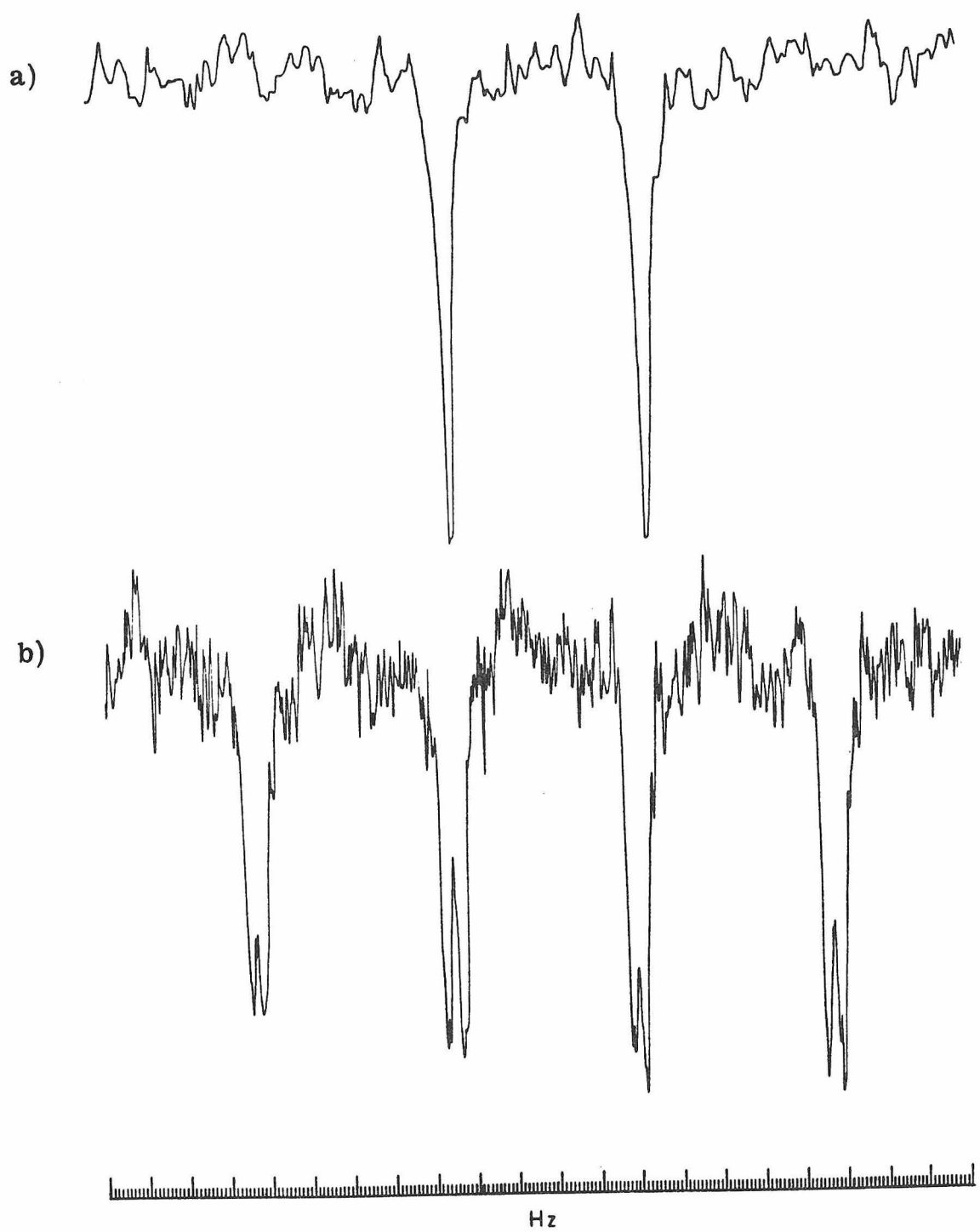
- (a) Proton-decoupled spectrum: 435 scans,  $83^\circ$  pulse flip angle, 4.1-sec data acquisition time, 6.0-sec pulse repetition rate, 0.25 Hz line broadening. The line width is 1.5 Hz.
- (b) Proton-coupled spectrum: 1734 scans,  $83^\circ$  pulse flip angle. 4.1-sec data acquisition time, 1.9-sec decoupler-on pulse delay, 0.25 Hz line broadening. The line width is 3.5 Hz.



Hz

Figure II.4.  $^{15}\text{N}$  NMR spectra of glycyloleucine amide resonances.

- (a) Proton-decoupled spectrum: 1000 scans,  $83^\circ$  pulse flip angle, 1.2-sec data acquisition time and pulse repetition rate, 0.93 Hz line broadening. The upfield resonance was assigned to Gly-aIle (see Experimental section).
- (b) Proton-coupled spectrum: 1391 scans,  $83^\circ$  pulse flip angle, 4.1-sec acquisition time, 1.9-sec decoupler-on pulse delay, 0.25 Hz line broadening.



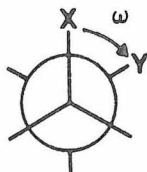
### Coupling constants and conformation

The  $^{15}\text{N}$  nucleus in an amino acid-dipolar ion is coupled equally to the three directly-bonded protons ( $\underline{J} \approx 75 \text{ Hz}$ )<sup>1d, 23</sup> and unequally to the  $\alpha$ - and  $\beta$ -hydrogens ( $\underline{J} = 0.5\text{-}1.5 \text{ Hz}$  and  $2\text{-}4 \text{ Hz}$ , respectively).<sup>1a, 8, 21</sup> Unless the pH is below zero,<sup>23</sup> rapid exchange causes the amine protons to be partially decoupled from the nitrogen and a single resonance line is seen. Under these conditions, the proton exchange rate is about equal to or greater than the lifetime of the proton-coupled state. In amides the exchange is slower<sup>1d</sup> and a  $\sim 90 \text{ Hz}$  doublet is observed for the NH resonance in dipeptides. Whereas the small two-bond coupling of the amide nitrogen to the  $\alpha$ -proton in the same residue and, in the dipeptides, the three-bond coupling to the  $\alpha$ -proton in the neighboring residue ( $\underline{J} < 1.5 \text{ Hz}$ )<sup>9, 24</sup> cannot be resolved, the three-bond coupling to the  $\beta$ -proton(s) can usually be seen<sup>1d</sup> in the  $^{15}\text{N}$  spectrum.

The  $^{15}\text{N}$  spectra of selected amino acids and dipeptides were recorded and the values of the observed coupling constants are reported in Tables II.3 and II.4. The spectra of the amino acids (Figure II.2) were especially sensitive to the presence of paramagnetic metal ions and solutions had to be treated with chelating agents before the coupling constants could be determined. Blomberg and co-workers<sup>1d</sup> have reported similar difficulties in obtaining small couplings from  $^{15}\text{N}$  NMR spectra. The proton-coupled spectrum of alanine exhibits a broad resonance ( $\nu_{\frac{1}{2}} = 11.25 \text{ Hz}$ ). While the quartet which is expected on the basis of rotational averaging of the methyl protons is not distinguishable, an estimate of the coupling can be made. Because the quartet should have

a 1:2:2:1 line intensity, one third of the width at half-height can be used as an upper limit for  ${}^3J_{\text{NH}\beta}$  (Table II.3). This is consistent with the values of 3.10 Hz and 3.1 Hz previously<sup>9,10</sup> reported from proton NMR studies. Figure II.3 shows the proton-decoupled and proton-coupled  ${}^{15}\text{N}$  NMR spectra of the glycylglycine amide resonance. As indicated above, the small  ${}^2J_{\text{NH}\alpha}$  and  ${}^3J_{\text{NH}\alpha}$  broaden the resonance lines but are not resolvable. When a peptide residue possesses a  $\beta$ -proton, as in the case of Gly-Ile, the  ${}^3J_{\text{NH}\beta}$  coupling can be seen in the amide spectrum (Fig. II.4).

Vicinal coupling constants have been used to determine the conformation of molecules in solution by relating the dihedral angle,  $\omega$ , between the interacting nuclei to the observed coupling constant and



conformational equilibria. Because both the barriers and the energy differences between the different conformations resulting from rotation about the  $\text{C}_\alpha\text{-C}_\beta$  bond in amino-acid residues are not large, the observed couplings reflect what might be called average molecular conformations. The "average conformation" has been defined in several ways resulting in a variety of physical interpretations.<sup>26</sup> Before applying this type of analysis to the NH couplings, an outline of the assumptions and limitations inherent in the approach is presented.

The correlation of dihedral angle with three-bond coupling constants can be traced to the work of Karplus,<sup>27</sup> which used quantum mechanical, valence-bond methods to calculate vicinal proton coupling

constants in ethane molecular fragments. The results can be approximated by the equation

$${}^3J_{\text{HH}} = A + B \cos \omega + C \cos 2\omega \quad (\text{II. 1})$$

The values of the coefficients depend on the identity and orientation<sup>29</sup> of substituents in the molecular fragment as well as perturbations from ethane-like geometry associated with the substituent.<sup>27</sup> While several attempts have been made to refine the equation developed by Karplus using molecular orbital theory,<sup>29, 33</sup> the general form of the dependence is usually taken to be in accord with equation II.1. In practice, Karplus-type curves for a specific type of molecular fragment can be derived from experimental data. Coupling constants from molecules of known conformation are fitted to equation II.1, or an equivalent function, and the coefficients which result possess substantial (10-100%) error limits. Karplus curves of this kind<sup>21</sup> have been defined for three-bond  $\text{H}_\alpha\text{H}_\beta$ <sup>30</sup> and  $\text{NH}_\beta$ <sup>8</sup> coupling constants for amino-acid-side chain conformations.

The calculation of dihedral angles from the coupling constants is less ambiguous for rigid than for mobile structures. Since  $\omega$  can assume values between 0 and 360°, up to four conformations are consistent with an observed coupling constant and additional input is required to assign the conformation of a rigid molecule. For acyclic molecules, the static picture is no longer applicable and the observed coupling becomes an average of the coupling interactions for all values

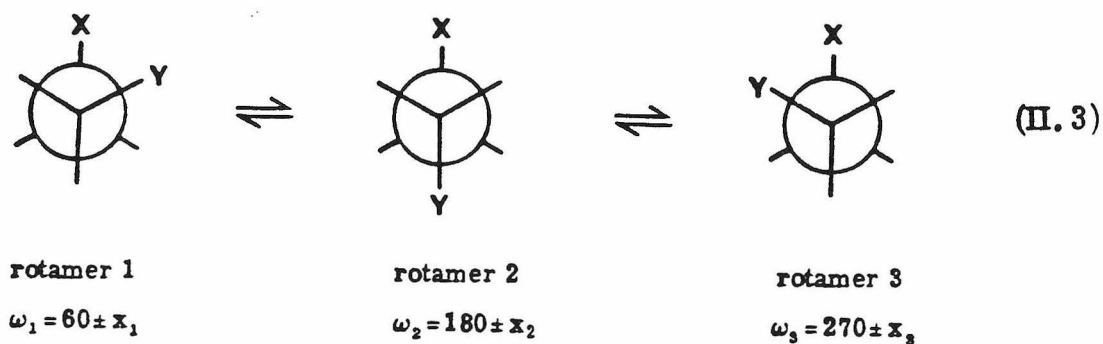
$$J = \int_{\omega=0}^{360} p_\omega J_\omega \quad (\text{II. 2})$$

of  $\omega$ .<sup>28</sup> This complication introduces an additional parameter; the residence time of the molecule in a given conformation or the populations ( $p$ ) of the conformer.

One of the simplest dynamic conformational models results from the degeneracy of the  $\omega$  values from the Karplus curve. Any linear combination of the populations of the rotamers corresponding to a given  $J$  value is mathematically consistent with the data, but as Feeney implies,<sup>34</sup> the equilibrium which this model represents seldom approaches reality.

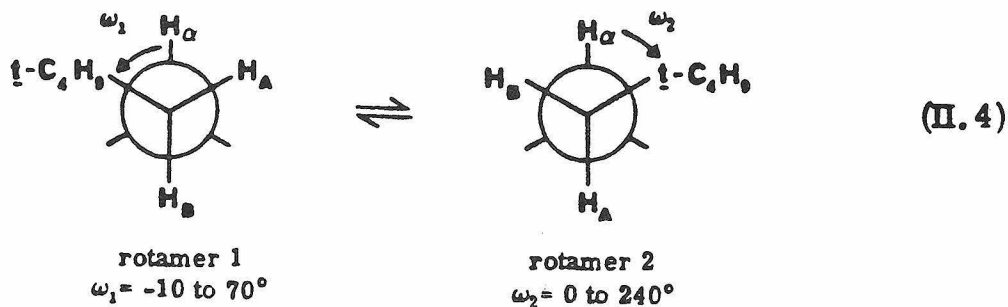
The Pachler-type analysis<sup>21</sup> of amino-acid conformations approximates equation II.2 by considering only the three staggered conformers where  $\omega = 60, 180$  and  $270^\circ$ . Because coupling constants for each rotamer are available from the Karplus equation, the experimental couplings are interpreted in terms of rotamer populations. Uncertainties in coupling constants are expressed as variations in populations and, when combined with the error limits for the coefficients in the Karplus equation, can be in excess of 10% of the total population. Despite the limitations of the model, the Pachler analysis is commonly<sup>21</sup> used for quantitative determination of side-chain conformations of amino-acid residues from  $H_\alpha H_\beta$ ,<sup>31</sup>  $CH_\beta$ ,<sup>32</sup> and  $NH_\beta$ <sup>10,11</sup> coupling constants.

A model which treats both the dihedral angle and rotamer populations as variables is used here to provide a qualitative picture of side-chain conformations. An equilibrium between staggered rotamers with tetrahedral carbon atoms (equation II.3) is considered. Because molecular geometry seldom results in perfectly staggered (i.e.,  $\omega = 60, 180$



$$J = p_1 J_1 + p_2 J_2 + p_3 J_3, \quad 1 = p_1 + p_2 + p_3$$

or  $270^\circ$ ) configurations for the lowest energy conformations, the value of  $\omega$  in each rotamer is allowed to vary. The Karplus equation relates  $\omega$  to  $J$  for the individual rotamers. A computer program calculates average coupling constants for all possible combinations of  $\omega_1$ ,  $\omega_2$ ,  $\omega_3$ ,  $p_1$ ,  $p_2$  and  $p_3$  and selects for only those values which give reasonable agreement with observed coupling constants. Whereas the results of this type of analysis do not provide an inherently "better" description of molecular structure than the Pachler method, the uncertainties in observed coupling constants and Karplus curves present a different sort of picture. Usually, the acceptable data which result are clustered about certain conformations. The range of and trends in  $\omega$  and  $p$  allow qualitative statements about the interaction between substituents to be made. As an example, consider the conformational equilibria for  $\delta$ -methylleucine from the previous section. The results (Appendix II. C) indicate as one possibility an equilibrium in which rotamers 1 and 2 (equation II.4) are about equally populated and the dihedral angle between the tert-butyl substituent and  $H_\alpha$  is less than  $50^\circ$ . The residence time of rotamer 1 increases when the tert-butyl group is closer to  $H_\alpha$  (i.e.,  $\omega_1$  decreases). These results lead to the conclusion that



the bulky substituent prefers to be closer to  $H_\alpha$ , thus minimizing the interaction energy<sup>35</sup> with the amino and carboxyl groups.

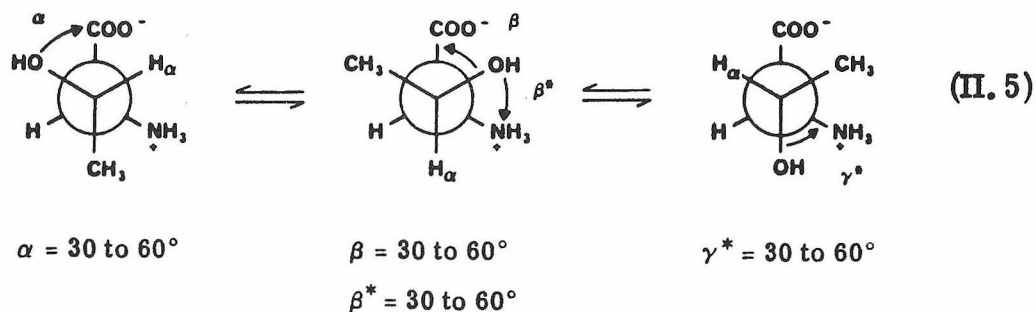
The conformations of the isomeric threonines can be considered within the context of the model. In order to more accurately "fix" the conformations, three-bond  $H_\alpha H_\beta$  and  $^{13}\text{C} H_\beta$  coupling constants (Table II. 5) were determined and used in the calculations (Appendix II. D). The dihedral angles were varied in  $5^\circ$  increments over a  $30^\circ$

Table II. 5. Threonine vicinal coupling constants

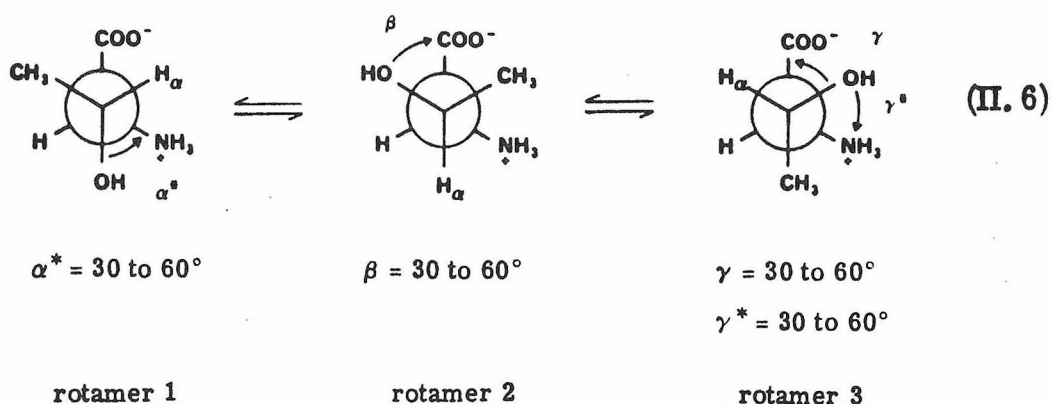
	$^3J_{H_\alpha H_\beta}, \text{Hz}$	$^3J_{H_\beta ^{13}\text{C}=\text{O}}, \text{Hz}$
Thr	3.90	1.5
aThr	4.95	2.0

range for the conformers in which the hydroxyl group is gauche to either the amino or carboxylate substituent (equations II. 5 and II. 6) to optimize hydrogen-bonding interactions. Sets of  $\alpha$ ,  $\beta$ ,  $\gamma$ ,  $p_1$ ,  $p_2$  and  $p_3$  were selected for which the calculated three-bond coupling constants of  $H_\alpha$  to  $H_\beta$ ,  $^{13}\text{C}=\text{O}$ , and  $^{15}\text{N}$  were in accord with the observed values. Two separate analyses of the data were performed. In the initial set of calculations, the Karplus curves used for the HH and CH coupling constants<sup>30b, 32a</sup> were derived from data for amino

## L-allothreonine



## L-threonine



acids with  $\beta$ -hydroxyl substituents and the one used for the NH coupling constants<sup>8</sup> was derived from amino acids with aliphatic side chains.

Several sets of allowed conformations resulted for allothreonine (Table D.3). The three rotamers (equation II.5) were about equally populated but substantial deviations of the dihedral angle from the standard  $60^\circ$  value of the classical staggered conformations were found. In rotamer 1,  $\alpha$  ranged from  $30$  to  $45^\circ$  with the population decreasing from  $40$  to  $20\%$  as the dihedral angle between the hydroxyl and carboxyl groups increased. Rotamer 3 showed a similar preference for the hydroxyl being closer to the amino group than in a staggered conformation. The range of values of  $\beta$  tested for

rotamer 2 allows the hydroxyl to interact with the carboxylate or amino substituents. Only conformers of this rotamer in which the hydroxyl was close to the carboxylate group ( $\beta \approx 30^\circ$ ) were consistent with the coupling constant data. The calculations for the threonine molecule resulted in a single conformational equilibrium (Table D.4) in which rotamer 3 predominates (equation II.6) and the dihedral angle between the hydroxyl and carboxylate groups is  $45^\circ$ . Rotamer 1 was not populated and rotamer 2 was in a staggered conformation ( $\beta = 60^\circ$ ). These results indicate that for both allothreonine and threonine the hydroxyl group prefers being near to the carboxylate. Although the exact dihedral angles and populations are not known, the preferred conformation of the amino acids is a six-membered ring with a hydrogen bond between these substituents.

For a further test of the validity of this type of coupling constant analysis the effect of changing the form of the Karplus curve was explored. A second set of calculations was performed in which the HH Karplus curve used for amino acids with  $\beta$ -hydroxyl substituent was replaced with one derived for amino acids with aliphatic side chains.<sup>30b</sup> The dynamic picture which results (Tables D.1 and D.2) is at variance with the one above. No dramatic preference of the hydroxyl for interaction with either the carboxylate or amino groups was found. This might be expected when the Karplus curves do not take account of the presence of the hydroxyl group. In allothreonine, the residence time of rotamer 1 is 40 to 50%; however, no preference for a specific OH, COO<sup>-</sup> dihedral angle is seen. Rotamer 3 is populated 20-30% of the time with a dihedral angle of about  $35$  to  $45^\circ$ . In rotamer 2, the

hydroxyl can reside near either the  $\text{NH}_3^+$  or  $\text{COO}^-$  groups with a slight bias toward the latter. The single conformational equilibrium calculated for threonine has rotamers 1 and 3 each populated 50% of the time, with the hydroxyl slightly closer to the amino than the carboxylate substituent.

The results for analyses of the threonines indicate that the method is capable of providing a viable description of the conformational equilibria when interaction between substituents on the  $\alpha$ - and  $\beta$ -carbons are considered. For the results to be valid, Karplus curves which reflect the nature of the interacting substituents should be employed.

## Conclusion

The structure and conformation of amino acids and peptides can be examined using natural-abundance  $^{15}\text{N}$  NMR spectroscopy. Chemical shift data are useful for determining the presence of substituents at the  $\alpha$ ,  $\beta$ , and  $\gamma$  carbons in the amino acid residue. The inability to distinguish between different  $\delta$ -substituents, however, limits the use of amide chemical shift data in peptide sequence determination.

Vicinal  $\text{H}_\beta$ ,  $^{15}\text{N}_\alpha$  coupling constants for amino acid residues can be determined from nitrogen NMR spectra. This technique is restricted to residues with nitrogen bonded to at least one proton because the short  $T_1$  and significant nuclear Overhauser enhancement allow spectra to be obtained in only several hours and to residues with a single or equivalent  $\beta$ -hydrogens because limited resolution makes it difficult to distinguish small differences between non-equivalent couplings to diastereotopic  $\beta$ -hydrogens.

The NH vicinal coupling constants used in conjunction with HH and CH coupling constants and Karplus analyses yield information on the conformational equilibrium about the  $\text{C}_\alpha$ - $\text{C}_\beta$  bond. When the traditional Pachler analysis of coupling constants for the threonines did not generate a set of consistent populations for the staggered rotamers, an alternative approach was employed in which interaction between substituents was allowed by treating both the rotamer populations and dihedral angles as variables. For both threonine and allothreonine the hydrogen bond interaction between the hydroxyl

and carboxylate was favored over the amine-hydroxyl interaction. The success of this approach to conformational analysis suggests that applications to peptide systems be explored.

## APPENDIX II.A

Amino acid abbreviations

Abu	$\alpha$ -aminobutyric acid
Ala	alanine
Asn	asparagine
Gly	glycine
His	histidine
Hyp	<u>trans</u> -4-hydroxyproline
aHyp	<u>cis</u> -4-hydroxyproline
Ile	isoleucine
alle	alloisoleucine
Leu	leucine
$\delta$ -MeLeu	$\delta$ -methyllleucine
Nva	norvaline
Phe	phenylalanine
Pro	proline
Ser	serine
Thr	threonine
aThr	allothreonine

## APPENDIX II.B

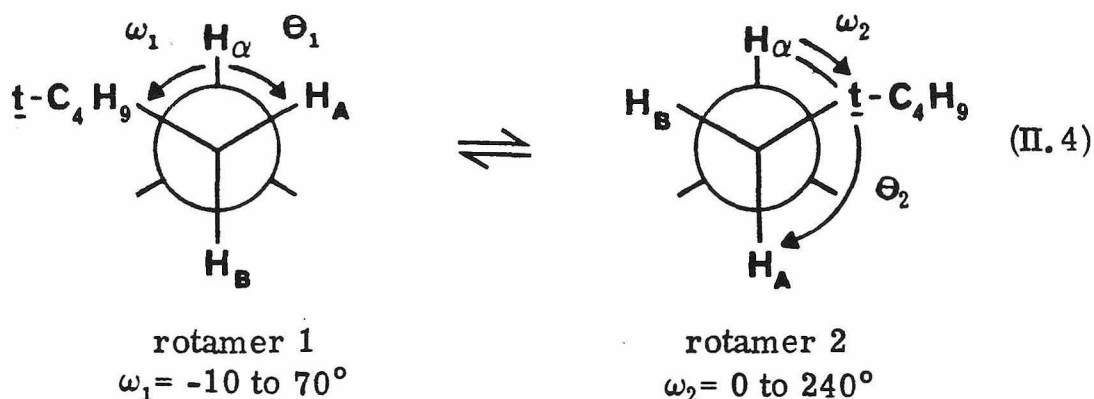
Absolute configuration of diastereomeric amino acids<sup>a</sup>

L- <i>isoleucine</i>	(2S, 3S)-2-amino-3-methylpentanoic acid
D- <i>isoleucine</i>	(2R, 3R)-2-amino-3-methylpentanoic acid
allo-L- <i>isoleucine</i>	(2S, 3R)-2-amino-3-methylpentanoic acid
allo-D- <i>isoleucine</i>	(2R, 3S)-2-amino-3-methylpentanoic acid
L- <i>threonine</i>	(2S, 3R)-2-amino-3-hydroxybutyric acid
D- <i>threonine</i>	(2R, 3S)-2-amino-3-hydroxybutyric acid
allo-L- <i>threonine</i>	(2S, 3S)-2-amino-3-hydroxybutyric acid
allo-D- <i>threonine</i>	(2R, 3R)-2-amino-3-hydroxybutyric acid
4-hydroxy-L- <i>proline</i>	(2S, 4R)-4-hydroxy-2-pyrrolidine carboxylic acid
4-hydroxy-D- <i>proline</i>	(2R, 4S)-4-hydroxy-2-pyrrolidine carboxylic acid
allo-4-hydroxy-L- <i>proline</i>	(2S, 3S)-4-hydroxy-2-pyrrolidine carboxylic acid
allo-4-hydroxy-D- <i>proline</i>	(2R, 4R)-4-hydroxy-2-pyrrolidine carboxylic acid

---

<sup>a</sup>W. Klyne and J. Buckingham, "Atlas of Stereochemistry",  
Oxford University Press, 1974.

## APPENDIX II.C

A model for the rotamer populations in  $\delta$ -methyllleucine.

Coupling constants were calculated based on the dynamic equilibrium in Eq. II.4. The coupling was assumed to be a weighted average of the coupling in the individual rotamers, where

$$\underline{J}_{\text{calc}} = \underline{p}_1 J_{\theta_1} + \underline{p}_2 J_{\theta_2}, \quad 1 = \underline{p}_1 + \underline{p}_2$$

$$\underline{J}_{\theta} = \begin{cases} 10.5 \cos \theta & 0-90^\circ, 180-360^\circ \\ 13.7 \cos \theta & 90-180^\circ \end{cases}$$

the angular dependence of  $J$  has been previously defined.<sup>22</sup> A BASIC computer program (Figure C.1) was used to find sets of  $\omega_1$ ,  $\omega_2$ ,  $\underline{p}_1$ , and  $\underline{p}_2$  (Table C.1) in which the calculated values of  $J_{\text{AX}}$  and  $J_{\text{BX}}$  were within the limits of the experimental error of the observed couplings. Analysis of the ABX portion of  $\delta$ -methyllleucine spectra (Figure C.2) in acidic, basic, and neutral solution yielded the observed couplings.<sup>25</sup>

```

TYPE NTC4H9.BAS
10 REM DEFINITIONS, ETC.
20 OPEN #1,"DATFIL",OUTPUT
32 PI=3.141592654
33 PII=PI/180
34 PIT=120*PII
99 GO TO 10000
1099 REM
1100 REM SUBROUTINE FOR X,Y
1101 IF T< 90 THEN 1140
1110 IF T<150 THEN 1170
1120 IF T<270 THEN 1200
1130 IF T<330 THEN 1230
1140 X=10.5
1150 Y=13.7
1160 GOTO 1300
1170 X=13.7
1180 Y=13.7
1190 GOTO 1300
1200 X=13.7
1210 Y=10.5
1220 GOTO 1300
1230 X=10.5
1240 Y=10.5
1300 RETURN
9998 REM
9999 REM MAIN PROGRAM
10000 READ A,B
10005 PRINT #1
10006 PRINT #1
10007 PRINT #1
10010 PRINT #1, A,B
10020 PRINT #1
10030 PRINT #1
10040 FOR T1=50 TO 130
10042 PRINT T1
10043 T=T1
10044 GOSUB 1100
10046 T1T=T1*PII
10048 S=Y*COS(T1T+PIT)**2
10050 R=X*COS(T1T)**2
10060 FOR T2=120 TO 360
10090 T=T2
10120 GOSUB 1100
10130 T2T=T2*PII
10140 Q=Y*COS(T2T+PIT)**2
10144 P=X*COS(T2T)**2
10150 FOR N=0.1 TO 0.9 STEP 0.1
10160 B1=(1-N)*S+N*Q
10170 IF B1<B-0.06 THEN 13000
10180 IF B1>B+0.06 THEN 13000
10190 A1=(1-N)*R+N*P
10200 IF A1<A-0.06 THEN 13000
10210 IF A1>A+0.06 THEN 13000
10220 PRINT #1, T1,N,T2,A1,B1
13000 NEXT N
13010 NEXT T2
13020 NEXT T1
13040 GOTO 10000
20010 DATA 4.52, 7.88
65534 END

```

Figure 1. Computer program for calculating rotamer populations in  $\delta$ -methylleucine.

Table C.1. Calculated rotamer conformations and populations for  $\delta$ -methylleucine.

Dipolar ion ( $J_{AX} = 4.52$ ,  $J_{BX} = 7.88$ )

$\Theta_1$	$\omega_1$	$P_1$	$\Theta_2$	$\omega_2$	$J_{AX}$ — calc	$J_{BX}$ — calc
71	49	.4	147	27	4.52222	7.93574
72	48	.4	148	28	4.54273	7.87135
99	21	.4	207	87	4.55169	7.91866
100	20	.4	208	88	4.52005	7.84427
107	13	.5	221	101	4.48721	7.87961
115	5	.6	229	109	4.51676	7.87349
128	-8	.7	236	116	4.55661	7.89099
129	-9	.7	237	117	4.47244	7.85771

Cation ( $J_{AX} = 5.17$ ,  $J_{BX} = 6.35$ )

$\Theta_1$	$\omega_1$	$P_1$	$\Theta_2$	$\omega_2$	$J_{AX}$ — calc	$J_{BX}$ — calc
75	45	.5	147	27	5.16976	6.4099
76	44	.5	147	27	5.12534	6.34833
86		.5	350		5.11724	6.33494
87		.5	351		5.1359	6.31789
87		.5	352		5.16269	6.39943
88		.5	352		5.15471	6.3015
88		.5	353		5.17842	6.38603
89		.5	354		5.19424	6.3732
90		.5	355		5.21012	6.36095
91	29	.4	165	45	5.11541	6.32087
91	29	.4	166	46	5.16173	6.35863
91	29	.4	167	47	5.2052	6.39855
91		.5	356		5.22654	6.3493
111		.4	210		5.16567	6.40548
112		.4	211		5.17987	6.32853
123		.5	227		5.21801	6.39617
124		.5	228		5.20396	6.33942

Anion ( $J_{AX} = 6.18$ ,  $J_{BX} = 6.35$ )

$\Theta_1$	$\omega_1$	$P_1$	$\Theta_2$	$\omega_2$	$J_{AX}$ — calc	$J_{BX}$ — calc
77	43	.5	158	38	6.1544	6.36614
77	43	.5	159	39	6.23594	6.39293
78	42	.5	159	39	6.19721	6.32436
114	6	.5	211	91	6.16617	6.38265
115	5	.5	212	92	6.14987	6.34646
116	4	.5	213	93	6.13443	6.30991

## a) Dipolar ion

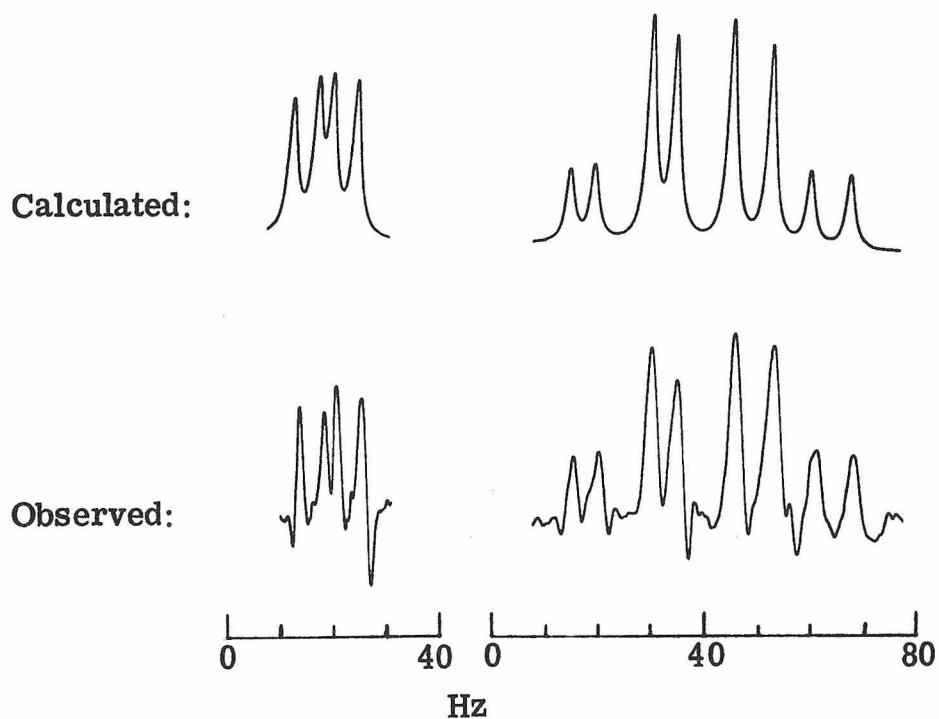
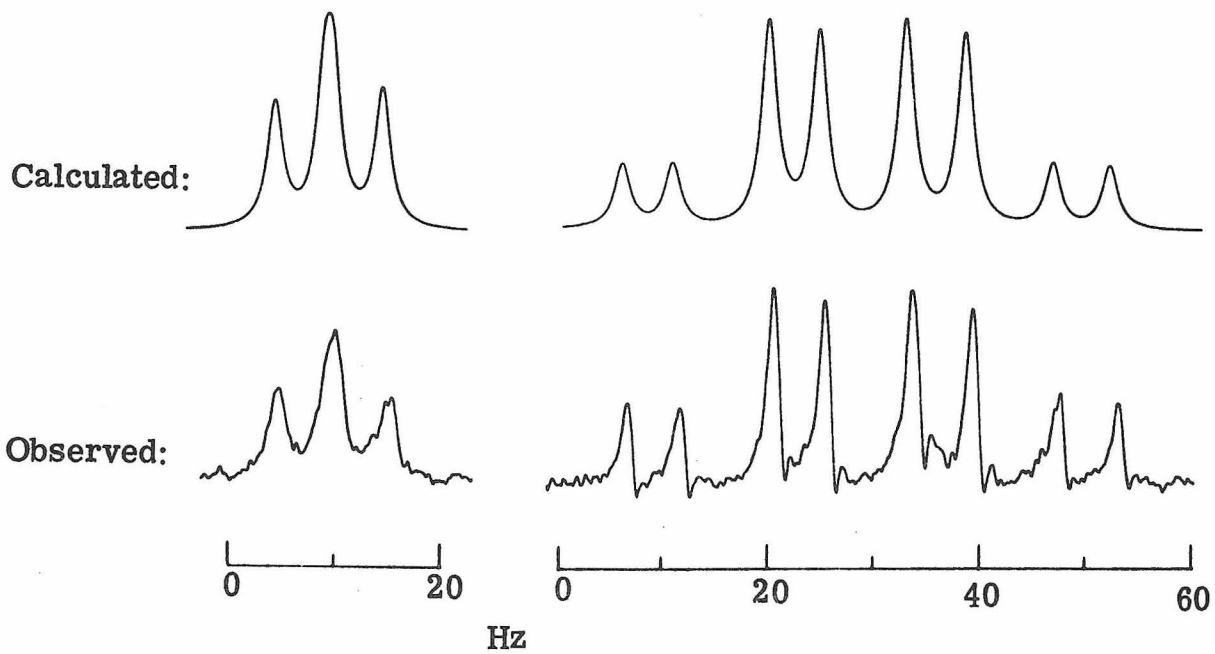


Figure C.2. 90 MHz Proton NMR spectra of  $\delta$ -methyllucine.

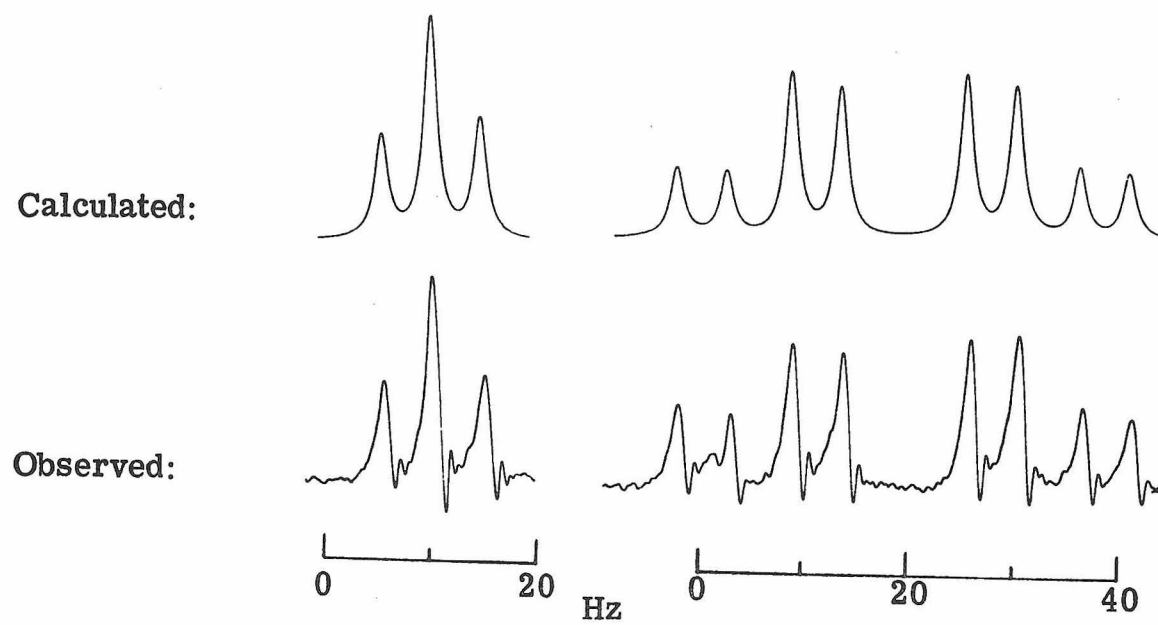
The following parameters (in Hz) were used for the calculated spectra.

	$\Delta\nu_{AB}$	$\Delta\nu_{AX}$	$J_{AB}$	$J_{AX}$	$J_{BX}$
dipolar ion	28.65	186.75	15.5	7.88	4.52
cation	26.25	243.63	15.5	6.35	5.17
anion	33.8	174.23	14.5	6.35	6.18

## b) Cation



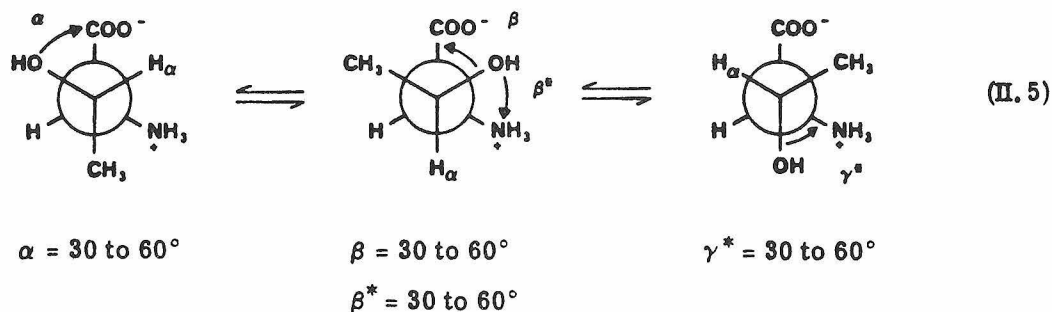
## c) Anion



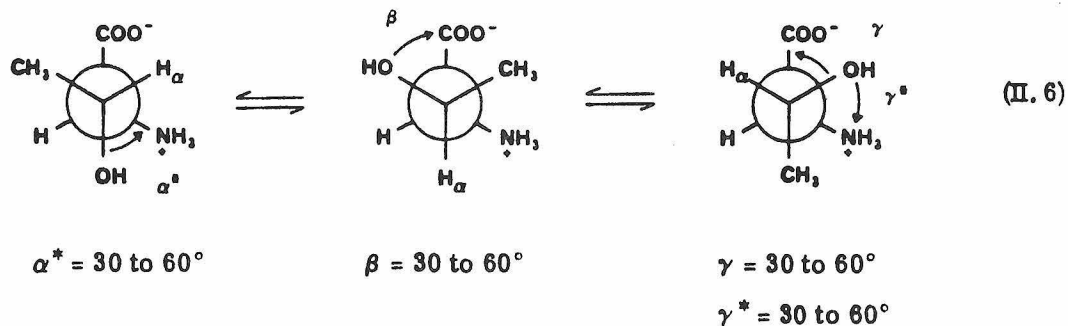
## APPENDIX II.D

A model for the rotamer populations in threonine and allothreonine

L-allothreonine



L-threonine



Coupling constants were calculated on the basis of the dynamic equilibria above.

$$J_{\text{HX}}^{\text{-calc}} = P_1 J_{1, \text{HX}} + P_2 J_{2, \text{HX}} + P_3 J_{3, \text{HX}} \quad , \quad 1 = P_1 + P_2 + P_3$$

$$J_{\text{HH}} = 9.4 \cos^2 \theta - 1.4 \cos \theta + 1.6 \quad (\text{A})$$

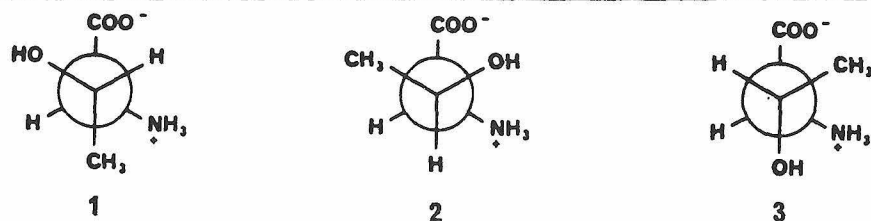
$$J_{\text{HH}} = 8.65 \cos^2 \theta - 1.29 \cos \theta + 1.47 \quad (\text{B})$$

$$J_{\text{CH}} = \begin{cases} 6 \cos^2 \theta & 0-90^\circ, 180-360^\circ \\ 7.6 \cos^2 \theta & 90-180^\circ \end{cases}$$

$$J_{\text{NH}} = 4.2 \cos^2 \theta - \cos \theta + 0.2$$

Two sets of calculations were done, using different Karplus curves for the proton-proton coupling constants.<sup>30b</sup> Equation A was derived for amino acids with an aliphatic side chain, and equation B was derived for amino acids containing a  $\beta$ -hydroxyl group. The Karplus curve for  $\text{CH}_\beta$  couplings was derived from data in ref. 32a and that for the  $\text{NH}_\beta$  couplings taken directly from ref. 8.

Table D.1. Calculated rotamer conformations and populations for allothreonine using equation A.



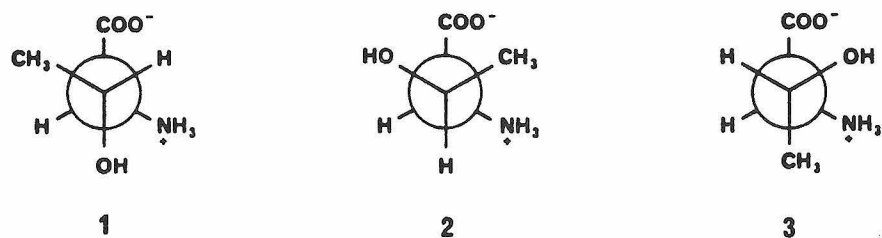
$\alpha, \beta, \gamma$  = angle between -OH and  $-\text{CO}_2^-$   
 $\alpha^*, \beta^*, \gamma^*$  = angle between -OH and  $-\text{NH}_3^+$

Rotamer Conformations (populations)			Calculated Coupling Constants		
$\alpha$	$\beta$	$\gamma$	$J_{\text{HH}}$	$J_{\text{CH}}$	$J_{\text{NH}}$
30 ( 0.4 )	30 * ( 0.3 )	40 * ( 0.3 )	5.025	1.92057	2.63103
30 ( 0.5 )	50 * ( 0.2 )	35 * ( 0.3 )	5.02914	1.79566	2.92113
30 ( 0.5 )	40 ( 0.3 )	35 * ( 0.2 )	4.87741	2.22761	2.88442
35 ( 0.4 )	30 * ( 0.3 )	45 * ( 0.3 )	4.97321	1.84882	2.465
35 ( 0.4 )	40 * ( 0.3 )	40 * ( 0.3 )	4.89783	2.24209	2.50298
35 ( 0.5 )	55 ( 0.2 )	35 * ( 0.3 )	5.01354	1.85273	2.91046
35 ( 0.5 )	45 ( 0.3 )	45 * ( 0.2 )	4.85916	2.23044	2.59432
35 ( 0.5 )	40 ( 0.3 )	40 * ( 0.2 )	5.01958	2.17645	2.72075
35 ( 0.5 )	35 ( 0.3 )	40 * ( 0.2 )	4.9923	2.03593	2.8109
35 ( 0.5 )	30 ( 0.3 )	40 * ( 0.2 )	5.00748	1.87316	2.89636
40 ( 0.5 )	55 ( 0.2 )	40 * ( 0.3 )	4.99419	1.80948	2.72839
40 ( 0.5 )	50 ( 0.2 )	40 * ( 0.3 )	4.9009	1.77519	2.78526
40 ( 0.5 )	40 ( 0.3 )	50 * ( 0.2 )	4.87556	2.13994	2.48856

Table D.1. (continued)

Rotamer Conformations (populations)			Calculated Coupling Constants		
$\alpha$	$\beta$	$\gamma$	$J_{HH}$	$J_{CH}$	$J_{NH}$
40 ( 0.5 )	30 ( 0.3 )	50 * ( 0.2 )	4.86346	1.83665	2.66417
45 ( 0.4 )	35 * ( 0.2 )	35 * ( 0.4 )	4.94933	1.83796	2.81182
45 ( 0.4 )	50 * ( 0.2 )	30 * ( 0.4 )	4.92979	2.23495	2.86701
45 ( 0.5 )	60 ( 0.2 )	45 * ( 0.3 )	5.01727	1.84155	2.47181
45 ( 0.5 )	55 ( 0.2 )	45 * ( 0.3 )	4.90472	1.83001	2.52345
45 ( 0.5 )	40 ( 0.2 )	40 * ( 0.3 )	5.03812	1.75372	2.75361
45 ( 0.5 )	30 ( 0.3 )	55 * ( 0.2 )	4.8952	1.92008	2.45286
50 ( 0.4 )	40 * ( 0.2 )	35 * ( 0.4 )	4.95499	2.05161	2.69333
50 ( 0.5 )	45 ( 0.2 )	45 * ( 0.3 )	4.92707	1.8897	2.49022
50 ( 0.5 )	40 ( 0.2 )	45 * ( 0.3 )	4.88167	1.81372	2.55136
55 ( 0.4 )	30 * ( 0.2 )	40 * ( 0.4 )	4.8818	1.84943	2.54653
55 ( 0.4 )	40 * ( 0.2 )	35 * ( 0.4 )	5.04618	2.19952	2.57958
55 ( 0.5 )	35 ( 0.2 )	45 * ( 0.3 )	4.97747	1.90493	2.46927
55 ( 0.5 )	30 ( 0.2 )	45 * ( 0.3 )	4.98759	1.79641	2.52625
60 ( 0.5 )	60 ( 0.1 )	40 * ( 0.4 )	4.98998	1.79077	2.55326
60 ( 0.5 )	55 ( 0.1 )	40 * ( 0.4 )	4.9337	1.785	2.57908
60 ( 0.5 )	50 ( 0.1 )	40 * ( 0.4 )	4.88706	1.76785	2.60751

Table D.2. Calculated rotamer conformations and populations for threonine using equation A.



$\alpha, \beta, \gamma$  = angle between  $-\text{OH}$  and  $-\text{CO}_2^-$   
 $\alpha^*, \beta^*, \gamma^*$  = angle between  $-\text{OH}$  and  $-\text{NH}_3^+$

Rotamer Conformations (populations)			Calculated Coupling Constants		
$\alpha$	$\beta$	$\gamma$	$J_{\text{HH}}$	$J_{\text{CH}}$	$J_{\text{NH}}$
45 *		50	3.94252	1.85097	2.74034
( 0.5 )		( 0.5 )			

```

100 MARGIN 120
110 DEF FNA(X)=INT(57.2958*X+0.5)
120 A=0.0872664
200 FOR T1=2.6180 TO 3.1416 STEP A
210 H=COS(T1)
220 H1=9.4*H*H-1.4*H+1.6
230 N=COS(T1-2.0944)
240 N1=4.2*N*N-N+0.2
250 C=COS(T1+2.0944)
260 IF C>0 THEN 290
270 C1=7.6*C*C
280 GO TO 300
290 C1=6*C*C
300 FOR T2=0.5236 TO 1.5708 STEP A
310 H=COS(T2)
320 H2=9.4*H*H-1.4*H+1.6
330 N=COS(T2-2.0944)
340 N2=4.2*N*N-N+0.2
350 C=COS(T2+2.0944)
360 IF C>0 THEN 390
370 C2=7.6*C*C
380 GO TO 400
390 C2=6*C*C
400 FOR T3=5.2360 TO 5.7596 STEP A
410 H=COS(T3)
420 H3=9.4*H*H-1.4*H+1.6
430 N=COS(T3-2.0944)
440 N3=4.2*N*N-N+0.2
450 C=COS(T3-4.1888)
460 IF C>0 THEN 490
470 C3=7.6*C*C
480 GO TO 500
490 C3=6*C*C
500 FOR P1=0 TO 1 STEP 0.1
600 FOR P2=0 TO 1-P1 STEP 0.1
610 P3=1-P1-P2
620 H9=P1*H1+P2*H2+P3*H3
630 IF H9>5.05 THEN 900
640 IF H9<4.85 THEN 900
650 N9=P1*N1+P2*N2+P3*N3
660 IF N9>2.95 THEN 900
670 IF N9<2.45 THEN 900
680 C9=P1*C1+P2*C2+P3*C3
690 IF C9>2.25 THEN 900
700 IF C9<1.75 THEN 900
750 IF T2<1.047 THEN 950
800 PRINT TAB(10);FNA(T1-2.0944);TAB(20);FNA(2.0944-T2);TAB(30);FNA(
T3-4.7124);"*";
810 PRINT TAB(40);H9;TAB(50);C9;TAB(60);N9
820 PRINT TAB(10);"(";P1;")";TAB(20);"(";P2;")";TAB(30);"(";P3;")"
830 PRINT
900 NEXT P2
910 NEXT P1
920 NEXT T3
930 NEXT T2
940 NEXT T1
945 GO TO 999
950 PRINT TAB(10);FNA(T1-2.0944);TAB(20);FNA(T2);"*";TAB(30);FNA(T3-
4.7124);"*";
960 GO TO 810
999 END

```

Figure D.1. Computer program for calculating allothreonine rotamer populations using equation A.

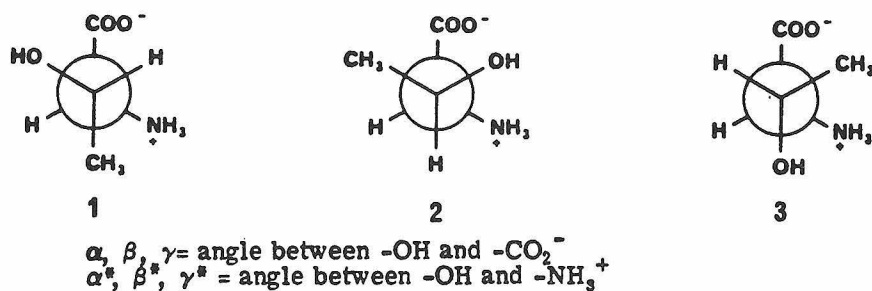
```

100 MARGIN 120
110 DEF FNA(X)=INT(57.2958*X+0.5)
120 A=0.0872664
200 FOR T1=3.1416 TO 3.6652 STEP A
210 H=COS(T1)
220 H1=9.4*H*H-1.4*H+1.6
230 N=COS(T1-2.0944)
240 N1=4.2*N*N-N+0.2
250 C=COS(T1+2.0944)
260 IF C>0 THEN 290
270 C1=7.6*C*C
280 GO TO 300
290 C1=6*C*C
300 FOR T2=0.5236 TO 1.0472 STEP A
310 H=COS(T2)
320 H2=9.4*H*H-1.4*H+1.6
330 N=COS(T2-2.0944)
340 N2=4.2*N*N-N+0.2
350 C=COS(T2+2.0944)
360 IFC>0 THEN 390
370 C2=7.6*C*C
380 GO TO 400
390 C2=6*C*C
400 FOR T3=4.7124 TO 5.7596 STEP A
410 H=COS(T3)
420 H3=9.4*H*H-1.4*H+1.6
430 N=COS(T3-2.0944)
440 N3=4.2*N*N-N+0.2
450 C=COS(T3-4.1888)
460 IF C>0 THEN 490
470 C3=7.6*C*C
480 GO TO 500
490 C3=6*C*C
500 FOR P1=0 TO 1 STEP 0.1
600 FOR P2=0 TO 1-P1 STEP 0.1
610 P3=1-P1-P2
620 H9=P1*H1+P2*H2+P3*H3
630 IF H9>4.00 THEN 900
640 IF H9<3.80 THEN 900
650 N9=P1*N1+P2*N2+P3*N3
660 IF N9>2.95 THEN 900
670 IF N9<2.45 THEN 900
680 C9=P1*C1+P2*C2+P3*C3
690 IF C9>1.90 THEN 900
700 IF C9<1.10 THEN 900
750 IF T3<5.236 THEN 950
800 PRINT TAB(10);FNA(4.1888-T1);"*";TAB(20);FNA(T2);TAB(30);FNA(6.2
832-T3);
810 PRINT TAB(40);H9;TAB(50);C9;TAB(60);N9
820 PRINT TAB(10);"(";P1;")";TAB(20);"(";P2;")";TAB(30);"(";P3;")"
830 PRINT
900 NEXT P2
910 NEXT P1
920 NEXT T3
930 NEXT T2
940 NEXT T1
945 GO TO 999
950 PRINT TAB(10);FNA(4.1888-T1);"*";TAB(20);FNA(T2);TAB(30);FNA(T3-
4.1888);"*";
960 GO TO 810
999 END

```

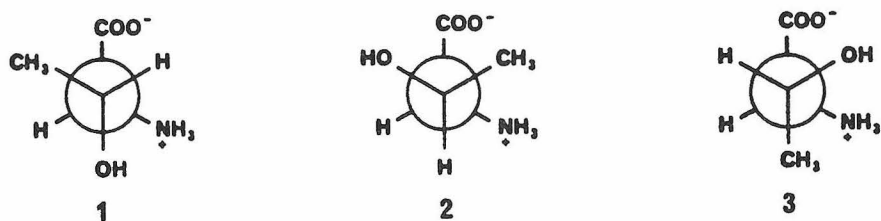
Figure D.2. Computer program for calculating threonine rotamer populations using equation A.

Table D.3. Calculated rotamer conformations and populations for allothreonine using equation B.



Rotamer Conformations (populations)			Calculated Coupling Constants		
$\alpha$	$\beta$	$\gamma$	$J_{\text{HH}}$	$J_{\text{CH}}$	$J_{\text{NH}}$
30 ( 0.3 )	50 ( 0.3 )	40 * ( 0.4 )	5.17083	2.49199	3.23621
30 ( 0.4 )	40 ( 0.3 )	30 * ( 0.3 )	5.04125	2.46328	3.18317
30 ( 0.4 )	35 ( 0.3 )	30 * ( 0.3 )	5.01111	2.32276	3.27331
30 ( 0.3 )	35 ( 0.4 )	50 * ( 0.3 )	5.09342	2.5513	3.07933
30 ( 0.2 )	35 ( 0.4 )	55 * ( 0.4 )	5.07489	2.51525	3.19888
30 ( 0.4 )	30 ( 0.4 )	35 * ( 0.2 )	4.98243	2.49431	3.06003
30 ( 0.4 )	30 ( 0.4 )	40 * ( 0.2 )	5.12284	2.42036	3.0388
30 ( 0.3 )	30 ( 0.4 )	45 * ( 0.3 )	4.8878	2.40056	3.26414
30 ( 0.3 )	30 ( 0.4 )	50 * ( 0.3 )	5.10983	2.33426	3.19328
35 ( 0.3 )	30 ( 0.4 )	40 * ( 0.3 )	4.8687	2.50422	3.23076
35 ( 0.3 )	30 ( 0.4 )	45 * ( 0.3 )	5.08865	2.41424	3.17868
40 ( 0.3 )	30 ( 0.4 )	40 * ( 0.3 )	5.04154	2.54483	3.14061
45 ( 0.2 )	30 ( 0.4 )	50 * ( 0.4 )	5.14455	2.43274	3.25151

Table D.4. Calculated rotamer conformations and populations for threonine using equation B.



$\alpha, \beta, \gamma$  = angle between  $-\text{OH}$  and  $-\text{CO}_2^-$   
 $\alpha^*, \beta^*, \gamma^*$  = angle between  $-\text{OH}$  and  $-\text{NH}_3^+$

Rotamer Conformations (populations)			Calculated Coupling Constants		
$\alpha$	$\beta$	$\gamma$	$J_{\text{HH}}$	$J_{\text{CH}}$	$J_{\text{NH}}$
	60 ( 0.3 )	45 ( 0.7 )	4.31429	2.56135	3.78419

```

100     MARGIN 120
110     DEF FNA(X)=INT(57.2958*X+0.5)
120     A=0.0872664
130     S=2.3
200     FOR T1=2.6180 TO 3.1416 STEP A
210     H=COS(T1)
220     H1=8.65*H*H-1.29*H+1.47
230     N=COS(T1-2.0944)
240     N1=4.2*N*N-N+0.2
250     C=COS(T1+2.0944)
260     IF C>0 THEN 290
270     C1=7.6*C*C
280     GO TO 300
290     C1=6*C*C
300     FOR T2=0.5236 TO 1.5708 STEP A
310     H=COS(T2)
320     H2=9.4*H*H-1.29*H+1.47
330     N=COS(T2-2.0944)
340     N2=4.2*N*N-N+0.2
350     C=COS(T2+2.0944)
360     IF C>0 THEN 390
370     C2=7.6*C*C
380     GO TO 400
390     C2=6*C*C
400     FOR T3=5.2360 TO 5.7596 STEP A
410     H=COS(T3)
420     H3=9.4*H*H-1.29*H+1.47
430     N=COS(T3-2.0944)
440     N3=4.2*N*N-N+0.2
450     C=COS(T3-4.1888)
460     IF C>0 THEN 490
470     C3=7.6*C*C
480     GO TO 500
490     C3=6*C*C
500     FOR P1=0 TO 1 STEP 0.1
600     FOR P2=0 TO 1-P1 STEP 0.1
610     P3=1-P1-P2
620     H9=P1*H1+P2*H2+P3*H3
630     IF H9>4.95+S*0.1 THEN 900
640     IF H9<4.95-S*0.1 THEN 900
650     N9=P1*N1+P2*N2+P3*N3
660     IF N9>2.7+S*0.25 THEN 900
670     IF N9<2.7-S*0.25 THEN 900
680     C9=P1*C1+P2*C2+P3*C3
690     IF C9>2.0+S*0.25 THEN 900
700     IF C9<2.0-S*0.25 THEN 900
750     IF T2<1.047 THEN 950
800     PRINT TAB(10);FNA(T1-2.0944);TAB(20);FNA(2.0944-T2);TAB(30);FNA(
T3-4.7124);"*";
810     PRINT TAB(40);H9;TAB(50);C9;TAB(60);N9
820     PRINT TAB(10);"(";P1;")";TAB(20);"(";P2;")";TAB(30);"(";P3;")"
830     PRINT
900     NEXT P2
910     NEXT P1
920     NEXT T3
930     NEXT T2
940     NEXT T1
945     GO TO 999
950     PRINT TAB(10);FNA(T1-2.0944);TAB(20);FNA(T2);"*";TAB(30);FNA(T3-
4.7124);"*";
960     GO TO 810
999     END

```

Figure D.3. Computer program for calculating  
allothreonine rotamer populations using equation B.

```

100 MARGIN 120
110 DEF FNA(X)=INT(57.2958*X+0.5)
120 A=0.0872664
130 S=4.5
200 FOR T1=3.1416 TO 3.6652 STEP A
210 H=COS(T1)
220 H1=8.65*H*H-1.29*H+1.47
230 N=COS(T1-2.0944)
240 N1=4.2*N*N-N+0.2
250 C=COS(T1+2.0944)
260 IF C>0 THEN 290
270 C1=7.6*C*C
280 GO TO 300
290 C1=6*C*C
300 FOR T2=0.5236 TO 1.0472 STEP A
310 H=COS(T2)
320 H2=8.65*H*H-1.29*H+1.47
330 N=COS(T2-2.0944)
340 N2=4.2*N*N-N+0.2
350 C=COS(T2+2.0944)
360 IFC>0 THEN 390
370 C2=7.6*C*C
380 GO TO 400
390 C2=6*C*C
400 FOR T3=4.7124 TO 5.7596 STEP A
410 H=COS(T3)
420 H3=8.65*H*H-1.29*H+1.47
430 N=COS(T3-2.0944)
440 N3=4.2*N*N-N+0.2
450 C=COS(T3-4.1888)
460 IF C>0 THEN 490
470 C3=7.6*C*C
480 GO TO 500
490 C3=6*C*C
500 FOR P1=0 TO1 STEP0.1
600 FOR P2=0 TO 1-P1 STEP 0.1
610 P3=1-P1-P2
620 H9=P1*H1+P2*H2+P3*H3
630 IF H9>3.90+S*0.1 THEN 900
640 IF H9<3.90-S*0.1 THEN 900
650 N9=P1*N1+P2*N2+P3*N3
660 IF N9>2.7+S*0.25 THEN 900
670 IF N9<2.7-S*0.25 THEN 900
680 C9=P1*C1+P2*C2+P3*C3
690 IF C9>1.5+S*0.25 THEN 900
700 IF C9<1.5-S*0.25 THEN 900
750 IF T3<5.236 THEN 950
800 PRINT TAB(10);FNA(4.1888-T1);"*";TAB(20);FNA(T2);TAB(30);FNA(6.2
832-T3);
810 PRINT TAB(40);H9;TAB(50);C9;TAB(60);N9
820 PRINT TAB(10);"(";P1;";";TAB(20);"(";P2;";";TAB(30);"(";P3;";";
830 PRINT
900 NEXT P2
910 NEXT P1
920 NEXT T3
930 NEXT T2
940 NEXT T1
945 GO TO 999
950 PRINT TAB(10);FNA(4.1888-T1);"*";TAB(20);FNA(T2);TAB(30);FNA(T3-
4.1888);"*";
960 GO TO 810
999 END

```

Figure D.4. Computer program for calculating threonine rotamer populations using equation B.

References

1. (a) R. L. Lichter and J. D. Roberts, Spectrochim. Acta, 26A, 1813-14 (1970); (b) K. Kanamori, A. H. Cain and J. D. Roberts, J. Am. Chem. Soc., 100, 4979-81 (1978); (c) I. Yavari and J. D. Roberts, Biochem. Biophys. Res. Comm., 83, 635-40 (1978); (d) F. Blomberg, W. Maurer and H. Rüterjans, Proc. Natl. Acad. Sci. USA, 73, 1409-13 (1976); (e) F. Blomberg, W. Maurer and H. Rüterjans, J. Am. Chem. Soc., 99, 8149-59 (1977).
2. (a) C. A. Swenson and L. Koob, J. Phys. Chem., 74, 3376-80 (1970); (b) D. Gattegno, G. E. Hawkes and E. W. Randall, J. C.S. Perkin II, 1976, 1527-31; (c) V. Markowski, T. B. Posner, P. Loftus and J. D. Roberts, Proc. Natl. Acad. Sci. USA, 74, 1308-09 (1977); (d) T. B. Posner, V. Morkowski, P. Loftus and J. D. Roberts, J.C.S. Chem. Comm., 1975, 769-70.
3. D. G. Gust, R. B. Moon and J. D. Roberts, Proc. Natl. Acad. Sci. USA, 72, 4696-4700 (1975); (b) A. Lapidot and C. S. Irving, J. Am. Chem. Soc., 99, 5488-90 (1977).
4. R. M. Davidson, T. O. Matsunga, B. L. Kam and N. J. Oppenheimer, Abstracts, 1977 Pacific Conference on Chemistry and Spectroscopy, Anaheim, Ca., Oct. 1977, No. 161.
5. W. W. Bachovchin and J. D. Roberts, J. Am. Chem. Soc., 100, 8041-47 (1978).

References (continued)

6. M. Kainosho, K. Ajisaka, M. Kamisaku and A. Murai, Biochem. Biophys. Res. Comm., 64, 425-32 (1975).
7. M. Llinás, W. J. Horsley and M. P. Klein, J. Am. Chem. Soc., 98, 7554-58 (1976).
8. A. Demarco, M. Llinás and K. Wüthrich, Biopolymers, 17, 2727-42 (1978).
9. J. A. Sogn, W. A. Gibbons and E. W. Randall, Biochemistry, 12, 2100-05 (1973).
10. R. L. Lichter and J. D. Roberts, J. Org. Chem., 35, 2806-07 (1970).
11. A. J. Fischman, H. R. Wyssbrod, W. C. Agosta and D. Cowburn, J. Am. Chem. Soc., 100, 54-58 (1978).
12. E. Fischer and W. Schmitz, Ber., 39, 351-56 (1906).
13. D. N Harpp, L. Q. Bao, C. Coyle, J. G. Gleason and S. Horovitch, Org. Syntheses, 55, 27-31 (1976).
14. E. Ronwin, J. Org. Chem., 18, 127-32 (1953).
15. P. S. Pregosin, E. W. Randall and A. I. White, Chem. Comm., 1971, 1602-3.
16. (a) M. Witanowski, L. Stefaniak and H. Januszewski in "Nitrogen NMR", M. Witanowski and G. A. Webb, Eds., Plenum Press, London, 1973, Chapter 4; (b) M. Witanowski, L. Stefaniak and G. A. Webb, Ann. Reports NMR Spectroscopy, 7, 117-244 (1977).
17. (a) J. Reisse, R. Ottinger, P. Bickart and K. Mislow, J. Am. Chem. Soc., 100, 911-915 (1978); (b) P. J. Stiles, Tetrahedron,

References (continued)

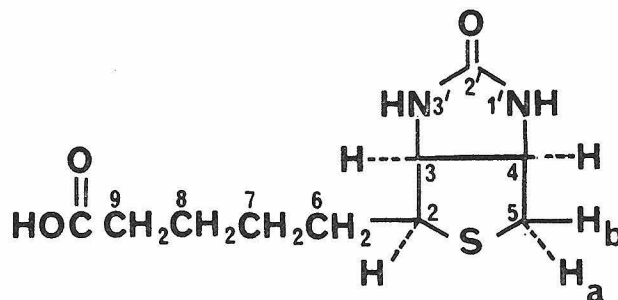
- 33, 2981-86 (1977).
18. J. P. Warren and J. D. Roberts, J. Phys. Chem., 78, 2507-11 (1974).
19. J. G. Batchelor, J. Mag. Res., 18, 212-14 (1975).
20. (a) J. I. Kroschwitz, M. Winokur, H. J. Reich and J. D. Roberts, J. Am. Chem. Soc., 91, 5927-28 (1969); (b) J. D. Roberts, F. J. Weigert, J. I. Kroschwitz and H. J. Reich, J. Am. Chem. Soc., 92, 1338-47 (1970).
21. For a review see V. F. Bystrov, Progress NMR Spectroscopy, 10, 41-81 (1976).
22. R. J. Abraham and K. A. McLauchlan, Mol. Physics, 5, 513-23 (1962).
23. R. A. Cooper, R. L. Lichter and J. D. Roberts, J. Am. Chem. Soc., 95, 3724-29 (1973).
24. J.-P. Marchal and D. Canet, J. Mag. Res., 31, 21-32 (1978).
25. "Nuclear Magnetic Resonance Spectrum Calculation Program, NMRCAL", Nicolet Instrument Corporation, Madison, Wisconsin, 1971.
26. For example: M. Montagut, B. Lemanceau and A. M. Bellocq, Biopolymers, 13, 2615-29 (1974).
27. (a) M. Karplus, J. Am. Chem. Soc., 85, 2870-71 (1963);  
(b) M. Karplus, J. Chem. Phys., 30, 11-15 (1959).
28. Dr. William H. Vine, personal communication.

References (continued)

29. (a) R. J. Abraham and G. Gatti, J. Chem. Soc. (B), 1969, 961-68; (b) R. J. Abraham, P. Loftus and A. W. Thomas, Tetrahedron, 33, 1227-34 (1977); (c) K. G. R. Pachler, J.C.S. Perkin II, 1972, 1936-40; (d) L. Phillips and V. Wray, J.C.S. Perkin II, 1972, 536-39.
30. (a) J. Feeny, J. Mag. Res., 21, 473-78 (1976); (b) K. D. Kopple, G. R. Wiley and R. Tauke, Biopolymers, 12, 627-36 (1973).
31. Recent examples include ref. 30a and M. Kainosho and K. Ajisaka, J. Am. Chem. Soc., 97, 5630-31 (1975).
32. (a) P. E. Hansen, J. Feeny and G. C. K. Roberts, J. Mag. Res., 17, 249-61 (1975); (b) W. G. Espersen and R. B. Martin, J. Phys. Chem., 80, 741-45 (1976); (c) J. Feeny, P. E. Hansen and G. C. K. Roberts, J.C.S. Chem. Comm., 1974, 465-66.
33. For example V. F. Bystrov, Yu. D. Gavrilov and V. N. Solkan, J. Mag. Res., 19, 123-29 (1975) or R. Wasyishen and T. Schaefer, Can. J. Chem., 50, 2989-3008 (1972).
34. J. Feeny in G. C. K. Roberts (Ed), "Drug Action at the Molecular Level", University Park Press, Baltimore, 1977, pp 55-72.
35. G. M. Whitesides, J. P. Sevenair and R. W. Gotez, J. Am. Chem. Soc., 89, 1135-44 (1967).

CHAPTER IIIBIOTINIntroduction

Biotin (1) is an essential cofactor for several enzymes involving carboxylation and carbonyl exchange reactions.<sup>1</sup> It appears to participate in the fixation, activation and transfer of carbon dioxide by forming a carboxybiotin. Lynen and coworkers<sup>2</sup> established one of the ureido nitrogens was the site of carboxylation and subsequently



1

demonstrated N1' was the point of attachment by X-ray crystallography. In addition, biotin forms a complex with the protein avidin with a dissociation energy<sup>3</sup> in excess of 20 kcal/mole. Substitution and modification of the N3' and N1' positions in biotin analogs led Green<sup>3</sup> to conclude that, while both ureido groups contribute to the association through hydrogen bonds with the protein, the interaction with N1' is more pronounced.

The chemical reactivity of the ureido nitrogens differs. Knappe and coworkers<sup>2</sup> found a 100:7 ratio of N1'- to N3'-acylated products from the reaction of methyl chloroformate with biotin methyl ester. The low proportion of N3' product was attributed to steric hindrance to approach of the reagent to N3' due to the presence of the carboxy-butyl side chain. Glasel<sup>6</sup> employed a similar argument to account for the difference in exchange rates for the ureido protons with ethanol.

The lack of physical methods to distinguish the two nitrogens in solution, suggested an examination of the <sup>15</sup>N NMR spectra could prove useful in providing an additional probe for protein systems involving biotin.

## Experimental

### Materials

2-Imidazolidinone (Aldrich), D, L-desthiobiotin (Sigma) and d-Biotin (Sigma and Calbiochem) were used without further purification. Dimethyl sulfoxide (DMSO) was dried over molecular sieves prior to use and solutions were degassed by bubbling argon gas for several minutes. Twice-distilled water and reagent-grade sodium bicarbonate were used. The aqueous solutions were prepared by filtering a mixture of 0.5 g of compound in 20 ml of 0.1 N NaHCO<sub>3</sub>.

### NMR Spectra

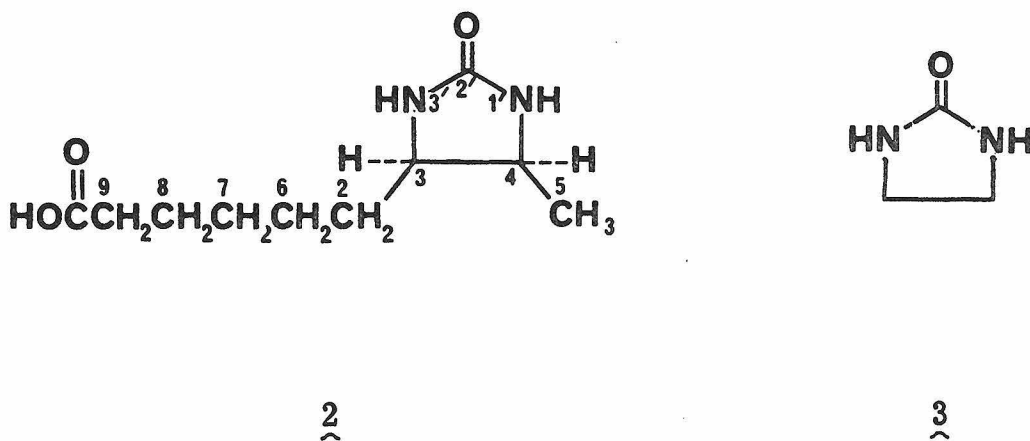
Proton spectra were recorded on Varian HR-220 (220 MHz) at 40° and Varian EM-390 (90 MHz) spectrometers at ambient probe temperatures.

The <sup>15</sup>N NMR spectra were recorded on a Bruker WH-180 Fourier-transform quadrature-detection spectrometer operating at 42 kGauss (18.25 MHz for <sup>15</sup>N and 180 MHz for <sup>1</sup>H) with 25-mm sample probe. The aqueous solutions and 2-imidazolidinone solutions were contained in 25-mm sample tubes with a concentric 5-mm capillary containing 1 M H<sup>15</sup>NO<sub>3</sub> in D<sub>2</sub>O for chemical-shift reference and deuterium field-frequency lock. The biotin and desthiobiotin solutions in DMSO, contained in 15-mm or 25-mm sample tubes, were locked on internal DMSO-d<sub>6</sub> and shifts are referenced to 1 M H<sup>15</sup>NO<sub>3</sub> in H<sub>2</sub>O contained in a concentric 5-mm capillary. Solution temperatures, measured by inserting a thermometer in the sample, were between 18 and 24° C. Chemical shifts are reported in ppm upfield of 1 M nitric acid with a precision of ± 0.1 ppm.

The nitrogen spectra in which a single proton resonance was irradiated during data acquisition were run in a gated decoupling mode to obtain a nuclear Overhauser enhancement. The decoupler modulation was switched off and on and a computer-activated relay was used to swap an attenuator into and out of the decoupler power transmission line prior to, and after, data acquisition, respectively. The nitrogen free-induction decays were treated with an exponential weighting function to increase the signal to noise ratio of the Fourier-transformed spectrum. The increase in peak width which resulted from this process is expressed as "line-broadening".

## Results

The  $^{15}\text{N}$  chemical shifts and one-bond NH coupling constants for biotin and its model compounds, desthiobiotin (2) and 2-imidazolidinone (3) are given in Table III.1. Two well-resolved resonances are present in



the proton decoupled spectra of desthiobiotin and biotin. For both, the upfield resonance was assigned to N3' as described below.

### Desthiobiotin

The two resonances were assigned on the basis of a selective decoupling experiment (Fig. III.1) in DMSO. The coupled spectrum shows two doublets with splitting of 90 and 91 Hz due to one-bond nitrogen proton couplings. By irradiating only the methyl protons at C5, the downfield nitrogen resonance is observed as a doublet of doublets. This is consistent with the assignment of the downfield nitrogen shift to N1' where the broadness of the resonances in the decoupled spectrum (Fig. III.1b) is due to coupling of the nitrogen to protons three bonds removed (typical<sup>4,5</sup>  $^3J_{\text{NH}} = 2-4$  Hz). The small 1.3-1.7 Hz splitting

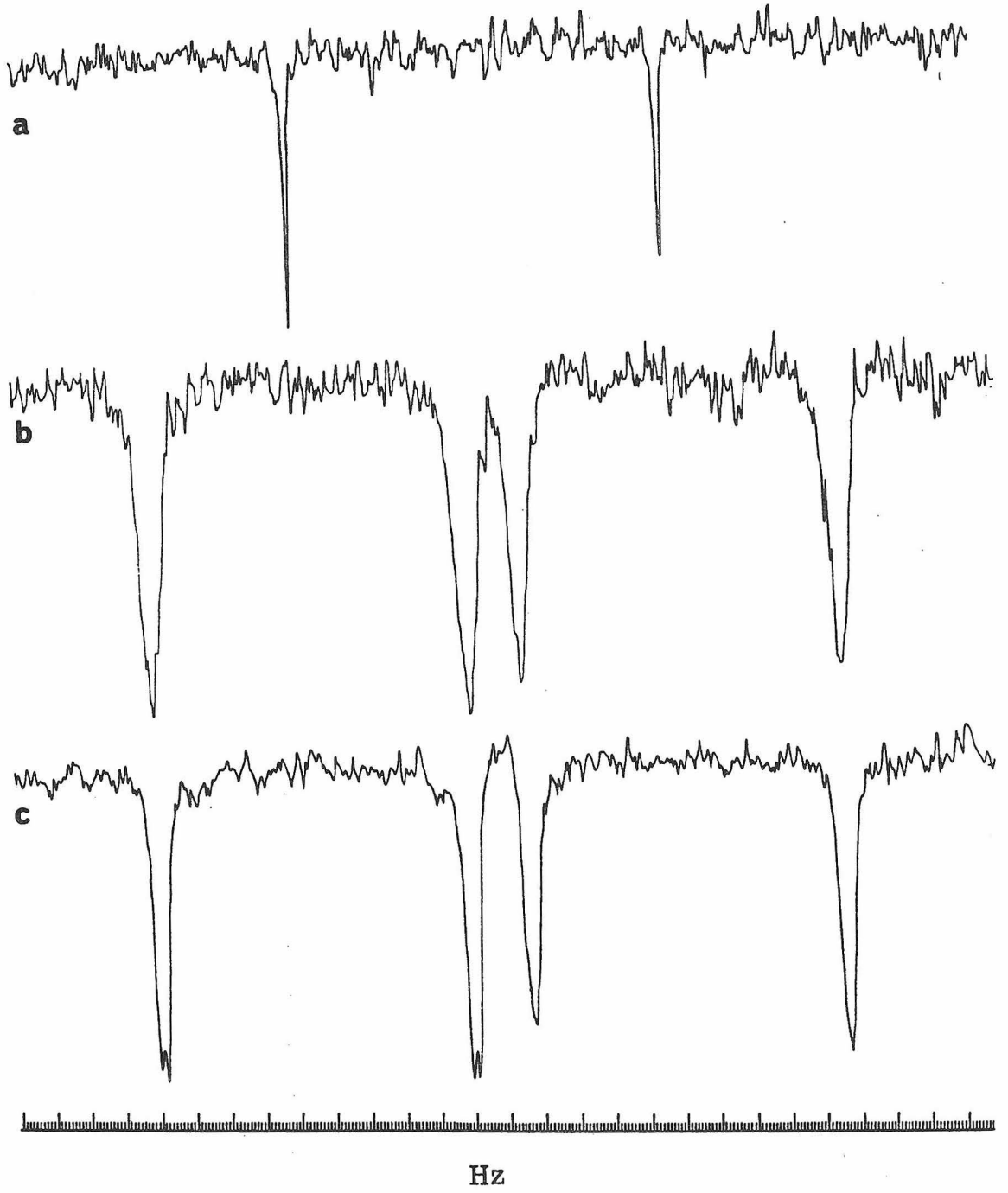
Table III.1.  $^{15}\text{N}$  NMR Chemical Shifts and Coupling Constants for Biotin and Model Compounds

	$\delta_{^{15}\text{N}}$ (ppm)	$^1J_{\text{NH}}$ (Hz)
<b>2-Imidazolidinone <u>3</u></b>		
1 M $\text{H}_2\text{O}$	294.0	
1.8 M $\text{H}_2\text{O}$	294.5	
1 M 0.1 N $\text{NaHCO}_3$	294.3	
2 M DMSO	296.7	93
<b>Desthiobiotin <u>2</u></b>		
sat'd soln in 0.1 N $\text{NaHCO}_3$	276.8	
	282.5	
0.7 M DMSO	279.3	90
	285.0	91
<b>Biotin <u>1</u></b>		
sat'd soln in 0.1 N $\text{NaHCO}_3$	283.6	
	292.6	
0.3 M DMSO	285.6	94
	294.7	92

Figure III.1.  $^{15}\text{N}$  NMR spectra of desthiobiotin in DMSO solution

- (a) Proton-decoupled spectrum: 1000 pulses,  $83^\circ$  pulse flip angle, 2.27 sec pulse repetition rate.
- (b) Proton-coupled spectrum: 6900 pulses,  $83^\circ$  pulse flip angle, 2 sec noise decoupler-on pulse delay, 4.27 sec pulse repetition rate.
- (c) Selective proton decoupling of the C5 methyl protons: 10745 pulses,  $83^\circ$  pulse flip angle, single-frequency decoupling of proton field at 263 Hz upfield of the DMSO resonance during the data acquisition time, 2 sec noise decoupler-on pulse delay, 4.27 sec pulse repetition rate.

Spectra were recorded with 1800 Hz spectral sweep width, 4096 data points of samples contained in a 15-mm tube with internal DMSO- $d_6$  lock. Line-broadening functions were set to 0.5 Hz.



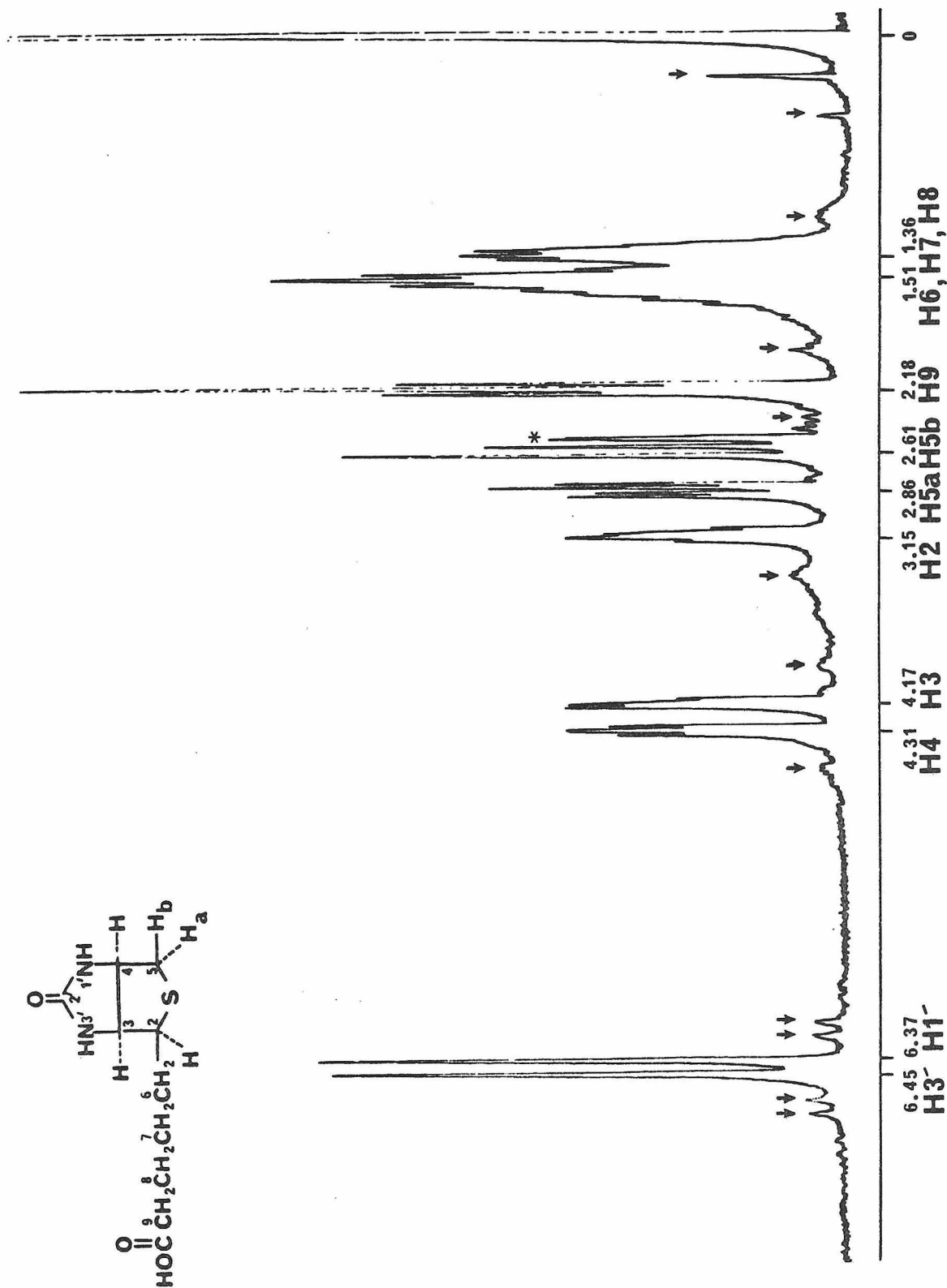


Figure III. 2. 220 MHz  $^1\text{H}$  NMR spectrum of biotin in dimethylsulfoxide- $d_6$ . The peak marked \* is the protio-impurity of the solvent 2.54  $\delta$ . Spinning side bands are designated with an  $\nabla$ .

in Figure III.1c is due then to the residual coupling of the proton at C3 to N1'.

## Biotin

### $^1\text{H}$ NMR Spectrum

An explicit assignment of biotin chemical shifts, necessary for the proton-nitrogen double resonance experiments, is presented in Figure III.2. Major features of the proton NMR were defined by Glasel<sup>6</sup> from spectra recorded at 60 MHz, where overlapping resonances were observed for H5a and H5b and also H4 and H3. The former were differentiated and assigned by Lett and Marquet<sup>7</sup> and also Griesser and coworkers<sup>8</sup> on the basis of coupling constants to H4 ( $^3J_{\text{H4}, \text{H5a}} = 5.0$ ,  $^3J_{\text{H4}, \text{H5b}} = 0$ ). Determination of the chemical shifts for H3 and H4 resulted from homonuclear decoupling experiments at 90 MHz. Upon irradiation of the H5a resonance, the doublet of doublets in the downfield portion of the H3, H4 multiplet collapsed to a doublet. A similar effect was noted on the upfield part of the multiplet when the H2 resonance was irradiated. Thus the downfield resonance (4.31  $\delta$ ) results from H4 and the upfield resonance (4.17  $\delta$ ) results from H3.

When about one equivalent of D<sub>2</sub>O was added to a biotin solution, diminution of the ureido proton signals occurred over several minutes. A differential rate of H-D exchange was observed in which the upfield signal equilibrated within about 5 minutes and the downfield signal equilibrated in 10-15 minutes (Figure III.3). The same effect was seen in equilibration of biotin with N-d<sub>2</sub>-benzamide or excess NaOD in D<sub>2</sub>O.

One of the ureido protons is coupled to H3 as evidenced by disappearance of a 1-2 Hz splitting in the signal at 4.17  $\delta$  after equilibration (Figure III.4). This coupling is not visible in either of the ureido resonances ( $\nu_{\frac{1}{2}} = 5$  Hz at 220 MHz) in dimethyl sulfoxide solution because of line broadening resulting from quadrupolar relaxation<sup>9a</sup> by the <sup>14</sup>N nuclei and/or intermediate rates of ureido proton exchange.

When the downfield ureido proton was irradiated, the three-bond coupling to H3 again disappeared while, on the contrary, irradiating the upfield ureido proton resulted in no discernible effect in the H3 or H4 resonances (Figure III.5). This means the downfield resonance (6.45  $\delta$ ) derives from H3' and the upfield resonance (6.37  $\delta$ ) derives from H1'.

The three-bond coupling constant of the ureido protons is expected to be small for biotin based on the relationship between dihedral angles and coupling constants. Measurements from molecular models indicate the HNCH dihedral angles are approximately 60°, occurring in the region of the Karplus curve for cyclic amides<sup>9b,c</sup> where the couplings range between 0 and 2 Hz. The differences in influence of the substituent groups on the ring geometry could cause the coupling between H1' and H4 to be so small as to result in only broadening and no visible splitting of the H4 resonance, while the H3', H3 coupling is discernible.

#### <sup>15</sup>N NMR Spectrum

The nitrogen resonances were assigned using proton off-resonance decoupling. Upon irradiation with a coherent decoupling field ( $\gamma H_2$ ), the biotin one-bond NH couplings (J) are reduced and the longer range splittings effectively removed. The residual coupling ( $J_r$ ), linearly

dependent on the shift difference ( $\Delta\nu$ ) between the resonance of the

$$J_{\text{r}} = \frac{J \Delta\nu}{\gamma H_2}$$

directly bonded proton and the decoupler frequency, goes to zero when the decoupler frequency coincides with the proton resonance.<sup>10</sup>

Figure III.5 shows the upfield resonance corresponds to the nitrogen directly bonded to H3' and the downfield resonance corresponds to the nitrogen directly bonded to H1'. Thus the resonance of N3' is 294.7 ppm and N1' is 285.6 ppm.

An additional experiment was performed in which only the methine proton at C2 was irradiated. Based on the results for des-thiobiotin, the resonance of N3' should experience three-bond couplings to both H4 and H2 as well as a direct (~90 Hz) coupling to H3' yielding a doublet of triplets. When H2 is irradiated, the nitrogen resonance should become a doublet of doublets in which a small (<2 Hz) residual coupling to H4 is present. This was observed for the upfield nitrogen resonance in biotin (Figure III.6) and confirms the above assignments.

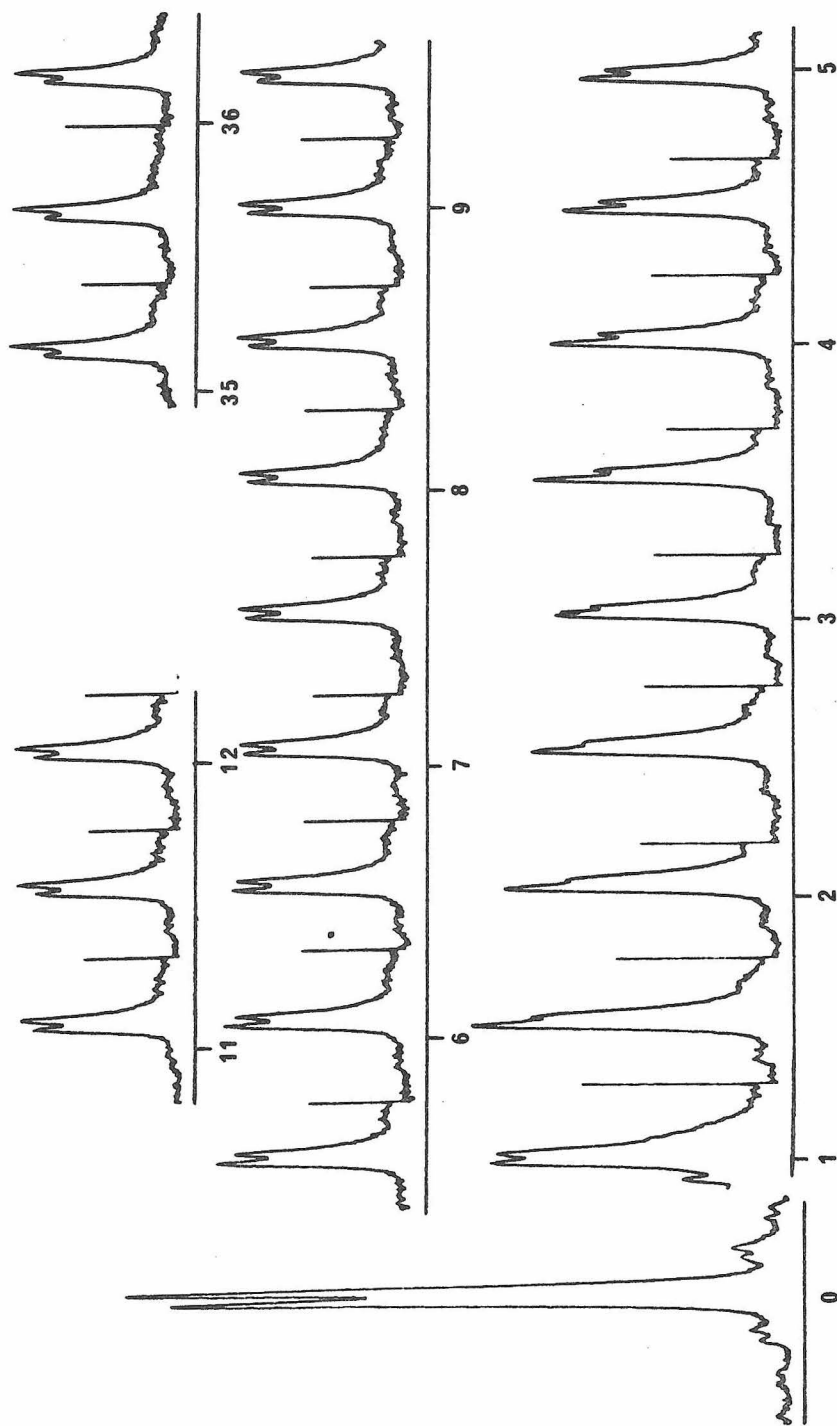


Figure III. 3. Biotin H-D exchange experiment. The ureido resonances are shown as a function of minutes elapsed after the addition of ca. one equivalent of D<sub>2</sub>O to biotin in dimethyl sulfoxide-d<sub>6</sub>. Spectra were recorded at 90 MHz and a sweep rate of 10 ppm/5 min.

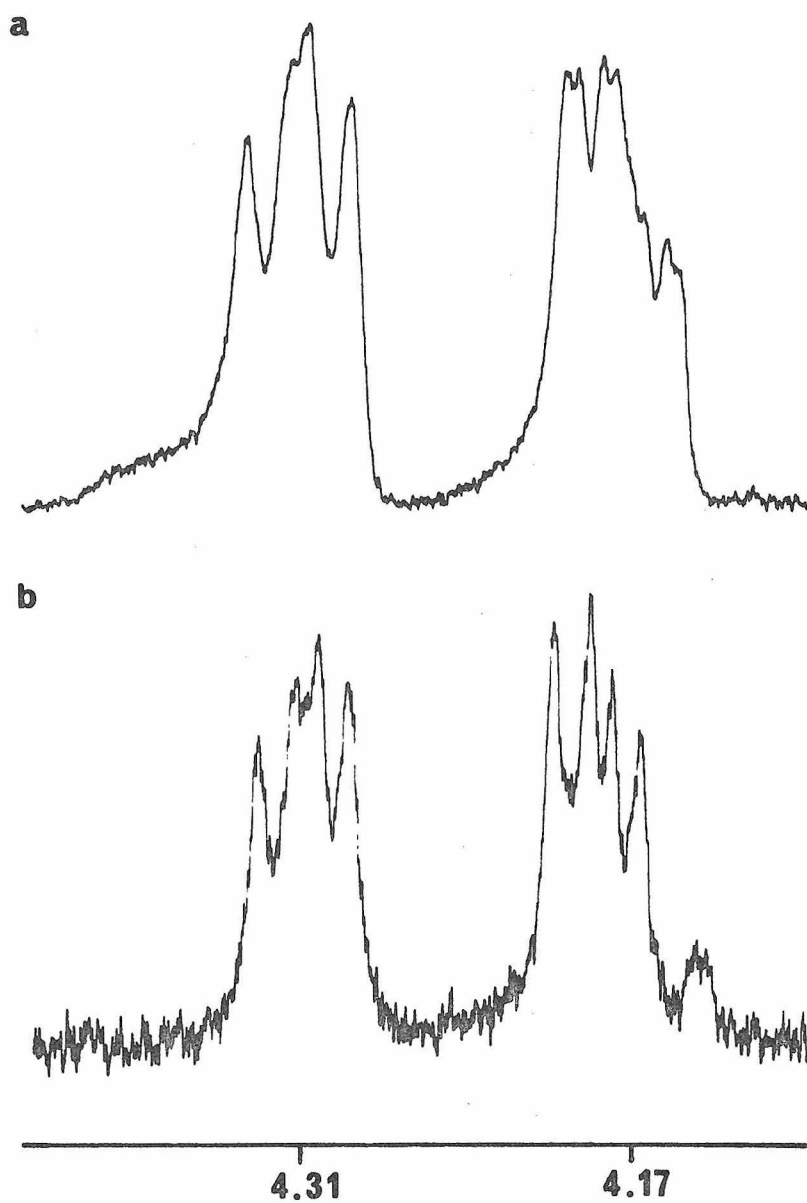


Figure III.4. Effect of ureido H-D exchange on H4 and H3 resonances. The 220 MHz spectrum of biotin in DMSO- $d_6$  in the absence (a) and presence (b) of aqueous NaOD solution.

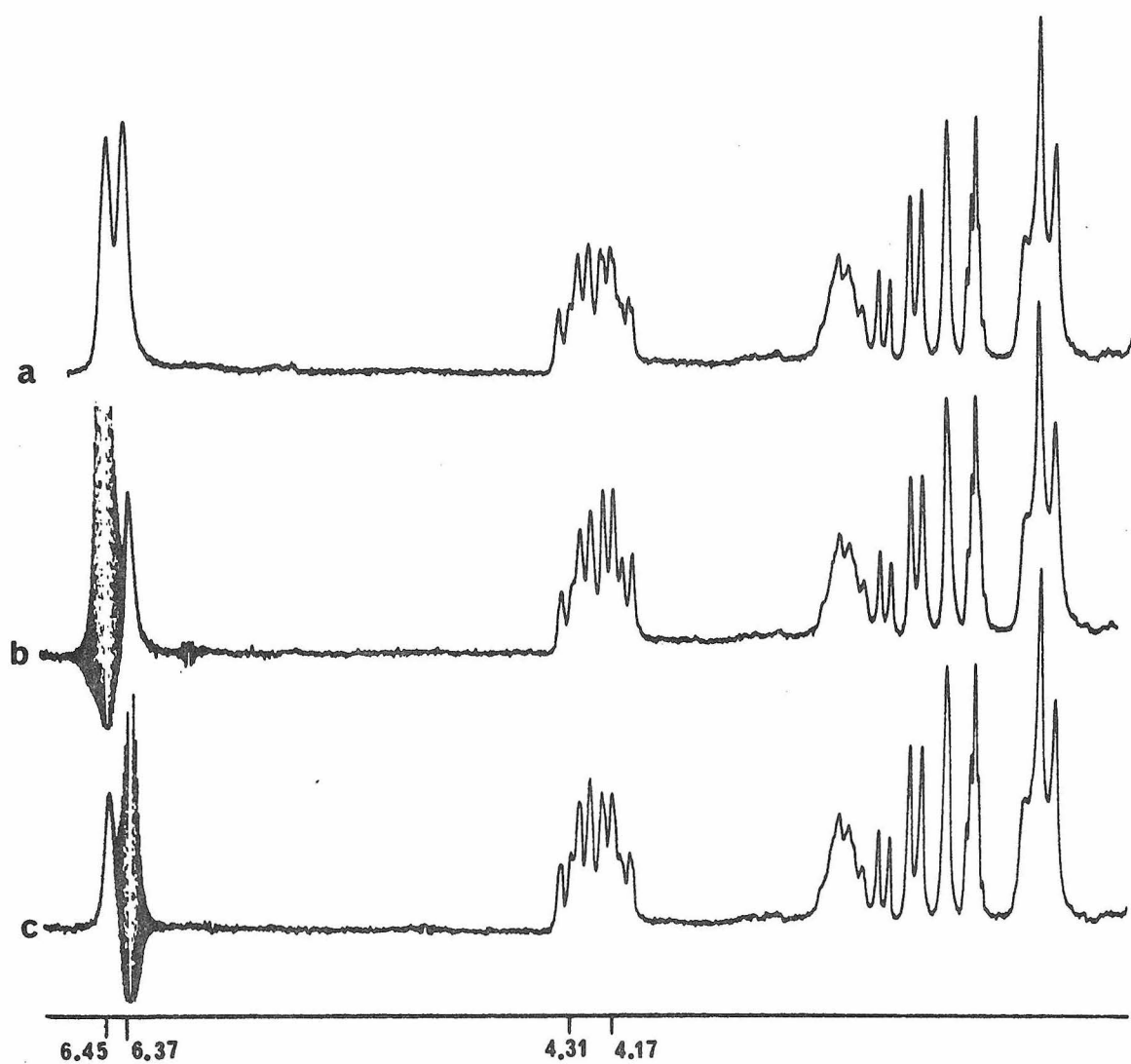


Figure III.5. Selective proton decoupling to assign biotin ureido resonances. (a) Proton-coupled spectrum at 90 MHz in dimethyl sulfoxide- $d_6$ . (b) Irradiation at 6.45  $\delta$  sharpens multiplet at 4.17  $\delta$ . (c) Irradiation at 6.37  $\delta$  leaves multiplets at 4.31 and 4.17  $\delta$  unaffected.

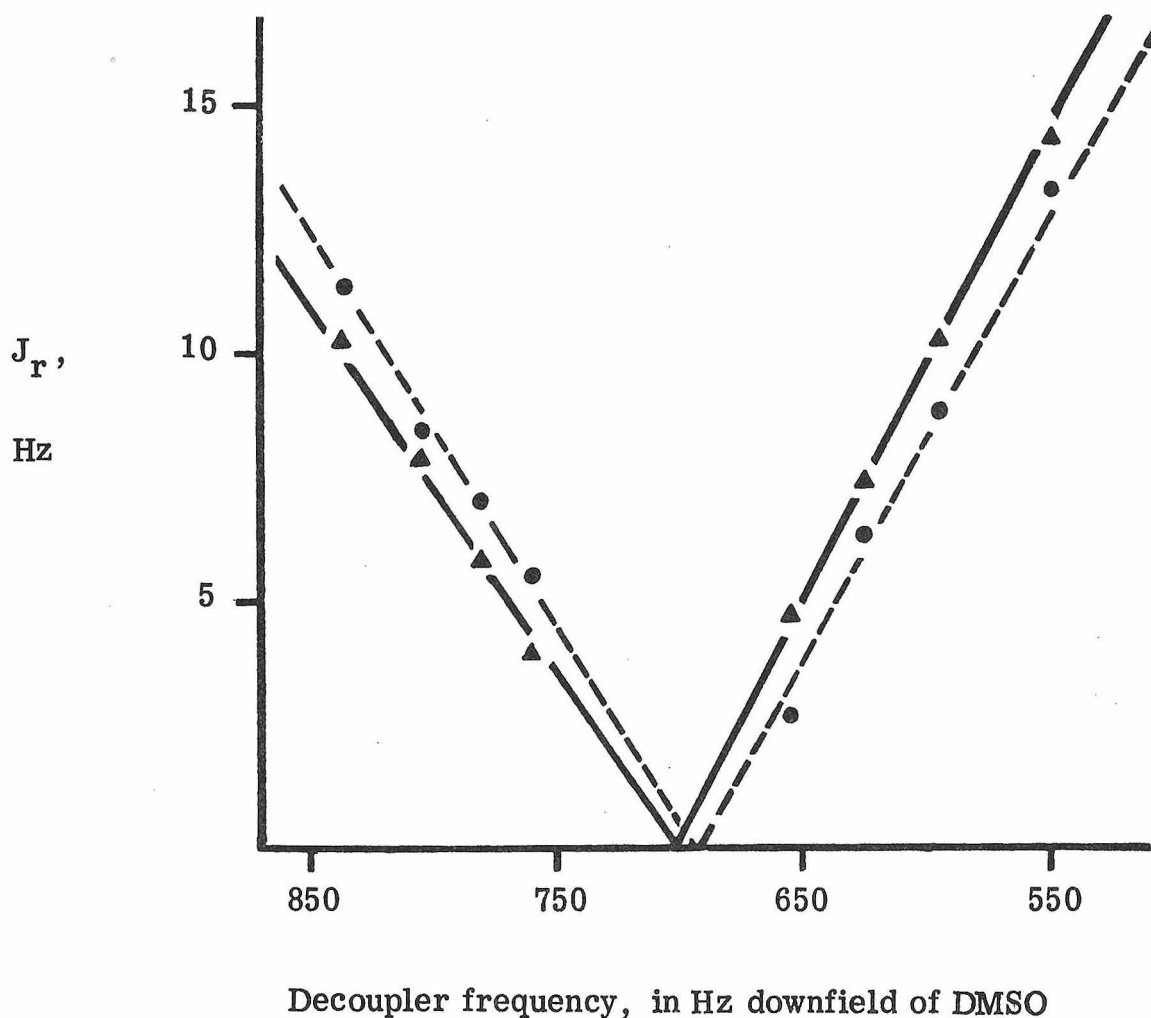
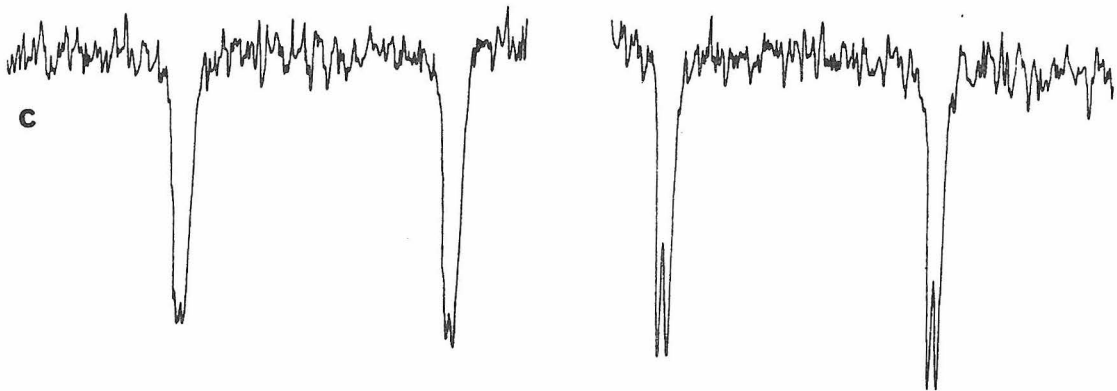
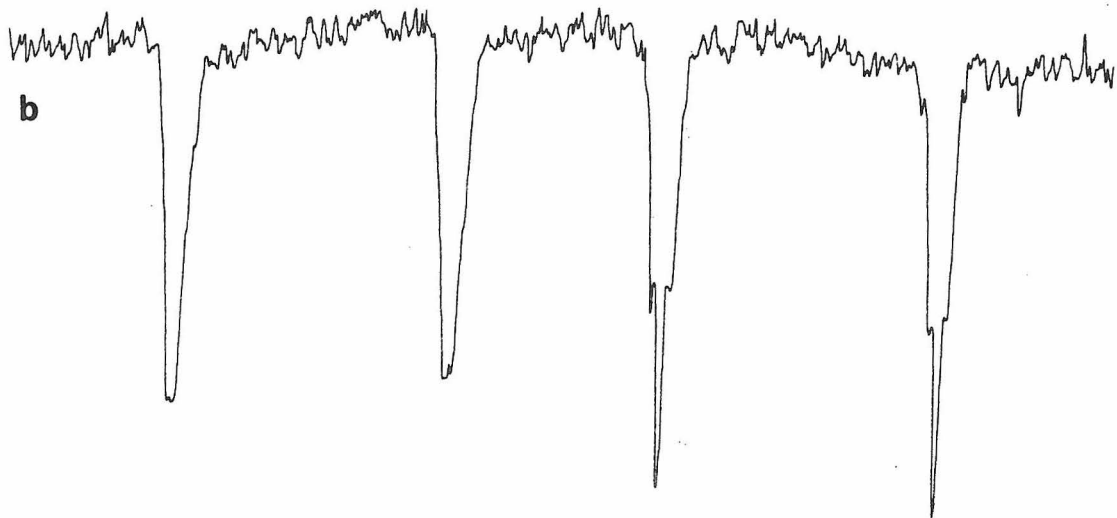
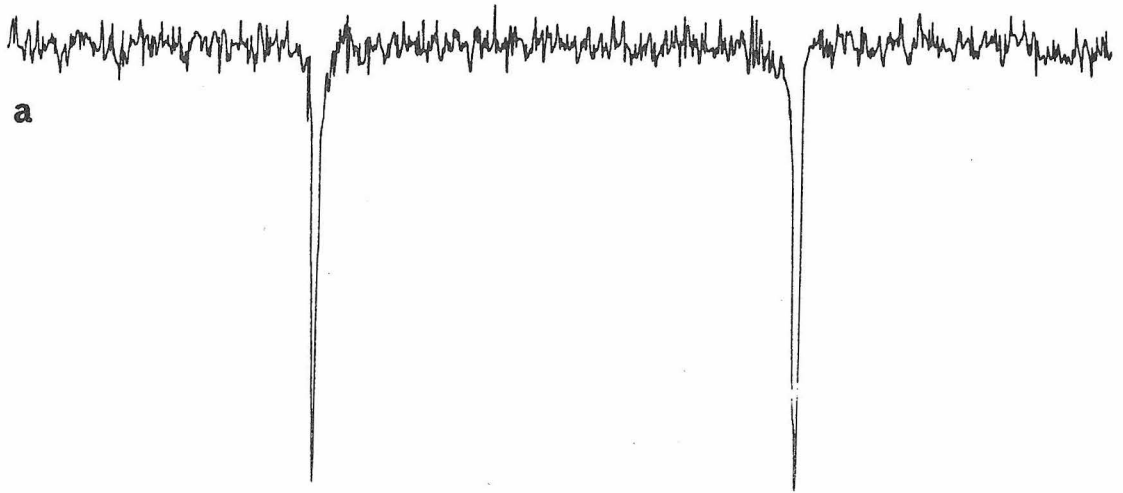


Figure III.6. Plot of nitrogen residual splittings,  $J_r$ , as a function of proton-decoupler position for biotin. The resonance centered at 285.6 ppm is represented as --●---●-- and that at 294.7 ppm as --▲---▲-- . The line represents the linear least-squares fit of the data. The average values of the proton-decoupler positions where the residual splittings are zero were 685.6 Hz and 707.6 Hz downfield of DMSO, respectively.

Figure III. 7.  $^{15}\text{N}$  NMR spectra of biotin in DMSO solution

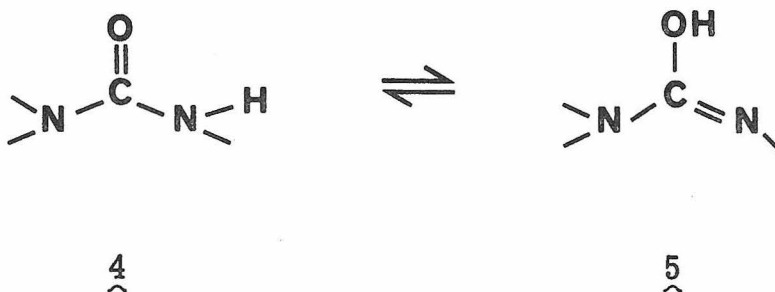
- (a) Proton-decoupled spectrum: 900 pulses, 4.10 sec pulse-repetition rate,  $45^\circ$  pulse flip angle.
- (b) Proton-coupled spectrum: 7664 pulses, 2.4 sec noise decoupler-on pulse delay, 6.5 sec pulse-repetition rate,  $90^\circ$  pulse flip angle.
- (c) Selective proton decoupling of the 2-C methine proton. 1952 pulses, single-frequency decoupling of the proton field at 104 Hz downfield of the DMSO resonance during data acquisition, 2.9 sec noise decoupler-on pulse delay, 7.0 sec pulse-repetition rate,  $77^\circ$  pulse flip angle. There is a  $90^\circ$  phase shift between the two halves of the spectrum and each portion was phased separately.

Spectra were recorded with either a 2000-Hz spectral width and 8192 data points or a 1000-Hz spectral width and 4096 data points. Line-broadening functions between 0.2 and 0.8 Hz were used.

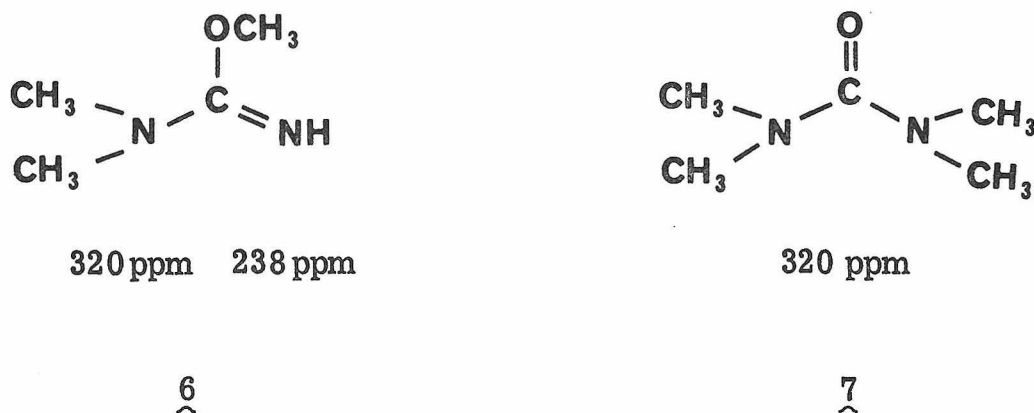


Discussion

Nitrogen chemical shifts of ureas typically<sup>11</sup> fall within the 270 - 320 ppm range. The equilibrium concentration of the imino tautomer (5) is usually small and O-methylisourea (6) shows<sup>12</sup> that



the imine nitrogen should exhibit a substantial downfield shift compared to the tautomeric urea (7). The values and range of nitrogen chemical

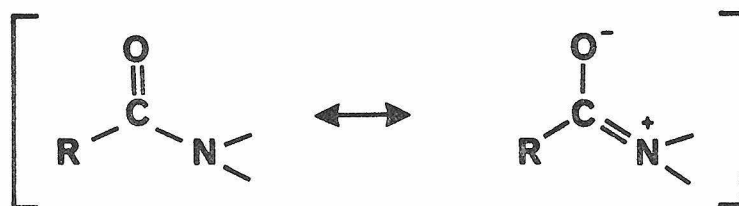


shifts observed among compounds (1), (2) and (3) and within the same compound reveal the nitrogens are of the urea type in dimethyl sulfoxide

and aqueous solutions. The shift differences are of the order of magnitude explained by alkyl substituent and solvent effects.

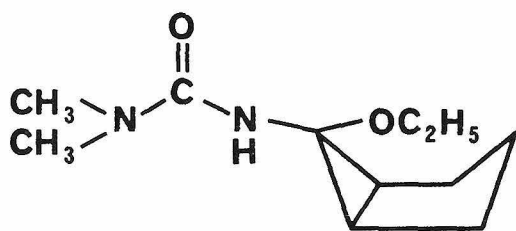
The chemical shifts of 2-imidazolidinone and those reported<sup>13</sup> for N-methyl-N'-isopropylurea in aqueous solution were 2.5 to 3.2 ppm downfield of those in dimethyl sulfoxide solution. Assuming comparable solvent effects for biotin and desthiobiotin, the upfield shifts for both compounds in aqueous solution correspond to the upfield shifts and assignments in dimethyl sulfoxide solution.

The solvent effect can arise from water-hydrogen bonding to the nitrogen lone pair and/or the oxygen. Duthaler and Roberts<sup>14</sup> proposed the former is the primary mechanism for solvent shifts in aliphatic amines between protic and non-hydrogen bonding solvents. Downfield shifts of 1 - 2.5 ppm resulted on changing the solvent from dimethyl sulfoxide to water. Llinàs and coworkers<sup>15</sup> attributed the 2.8 to 4.1 ppm downfield shifts observed on going from dimethyl sulfoxide to trifluoroethanol as solvent to stabilization of valence-bond structure (8) by hydrogen bonding to the oxygen in several amides.

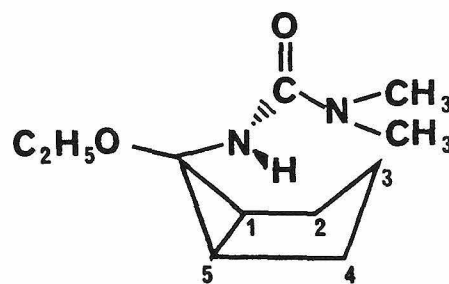


Changes in nitrogen chemical shift among the homologous ureas (1) through (3) correlate with known  $\beta$ -,  $\gamma$ -, and  $\delta$ -substituent effects. Downfield shifts in the range of 13 to 20 ppm result from replacing a hydrogen on the  $\alpha$ -carbon by a methyl group in acyclic amides<sup>16</sup> and amines.<sup>17</sup> A similar  $\beta$ -substituent effect in ureas can account for the majority of the differences observed between 2-imidazolidinone and desthiobiotin.

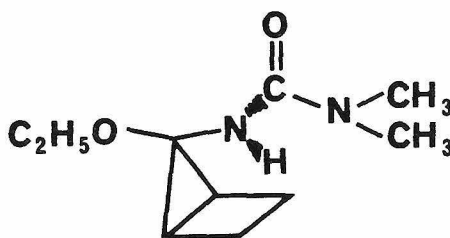
$\gamma$ -Substituent effects are dependent on molecular conformation, increasing with the degree of steric crowding at the nitrogen-induced by the  $\gamma$ -substituent. In acyclic amines, upfield shifts range from 2 to 6 ppm.<sup>18</sup> For cyclic compounds where the relationship between the nitrogen and  $\gamma$  carbon is fixed, the gauche effects are pronounced. Koch and coworkers<sup>19</sup> reported the NH nitrogen shift in urea (10)



9



10



11

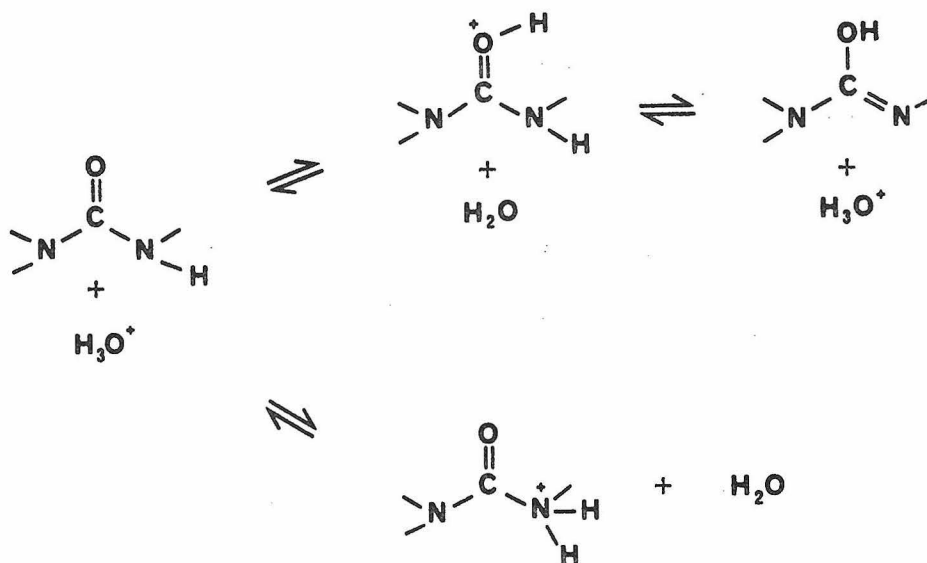
is 11.6 ppm upfield of the corresponding shift in (9). Data from the X-ray crystal structure of (10) indicate C4 and C2 make  $15^\circ$  and  $19^\circ$  dihedral angles<sup>20</sup> with the nitrogen. The NH shift of (10) is 4.1 ppm downfield of (11) suggesting a downfield  $\delta$  effect results when the  $\delta$ -carbon is proximal to the nitrogen.

The 5.7-ppm difference between the desthiobiotin resonances falls within the range expected for a  $\gamma$  effect on N3' due to C6. For biotin molecules in the crystal,<sup>21</sup> the sulfur is in the endo position forming  $84^\circ$  and  $86^\circ$  dihedral angles with N3' and N1' which constrains C6 to a pseudo-equatorial position and a  $43^\circ$  dihedral angle to N3'. Proton coupling constants<sup>7,8</sup> indicate the solution conformation is similar to that in the crystal. The differential interactions of N1' and N3' with C6 combined with the presence of a  $\gamma$ -sulfur atom result in a shift for N5' which is only 2 ppm downfield of 2-imidazolidinone and yet 9 ppm upfield of N1'.

The proton on N3' equilibrates with added D<sub>2</sub>O less rapidly than the proton on N1'. Similar results have been observed when N-d<sub>2</sub>-benzamide, excess aqueous NaOD or aqueous DCl were allowed to react with biotin.

In acidic solution, proton exchange via an O-protonated urea (Figure III. 8) is thought<sup>22</sup> to be slow relative to the N-protonated urea pathway. The relative rates of proton exchange in substituted ureas have been explained<sup>13,23</sup> by considering both steric and electronic effects on the mechanism in Figure III. 8. Since both acid- and base-catalyzed H-D equilibration involve removal and

## Acid-catalyzed exchange



## Base-catalyzed exchange

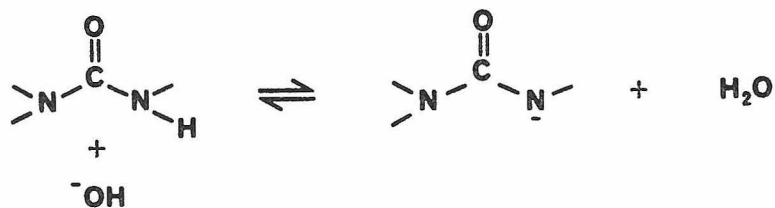


Figure III. 8. Schemes for urea proton exchange.

replacement of a proton on the nitrogens, steric hindrance to the approach of reagents by the carboxybutyl side chain can be expected<sup>2, 6</sup> to retard the exchange process at N3'.

The single-frequency decoupled spectra of biotin and desthiobiotin were recorded by combining noise-decoupler gating with coherent decoupling. The decoupler was set to the frequency of the proton. The sample was irradiated with broad-band, noise-modulated power in the proton region prior to data acquisition as is typical<sup>24</sup> of gated-decoupling experiments. During acquisition, the noise modulator is off and the decoupler power attenuated producing a narrow band of coherent radiation. As Bock and Pedersen<sup>25</sup> have emphasized, this technique improves the signal-to-noise ratio of the single-frequency decoupled spectrum by allowing a partial<sup>26</sup> nuclear Overhauser enhancement to be established. Figure III. 9 provides an example of the advantage of combining gated noise-decoupling with single-frequency decoupling for <sup>15</sup>N NMR.

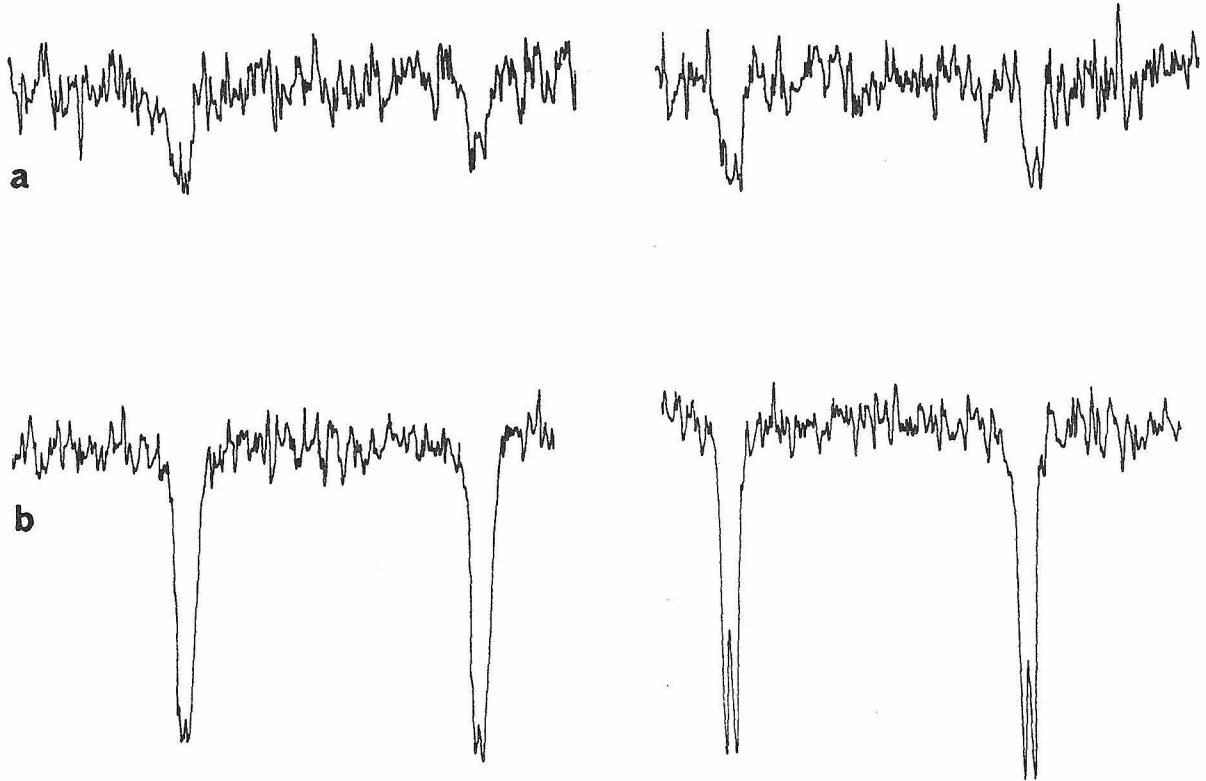


Figure III.9. Single-frequency decoupled biotin spectra, with and without gated noise decoupling. (a) 3374 scans,  $38^\circ$  pulse flip angle, 4.1 sec pulse-repetition rate. (b) (identical with Figure III.7c) 1952 scans,  $77^\circ$  pulse flip angle, 2.9 sec noise-decoupler on pulse delay, 7.0 sec pulse-repetition rate. The elapsed time for each experiment totaled 3.8 hr. The line-broadening function was set to 0.5 Hz.

## Conclusion

The differential exchange rates for the ureido protons of biotin were previously noted by Glasel.<sup>6</sup> We have established that the proton on the N1' nitrogen exchanges more readily with solvent than that on the N3' nitrogen. This was accomplished through assignment of the resonances of the nitrogen NMR spectrum and correlation of these resonances with the proton ureido spectrum, and also by assignment of the proton NMR spectrum by homonuclear decoupling experiments. Because the nitrogen resonances of biotin are separated by 9 ppm and the assignments are known, <sup>15</sup>N spectroscopy can be used to study <sup>15</sup>N enriched biotin mobility and binding in protein systems.

References

1. For reviews of biotin enzymes see (a) H. G. Wood and R. E. Barden, Ann. Rev. Biochem., 46, 385-413 (1977); (b) A. Marquet, Pure Appl. Chem., 49, 183-196 (1977).
2. (a) C. Bonnemere, J. A. Hamilton, L. K. Steinrauf and J. Knappe, Biochemistry, 4, 240-245 (1965); (b) J. Knappe, E. Ringelmann and F. Lynen, Biochem. Z., 335, 168-176 (1961).
3. N. M. Green, Adv. Protein Chem., 29, 84-133 (1975) and references therein.
4. T. Axenrod in "Nitrogen NMR," M. Witanowski and G. A. Webb, Eds., Plenum Press, London, 1973, Chapter 5.
5. M. J. O. Anteunis, F. A. M. Borremans, J. Geland, A. P. Marchand and R. W. Allen, J. Amer. Chem. Soc., 100, 4050-55 (1978).
6. J. A. Glasel, Biochemistry, 5, 1851-55 (1966).
7. R. Lett and A. Marquet, Tetrahedron, 30, 3365-77, 3379-92 (1974).
8. (a) R. Griesser and D. B. McCormick, Arch. Biochem. Biophys., 160, 667-8 (1974); (b) H. Sigel, D. B. McCormick, R. Griesser, B. Prijis and L. D. Wright, Biochemistry, 8, 2687-95 (1969).
9. (a) J. D. Roberts, J. Amer. Chem. Soc., 78, 4495 (1956); (b) V. N. Solkan and V. F. Bystrov, Tetrahedron Lett. 2261-64 (1973); (c) V. F. Bystrov, Prog. NMR Spectroscopy, 10, 41-81 (1976).

References (continued)

10. (a) F. W. Wehrli and T. Wirthlin, 'Interpretation of Carbon-13 NMR Spectra', Heyden, London, 1976, pp. 66-72; (b) G. E. Hawkes, E. W. Randall and W. E. Hull, J.C.S. Perkin II, 1977, 1268-75.
11. (a) M. Witanowski, L. Stefaniak and H. Januszewski in "Nitrogen NMR," M. Witanowski and G. A. Webb, Eds., Plenum Press, London, 1973, Chapter 4; (b) M. Witanowski, L. Stefaniak and G. A. Webb, Ann. Reports NMR Spectroscopy, 7, 117-244 (1977).
12. M. Witanowski, L. Stefaniak, S. Szymanski and G. A. Webb, Tetrahedron, 32, 2127-29 (1976).
13. I. Yavari and J. D. Roberts, Org. Mag. Res., submitted.
14. R. O. Duthaler and J. D. Roberts, J. Mag. Res., in press.
15. M. Llinàs, W. J. Horsley and M. P. Klein, J. Amer. Chem. Soc., 98, 7554-58 (1976).
16. P. W. Westerman and J. D. Roberts, J. Org. Chem., 43, 1177-79 (1978).
17. R. O. Duthaler, K. L. Williamson, D. D. Giannini, W. H. Bearden and J. D. Roberts, J. Amer. Chem. Soc., 99, 8406-8412 (1977).
18. R. O. Duthaler and J. D. Roberts, J. Amer. Chem. Soc., 100, 3889-95 (1978).
19. (a) R. C. Haltiwanger, J. M. Burns, G. C. Crockett and T. H. Koch, J. Amer. Chem. Soc., 100, 5110-16 (1978); (b) J. M. Burns, M. E. Ashley, G. C. Crockett and

References (continued)

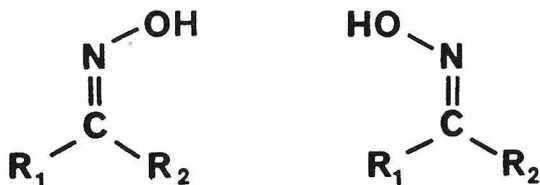
- T. H. Koch, J. Amer. Chem. Soc., 99, 6924-28 (1977).
20. Dihedral angles were calculated from the data in Ref. 19a.
21. G. T. De Titta, J. W. Edmonds, W. Stallings and J. Donohue, J. Amer. Chem. Soc., 98, 1920-26 (1976).
22. R. B. Martin, J.C.S. Chem. Commun., 1972, 793-4. See however J. F. Whidby and W. R. Morgan, J. Phys. Chem., 77, 2999-3002 (1973).
23. (a) L. C. Martinelli, C. D-W. Blaton and J. F. Whidby, J. Amer. Chem. Soc., 93, 5111-13 (1971); (b) R. S. Molday and R. G. Kallen, J. Amer. Chem. Soc., 94, 6739-45 (1972).
24. R. Freeman and H. D. W. Hill, J. Mag. Res., 5, 278-80 (1971).
25. K. Bock and C. Pederson, J. Mag. Res., 25, 227-30 (1977).
26. D. Shaw, "Fourier Transform NMR Spectroscopy", Elsevier Scientific Publishing Company, Amsterdam, 1976, pp. 290-93 and 187.

## CHAPTER IV

### OXIMES

#### Introduction

The configuration of oximes can be delineated by NMR spectroscopy from both chemical-shift and coupling-constant data. The chemical shifts of the protons<sup>1</sup> and carbons<sup>2</sup> in R<sub>1</sub> and R<sub>2</sub> are affected by the magnetic-field anisotropy of the hydroxyl group and the nitrogen lone pair of electrons. For example, the resonance of an  $\alpha$ -carbon in an R<sub>1</sub>-group cis to the hydroxyl will be shifted upfield of its resonance when the same R<sub>1</sub>-group is trans to the hydroxyl.



Comparison of the spectra for both geometric isomers yields the configurations. Recently the dependence<sup>3</sup> of <sup>15</sup>N chemical shifts on the structure of the R-groups was elucidated, providing an additional method of structure determination.

In proton NMR studies, Lehn and coworkers<sup>4</sup> observed that, for <sup>15</sup>N-enriched aldoximes, the two-bond nitrogen  $\alpha$ -proton coupling constant also depends on the configuration of the oxime. Specifically, when the lone pair is trans to the  $\alpha$ -proton (E-aldoximes) the observed coupling ranges between 2 and 3 Hz. In the cis-configuration (Z-aldoximes), the absolute value of the coupling

constants is between 13 and 16 Hz. Molecular orbital calculations<sup>5</sup> indicate that the differences in coupling constants are representative of the structural dependence of two-bond imine nitrogen couplings. The increased coupling in the Z-aldoximes appears<sup>5b</sup> to arise from interaction of the nitrogen lone pair with H<sub>α</sub>-C bonding orbitals. Similar experimental results are known for the C<sub>α</sub>-N couplings in ketoximes<sup>6</sup> and imines<sup>7</sup> and the H<sub>β</sub>-C<sub>α</sub> couplings in vinyl halides.<sup>8</sup>

The established stereochemical dependence of the two-bond coupling allows the configuration of a single aldoxime isomer to be determined. This study examines the prospects of obtaining the necessary coupling constants from <sup>15</sup>N NMR spectra.

## Experimental

The oxime and derivatives were prepared by literature methods: E and Z-benzaloxime,<sup>1b</sup> E- and Z-benzaloxime O-methyl ether,<sup>1b</sup> formamidoxime,<sup>16</sup> acetamidoxime,<sup>17</sup> benzamidoxime,<sup>17</sup> and N-methyl-benzaldonitrone.<sup>1b</sup>

The <sup>15</sup>N NMR spectra were recorded on a Bruker WH-180 Fourier-transform, quadrature-detection spectrometer operating at 42 kGauss. Oxime solutions (ca. 36 mole % in dimethyl sulfoxide) were contained in 25-mm sample tubes with a concentric 5-mm capillary containing 1M H<sup>15</sup>NO<sub>3</sub> in D<sub>2</sub>O for chemical-shift references and deuterium field-frequency lock. Solution temperatures, measured by inserting a thermometer in the sample, were between 17° and 25° C. The nitrogen chemical shifts are reported in ppm from 1M nitric acid with a precision of ± 0.1 ppm. Positive chemical shifts are upfield of the reference. An exponential weighting function was applied to the free induction decay to increase the signal-to-noise ratio of the Fourier transformed spectrum. The increase in peak width which results from this process is expressed as "line broadening". The NOE enhancement in the aldoxime spectra was eliminated with inverse-gated decoupling in order to observe the resonances.<sup>3</sup>

Table IV.1.  $^{15}\text{N}$  Chemical shifts and coupling constants.

<u>Oximes</u>		
	$\delta_{^{15}\text{N}}$ ppm	$^2J_{\text{NH}\alpha}$ Hz
	7.0	16.1
	3.7	3
	-9.4	15.9
	-10.7	2.4
	96.5	2.6
<u>Amidoximes</u>		
	$\delta_{^{15}\text{NOH}}$ ppm	$\delta_{\text{NH}_2}$ ppm
	90.9 $^2J_{\text{NH}} = 16$	310.0 $^1J_{\text{NH}} = 88, ^2J_{\text{NH}} = 5$
	98.6	306.4 $^1J_{\text{NH}} = 88$
	88.2	312.4 $^1J_{\text{NH}} = 87$

## Results and Discussion

The  $^{15}\text{N}$  NMR chemical shifts and coupling constants for E- and Z-benzaldoximes and three amidoximes are reported in Table IV.1. The benzaldoximes and benzamidoxime nitrogen chemical shifts are observed about 10 ppm downfield of the corresponding aliphatic compounds because of a second-order paramagnetic effect<sup>3, 8</sup> of the phenyl group on the C=N double bond. In contrast to aliphatic oximes,<sup>3</sup> the chemical shifts of Z-benzaldoxime and its O-methyl ether are upfield of the corresponding E-isomers. Comparison with the nitrogen shifts for isobutyraldoxime isomers in dimethyl sulfoxide solution<sup>3</sup> shows the downfield shifts of Z-benzaldoxime is not as large as in the E-isomer:

	$\delta$ , ppm	
	<u>E</u> -isomer	<u>Z</u> -isomer
isobutyraldoxime <sup>3</sup>	16.7	15.9
benzaldoxime	<u>3.7</u>	<u>7.0</u>
$\Delta\delta$	13	9

A similar difference in the effect of a phenyl substituent is observed for the O-methyl benzaldoxime ethers. This could result from an upfield steric compression in Z-benzaldoxime as previously noted for aliphatic oximes<sup>3</sup> and/or a smaller second-order paramagnetic effect in the Z-isomer from twisting of the phenyl ring out of the C=N-O plane.<sup>6a, 10</sup>

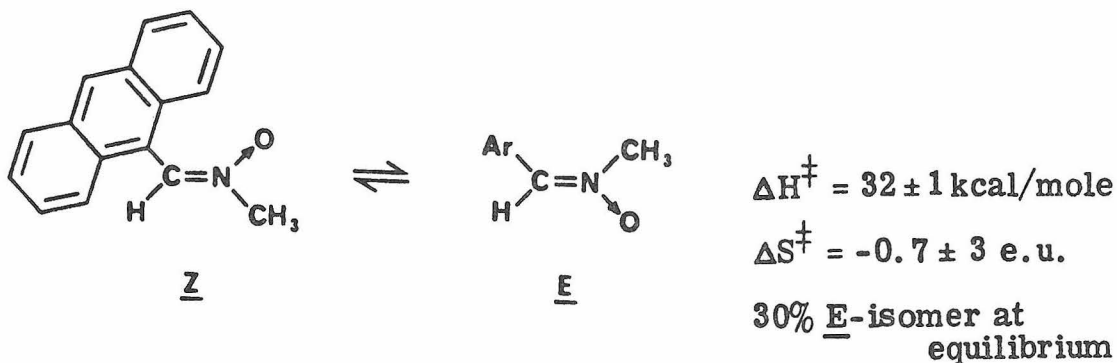
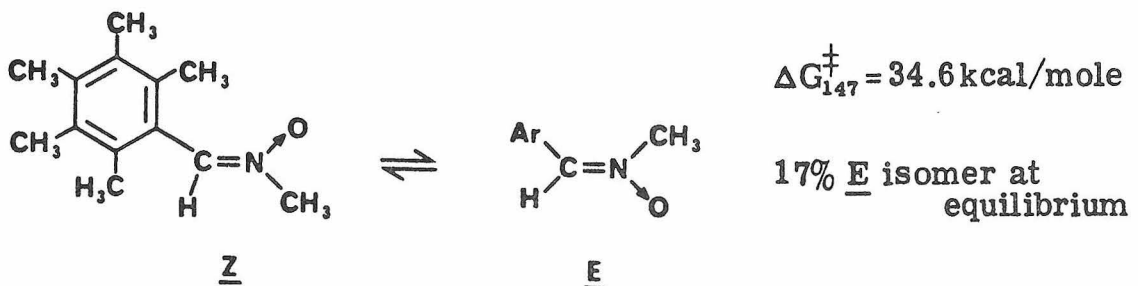
The  $\beta$ -substituent effect for the O-methyl group in the benzald-oximes (14.7 to 16.4 ppm) in dimethyl sulfoxide solution is significantly smaller than that previously reported<sup>11</sup> for acetone oxime (40 ppm) and acetaldehyde oxime (31 ppm). Webb and coworkers<sup>11</sup> have suggested that the large effects observed in the diethyl ether solutions of the aliphatic compounds reflect the loss of the hydrogen-bonded dimer structure<sup>3, 11</sup> of the oximes in addition to a  $\beta$ -substituent effect.

The nitrogens in E- and Z-benzaldoximes are coupled to both the hydroxyl and  $\alpha$ -protons. Oatis and Schultz<sup>12</sup> observed that the former coupling constants are between 1.5 and 2 Hz. However, the coupling to the hydroxyl proton was not observed in the <sup>15</sup>N spectrum of the benzaldoximes allowing the two-bond  $\text{NH}_{\alpha}$  coupling to be obtained directly from the proton-coupled spectrum. It was necessary to selectively decouple the methyl protons in the O-methyl benzald-oxime ether in order to observe  ${}^2J_{\text{NH}_{\alpha}}$ . For the benzaldoximes and their O-methyl ethers, the 2-3 Hz two-bond couplings in the E-isomers were readily observable and distinguishable from the ca. 16 Hz splitting in the Z-isomers. Figure IV. 1 demonstrates the difference in couplings observed for the isomeric benzaldoxime ethers.

That the nitrogen lone pair is necessary to observe large two-bond couplings to cis-substituents is supported by the coupling in N-methyl-Z-benzaldonitrone. The proton-coupled nitrogen spectrum in dimethyl sulfoxide solution showed a five-line multiplet ( $J \approx 2.6$  Hz). On selective decoupling of the  $\text{H}_{\alpha}$ -proton, a quartet ( $J = 2.57$  Hz) due

to the methyl protons was seen. A doublet (2.57 Hz) resulted when the methyl protons were irradiated. The magnitude of the observed coupling to  $H_{\alpha}$  is in marked contrast to the two-bond  $N-H_{\alpha}$  coupling of 16.1 Hz in Z-benzaldoxime.

It should be noted that the nitron configuration is assigned without direct experimental evidence. Support for the Z-isomer conformation follows. Only one N-methyl benzaldonitron is known.<sup>1b</sup> Buehler<sup>1b</sup> argues that because the  $^1H$  NMR of the methyl group shows no change from 100 to  $-60^{\circ}$  there is "little restriction" to rotation about the CN bond. Subsequent studies<sup>13, 14</sup> have shown, however, that when the C-alkyl group of aldonitrones is bulky two isomers are observed:



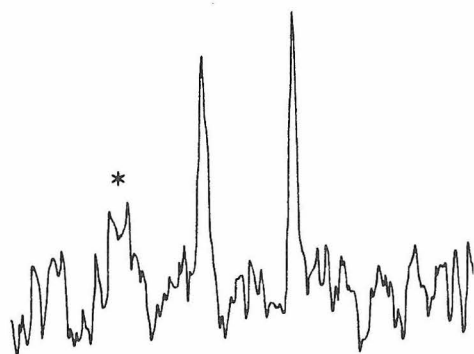
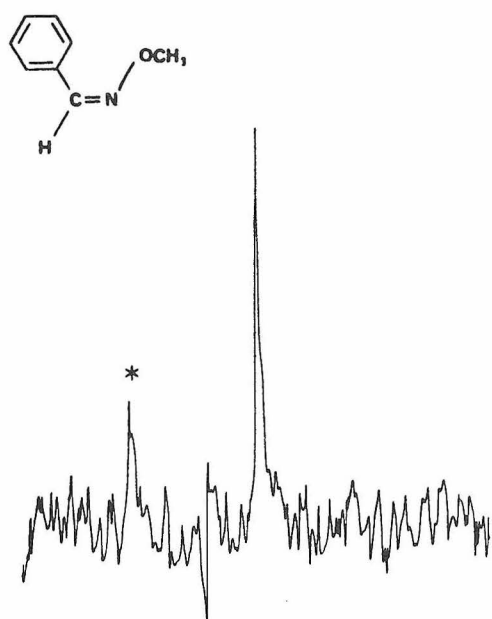
INDO and CNDO/2 calculations<sup>13</sup> for N-methylbenzaldonitrone predict that the Z-isomer (with a coplanar phenyl ring) is 3-4 kcal/mole more stable than the E-isomer (with an orthogonal phenyl ring). This corresponds to an E-isomer equilibrium concentration of less than 1%. The Z-configuration of the existing N-methylbenzaldonitrone isomer is also supported by the results from X-ray crystallographic studies<sup>15</sup> which show that p-chloro and p-nitro-N-methylbenzaldonitrones exist in the Z-configuration.

The nitrogen spectra of the amidoximes show only one pair of resonances for the oxime and amide nitrogens (Table IV.1). The presence of the ca. 90-Hz one-bond coupling in the amide resonance indicates that the amidoxime shifts arise from a single configurationally stable isomer and not an average of rapidly equilibrating structures. The two-bond  $\text{NH}_\alpha$  coupling constant in formamide oxime is 16 Hz (Figure IV.2), suggesting that the Z-isomer (1) is the one present in solution.

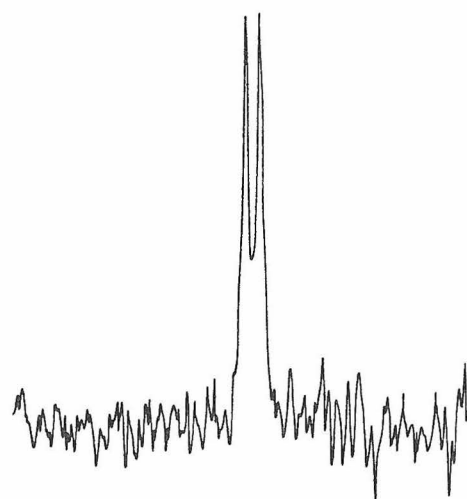
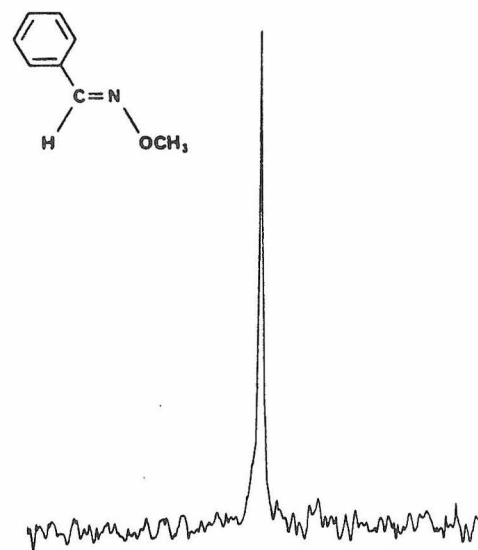
In summary, nitrogen NMR is useful for examining the configuration of oximes and oxime derivatives. The nitrogen chemical shifts of the isomeric benzaldoximes are different and, once they are assigned, can be used to distinguish the isomers. The values of the two-bond  $^{15}\text{N}, \text{H}_\alpha$  coupling constants for the E- and Z- oximes is characteristic of the configuration and the differences in magnitude are large. Coupling constants obtained from natural-abundance  $^{15}\text{N}$  spectra can be utilized for configuration assignment in aldoximes. An unfavorable nuclear Overhauser enhancement and long nitrogen relaxation time ( $T_1$ ) require that concentrated solutions of oxime be used if spectra are to be

obtained in a 2 to 3 hr period. When sufficient quantities of oxime are available, configuration assignment by this method is a viable alternative to obtaining the same information from the proton spectrum of aldoximes prepared from  $^{15}\text{N}$ -enriched hydroxylamine.

Figure IV.1.  $^{15}\text{N}$  NMR spectra of O-methylbenzaldoximes. The proton-decoupled (upper) and proton-coupled (lower) spectra are shown. The peaks marked with an \* are due to the E-isomer present in the Z-benzaldoxime sample. Spectra were recorded with between 100 and 147 scans, 4.1-sec data acquisition time, 45.9-sec pulse delay,  $83^\circ$  pulse flip angle and 0.25-Hz line broadening. The upper spectra were obtained with proton decoupling during data acquisition.



Hz



Hz

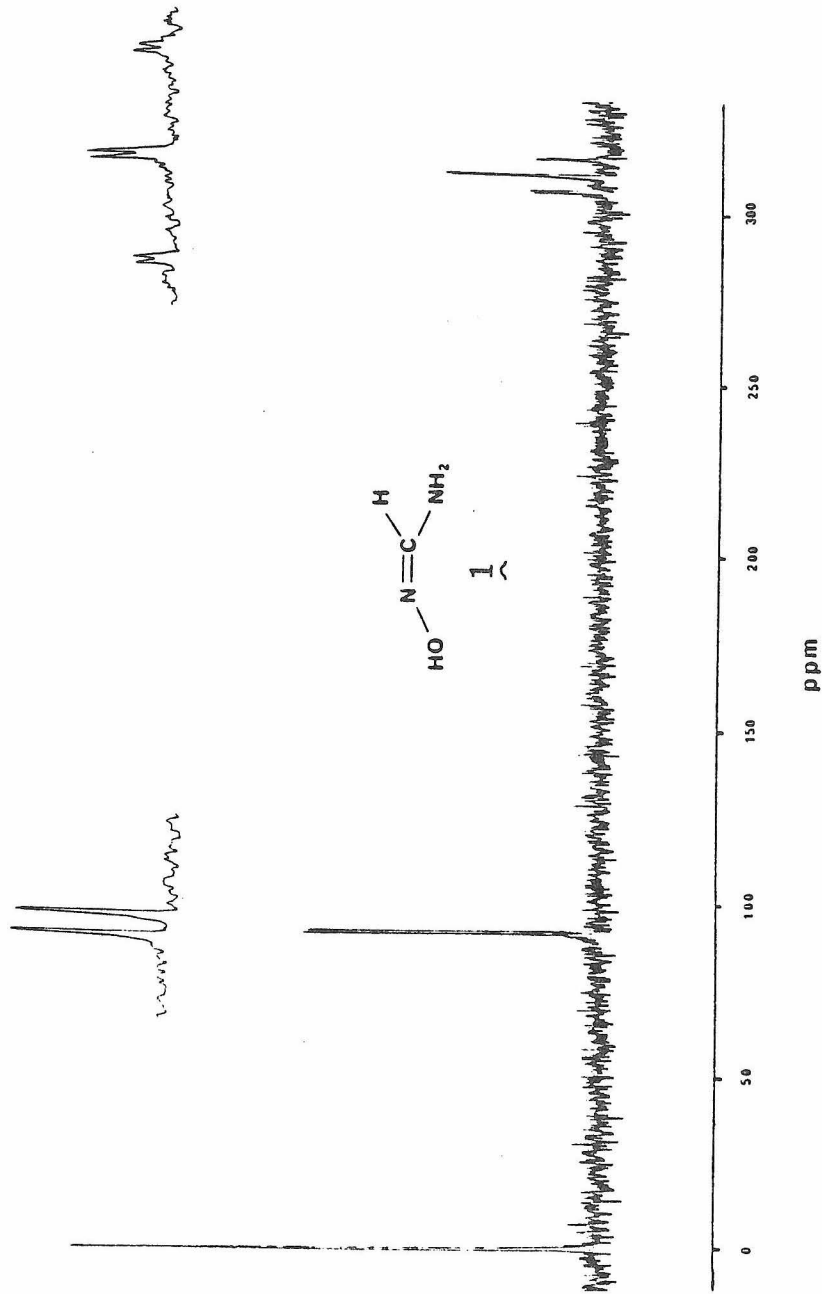


Figure IV.2. Proton-coupled  $^{15}\text{N}$  NMR spectrum of formamidoxime. The spectrum was recorded with 470 scans,  $85^\circ$  pulse-flip angle, 1.16 sec data acquisition time, 48.84-sec pulse delay and 1-Hz line-broadening.

REFERENCES

1. (a) For review see G. J. Martin and M. L. Martin, Prog. NMR Spectroscopy, 8, 166-259 (1972); (b) E. Buehler, J. Org. Chem., 32, 261-65 (1967).
2. (a) G. E. Hawkes, K. Herwig and J. D. Roberts, J. Org. Chem., 39, 1017-28 (1974); (b) G. C. Levy and G. L. Nelson, J. Am. Chem. Soc., 94, 4897-4901 (1972).
3. R. E. Botto, P. W. Westerman and J. D. Roberts, Org. Mag. Res., 11, 510-15 (1978).
4. (a) D. Crépeaux, J. M. Lehn and R. R. Dean, Mol. Physics, 16, 225-39 (1969); (b) D. Crépeaux and J. M. Lehn, Org. Mag. Res., 7, 524-26 (1975).
5. (a) R. Wasylishen and T. Schaffer, Can. J. Chem., 50, 2989-3008 (1972); (b) V. M. S. Gil and S. J. S. Formosinho-Simões, Mol. Physics, 15, 639-43 (1968); (c) S. Nagata, T. Yamabe, K. Hirao and K. Fukui, J. Phys. Chem., 79, 1863-67 (1975); (d) M. S. Gopinathan and P. T. Narasimhan, Mol. Physics, 22, 473-81 (1971).
6. (a) R. L. Lichter, D. E. Dorman and R. Wasylishen, J. Amer. Chem. Soc., 96, 930-32 (1974); (b) G. W. Buchanan and B. A. Dawson, Can. J. Chem., 55, 1437-39 (1977).
7. H. J. C. Yeh, H. Ziffer, D. M. Jering and D. R. Boyd, J. Amer. Chem. Soc., 95, 2741-43 (1973).

REFERENCES (continued)

8. (a) F. J. Weigert and J. D. Roberts, J. Phys. Chem., 73, 449-50 (1969); (b) C. J. Jameson and M. Damasco, Mol. Phys., 18, 491-504 (1970).
9. P. W. Westerman, R. E. Botto and J. D. Roberts, J. Org. Chem., 43, 2590-96 (1978).
10. K. Gram-Jensen, Acta Chem. Scand., 24, 3293-300 (1970).
11. M. Witanowski, L. Stefaniak, H. Janoszewski, S. Symanski and G. A. Webb, Tetrahedron, 29, 2833-36 (1973).
12. J. E. Oatis and H. P. Schultz, Org. Mag. Res., 11, 40-41 (1978).
13. J. Bjørge, D. R. Boyd and D. C. Neill, J.C.S. Chem. Comm., 1974, 478-9.
14. W. B. Jennings, D. R. Boyd and L. C. Waring, J.C.S. Perkin II, 1976, 610-13.
15. (a) K. Folting, W. N. Lipscomb and B. Jerslev, Acta Chem. Scand., 17, 2138-39 (1973); (b) F. Bachechi and L. Zambonelli, Acta Cryst., 31B, 2499-501 (1975).
16. J. U. Nef, Ann. 280, 291-342 (1894).
17. A. T. Fuller and H. King, J. Chem. Soc., 1947, 963-9.

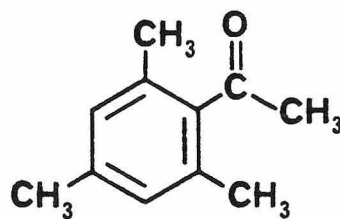
Part II

An Investigation of the Interaction of  
Grignard Reagents with Mesityl Ketones

## Introduction

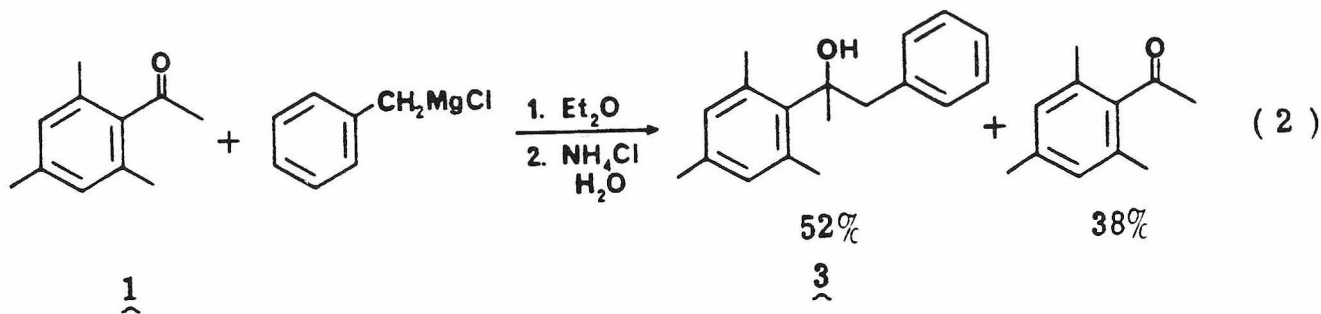
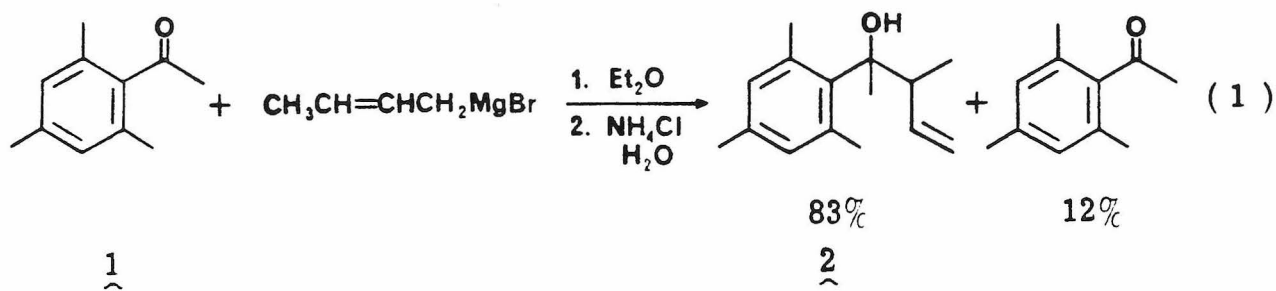
Interest in the reactions of Grignard reagents has undergone a resurgence in the past several years. Much of the early structural and mechanistic information on Grignard addition reactions was derived primarily from product studies and is subject to uncertainty resulting from the availability of limited analytical techniques. The principles underlying the mechanism for the simplest Grignard addition reactions are only now being defined by kinetic and spectroscopic investigations.<sup>1</sup> The existence of ketyl radical anions on the reaction pathway for selected substrates has been implicated by these studies. Thus a continuum of mechanisms appears to exist ranging from ionic to radical processes. This expanded framework for analyzing the mechanism of addition reactions offers the possibility of explaining the anomalous reactions of certain unsaturated Grignard reagents with hindered carbonyl compounds. The reactions of Grignard reagents with acetomesitylene are examined in this context.

Acetomesitylene (1) is often cited<sup>2</sup> as an example of a hindered ketone because of the effect of the two ortho-methyl groups on its molecular conformation and reactivity. The molecule, as indicated



1

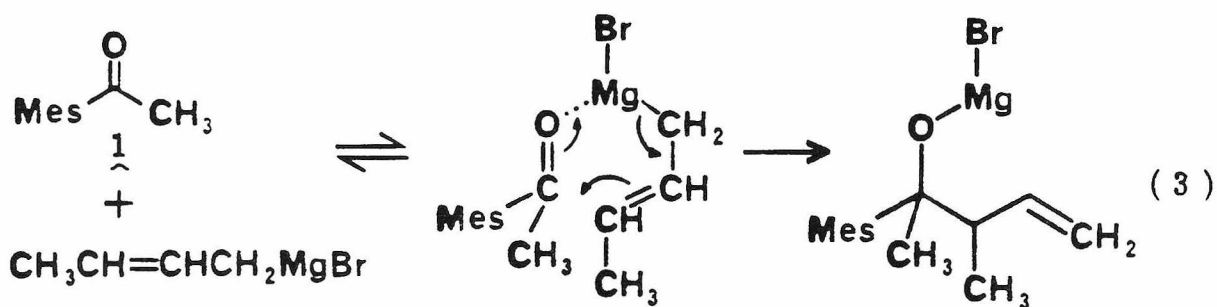
by dipole moment measurements,<sup>3</sup> NMR spectra,<sup>4</sup> uv spectra,<sup>2b,5</sup> and ir C=O absorptions,<sup>2c,6</sup> exhibits decreased resonance interaction between the aromatic ring and the carbonyl when compared with less hindered ketones, for example, acetophenone. The reactivity of the carbonyl group to Grignard-type additions has been reported to be overshadowed by the propensity of the molecule to undergo enolization.<sup>7</sup> In reactions with metallated alkyls, such as phenylsodium,<sup>8</sup> butyllithium,<sup>8,9</sup> and ethylmagnesium bromide,<sup>7,10</sup> acetomesitylene yields enolization products exclusively. Yet substantial amounts of addition products were observed by Young and Roberts<sup>11</sup> in the reactions with butenyl and benzyl Grignard reagents (equations 1 and 2). The tendency of resonance stabilized



Grignard reagents to yield addition products is related to the relative rates of enolization and addition.<sup>12</sup> Winstein proposed<sup>12</sup> that the base

strength of the carbanion corresponding to a Grignard reagent should affect the rate of enolization and hence the ratio of enolization to addition products. Thus the reaction of ethylmagnesium halide yields enolization products but both benzyl and butenylmagnesium halide, for which the corresponding carbanions are weaker bases, result in addition as well as enolization products.

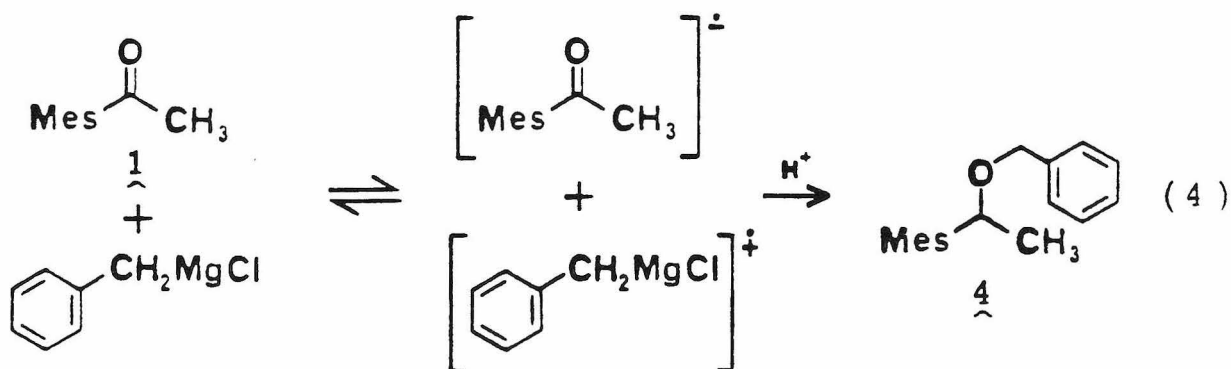
An alternate explanation for the addition products invokes separate mechanisms for the reactions of butenyl and benzyl Grignard reagents with acetomesitylene. Young and coworkers<sup>13</sup> had established that the butenyl Grignard reagent undergoes addition to ketones through a cyclic mechanism which results in rearrangement of the allylic moiety. The inability of a saturated alkyl Grignard



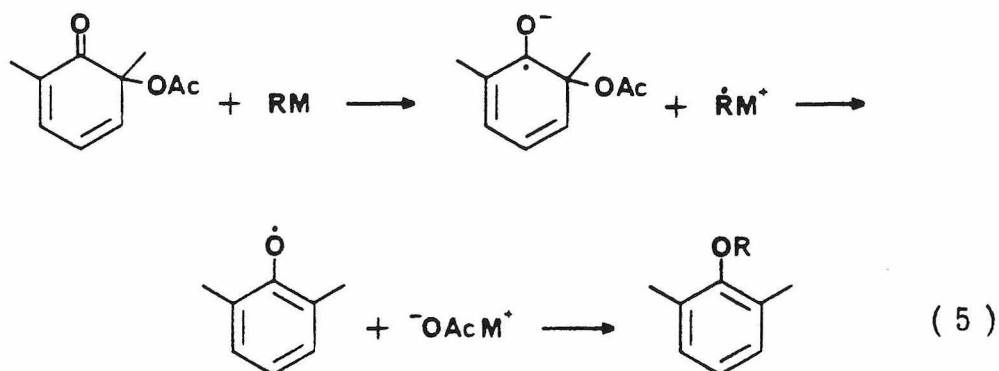
reagent to yield addition products could be attributed to steric hindrance at the carbonyl whereas the butenyl compound can utilize the cyclic mechanism for addition (equation 3).<sup>11a</sup>

A different mechanism for the addition of benzyl Grignard reagent to acetomesitylene has been proposed by Roberts.<sup>14</sup> A radical-type process in which the Grignard reagent transfers an

electron to the ketone yielding the ketyl radical anion of acetomesitylene may be involved. The existence of a single electron transfer (SET) mechanism has previously been demonstrated for several different Grignard additions to ketones.<sup>15</sup> Solutions of ketyl are typically colored<sup>16</sup> and the report of a "brilliant orange-red color" for the acetomesitylene reaction mixture<sup>11</sup> suggests the possibility of radical anion formation. The steric hindrance at the carbonyl carbon could preclude addition of the benzyl radical at that site. Instead, delocalization of the negative charge of the ketyl into the mesityl ring



could serve to stabilize the resonance structure in which the unpaired electron resides on oxygen. Then, recombination of the benzyl moiety with the less hindered oxygen yields, after quenching with acid, the benzyl ether 4 (equation 4). Precedent for this type of "wrong-end" addition can be found in two other cases where special features of the carbonyl compounds also facilitate the reaction. Benzyl Grignard reagents undergo addition to the carbonyl oxygen in o-quinol acetates to yield benzyl ethers. The addition is thought to proceed through a



radical pathway<sup>15c</sup> in which the ketyl loses acetate ion and the resulting phenoxy radical combines with the benzyl moiety (equation 5). The analogous "wrong-end" addition also occurs in several thioketones, in which the small C=S dipole and the ease of polarizability of the sulfur favor the addition.<sup>16</sup>

The original data used by Young and Roberts<sup>11</sup> for assignment of the structure of the addition product from acetomesitylene and benzyl Grignard reagent are insufficient to distinguish between the alcohol 3 and ether 4 structures. We have examined several aspects of the addition reaction to determine the role of a radical addition pathway. In particular, emphasis has been placed upon the spectral properties of the ketone-Grignard reagent reaction mixtures.

## Results and Discussion

The reactions of butenyl and benzyl Grignard reagents with acetomesitylene were repeated because of the uncertainty of the nature of the addition products. Butenylmagnesium bromide was allowed to react with the ketone and  $\alpha$ -methylallylmesitylmethylcarbinol (2) was isolated. This is the product of the cyclic rearrangement mechanism proposed by Young and Roberts<sup>11</sup> (equation 3). Benkeser and co-workers<sup>18</sup> recently reported that addition of butenyl Grignard reagents to hindered ketones is reversible and ultimately leads to the thermodynamically stable crotyl-substituted alcohol. However, we observed essentially no change in yield when the reaction mixture in ether was hydrolyzed within 5 min of mixing the reagents or when a tetrahydrofuran solution was heated at reflux for 2.5 hrs. This indicates that either the steric hindrance in the adduct is insufficient to promote rearrangement or the reaction is not reversible.

The addition product from the reaction of benzylmagnesium chloride with acetomesitylene was identified as the "normal" adduct (equation 2), benzylmesitylmethylcarbinol (3) from ir and NMR spectral data. This alcohol can be differentiated from the alternative benzyl ether structure (4) for the addition product. The presence of the hydroxyl group is demonstrated by a prominent OH stretching vibration in the ir region and also a D<sub>2</sub>O-exchangeable proton resonance in the NMR spectrum.

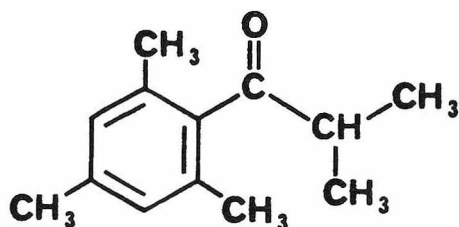
These results support the Winstein explanation for reactivity of butenyl and benzyl Grignard reagents. Normal addition to the

carbonyl can occur through either the polar or single electron transfer (SET) reaction or some combination of both.<sup>1</sup> The ketyl in the SET mechanism is probably stabilized by coordination of the magnesium to the oxygen. The tendency of Grignard reagents to reversibly complex ketones in addition reactions is well documented,<sup>19</sup> and the presence of a metal complex in the resulting radical anions,<sup>20</sup> and ketyls in general,<sup>17,21</sup> has been reported. This complexation serves to stabilize the ketyl resonance structure in which a negative charge resides on oxygen, making the addition of benzyl radical to oxygen unfavored (e.g., equation 4).

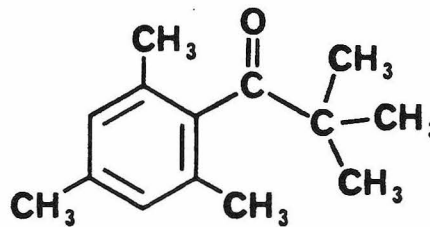
Steric hindrance caused by the mesityl group is not sufficient to prevent addition of the benzyl moiety to the carbonyl carbon. Recent reports in the literature reinforce this idea. Under extreme conditions, two other Grignard reagents yield carbonyl-addition products with acetomesitylene. Thus, a 17% yield of addition product was obtained when the ketone and phenylmagnesium bromide were heated at 165° for 14 hrs.<sup>22</sup> The yield of addition product was 43% after methylmagnesium bromide and acetomesitylene were allowed to react for three months.<sup>23</sup> These results indicate that both addition and enolization are slow. Contrary to the impression given by Kohler and Baltzly<sup>7</sup> that enolization is the dominant reaction, addition can be made to occur under forcing conditions.

Although a radical addition to the carbonyl oxygen does not occur, formation of the benzyl Grignard addition product 3 could still form through the ketyl radical anion. The origin of the orange color

observed in the reaction mixture of acetomesitylene and benzyl magnesium chloride in either ether or tetrahydrofuran was investigated in more detail. The "lifetime" of the color was temperature dependent, persisting for 5 min at room temperature and over 45 min at 0° C. Similar colors appeared in the reactions of benzyl Grignard reagent with both isobutyromesitylene 5 and pivaloylmesitylene 6. In the latter case, the orange color remained for at least two days. The uv-visible spectra of the reaction mixtures with acetomesitylene and pivaloylmesitylene indicate the absence of an absorption maximum in the



5



6

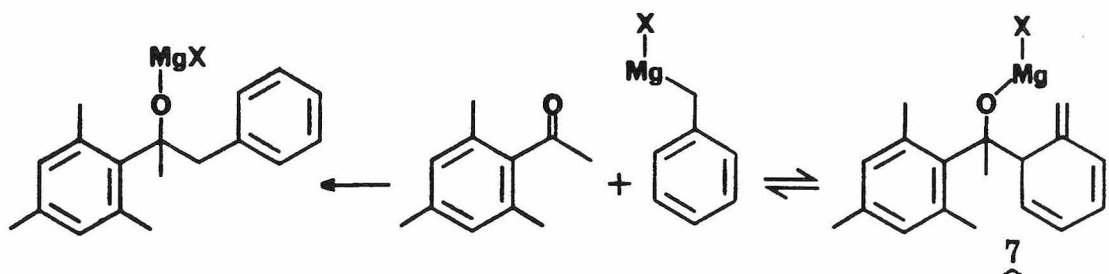
visible region and the observed color is due to the tail end of an absorption with a maximum in the uv (Figures 1 and 2).

An esr signal was seen for the reaction mixture of benzyl Grignard reagent and pivaloylmesitylene (Figure 3) and its origin is most probably the radical anion of pivaloylmesitylene. Similar ketyls were observed by Maruyama<sup>24</sup> and also Fauvarque and Rouget<sup>25</sup> in reaction mixtures of ketones with Grignard reagents. Because no esr signals could be detected for the reaction mixtures from either isobutyromesitylene or acetomesitylene, it is highly improbable that

the species responsible for the orange color is a stable ketyl radical anion.

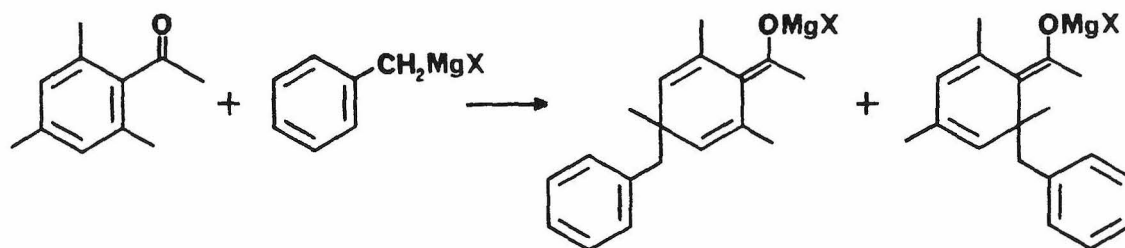
Several alternatives for the species giving rise to the orange color are possible. Because neither acetomesitylene ( $\lambda_{\text{max}} = 242 \text{ nm}$ ,  $\epsilon = 3600$ ) nor the Grignard reagent ( $\lambda_{\text{max}} = 266 \text{ nm}$ ,  $\epsilon = 1.26 \times 10^4$ )<sup>26</sup> can themselves account for the color, an interaction between them might. The color is formed immediately upon mixing the two reagents and dissipates over a period of several minutes (Figure 1b) indicating a stable species, possibly a reaction intermediate, is involved. The formation of a stable ketyl was ruled out previously; also if a ketyl were present it should exhibit an absorption maximum similar to that of the yellow acetophenone ketyl ( $\lambda_{\text{max}} = 440 \text{ nm}$ ).<sup>27</sup>

As an alternative, the color could be due to a species which is not on the pathway to observed products. At least two possibilities can be considered. The intermediate may be the methylenecyclohexadiene 7 from the "abnormal" addition of benzyl Grignard reagent to acetomesitylene. By analogy to the observations of Benkeser and co-workers with allylic Grignard reagents,<sup>18</sup> benzylmagnesium chloride may add initially to form 7 via a cyclic six-center transition state. Due to steric hindrance and loss of resonance energy, 7 may return to starting material and react via a four-center transition state to yield the observed products. The uv absorptions



of methylenecyclohexadienes are typically in the 300 nm region<sup>33</sup> and consistent with the wavelength variation seen in the acetomesitylene reaction mixture. Since methylenecyclohexadienes are colorless compounds,<sup>33</sup> the absorption is not strong enough or at high enough wavelength to allow a significant tail-end absorption into the visible region

Highly conjugated species can also result from 1,4 or 1,6-addition of the benzyl Grignard reagent to the carbonyl system.<sup>34</sup>



Species of this type have been isolated by Crossland and Holm<sup>35</sup> in additions to unsubstituted benzophenones. While the reaction mixtures were highly colored (reds and purples),<sup>35, 15a</sup> conjugate additions of this type are observed only in the case of unsubstituted aromatic rings or when the o- or p-substituent is a good leaving group.

The species responsible for the orange color is consistent with a charge-transfer type complex formed between acetomesitylene and benzyl Grignard reagent. The initial step in a reaction between ketone and Grignard reagent is generally thought to be complexation of the carbonyl oxygen by the magnesium.<sup>1, 28</sup> Several workers have reported spectroscopic evidence for this process.<sup>28</sup> A new carbonyl stretching absorption appears in the ir spectrum of acetone with butylmagnesium

bromide.<sup>29</sup> The uv spectra of several acetophenones<sup>30</sup> and benzophenones<sup>28, 31</sup> exhibit new absorptions, shifted to slightly longer wavelengths than the ketone  $\pi \rightarrow \pi^*$  transition, immediately upon mixing with Grignard reagents. The absorption maxima of the complexes are dependent upon the nature of the coordinated magnesium species and in several cases, characterized by strong end absorptions in the visible region yielding yellow reaction mixtures. The disappearance of the absorptions of these complexes serves as the basis of the kinetic studies reported by Ashby et al.<sup>28</sup> and also Smith et al.<sup>30, 31a</sup> Supportive evidence for the formation of a complex comes from the fact that variations in color were observed in the reactions of acetomesitylene. House and co-workers reported<sup>32</sup> that a yellow solution was formed when the ketone was added to dimethylmagnesium. When phenyl Grignard reagent, prepared from bromobenzene, was allowed to react with acetomesitylene, Kulibekov observed<sup>22</sup> that the colors of the reaction mixture varied from "straw yellow" to "red-orange" as the reaction progressed. Also, we found that the reaction mixture with butenyl Grignard reagent was pale yellow in tetrahydrofuran.

The last proposal for the source of the color in the reaction between acetomesitylene and benzyl Grignard reagent is consistent with the course of Grignard reactions with ketones. The presence of a stable ketyl radical ion is inconsistent with the spectroscopic evidence but radical character could possibly be involved in the transition state for the addition reaction. The possible intermediates which result from "abnormal", or 1,4- or 1,6-addition to acetomesitylene cannot be ruled out but the structural features of the ketones which promote

these reactions are not present in acetomesitylene. The simplest explanation of the Grignard addition to acetomesitylene involves Winstein's proposal of partitioning between addition and enolization reactions through an initial ketone-Grignard reagent complex.

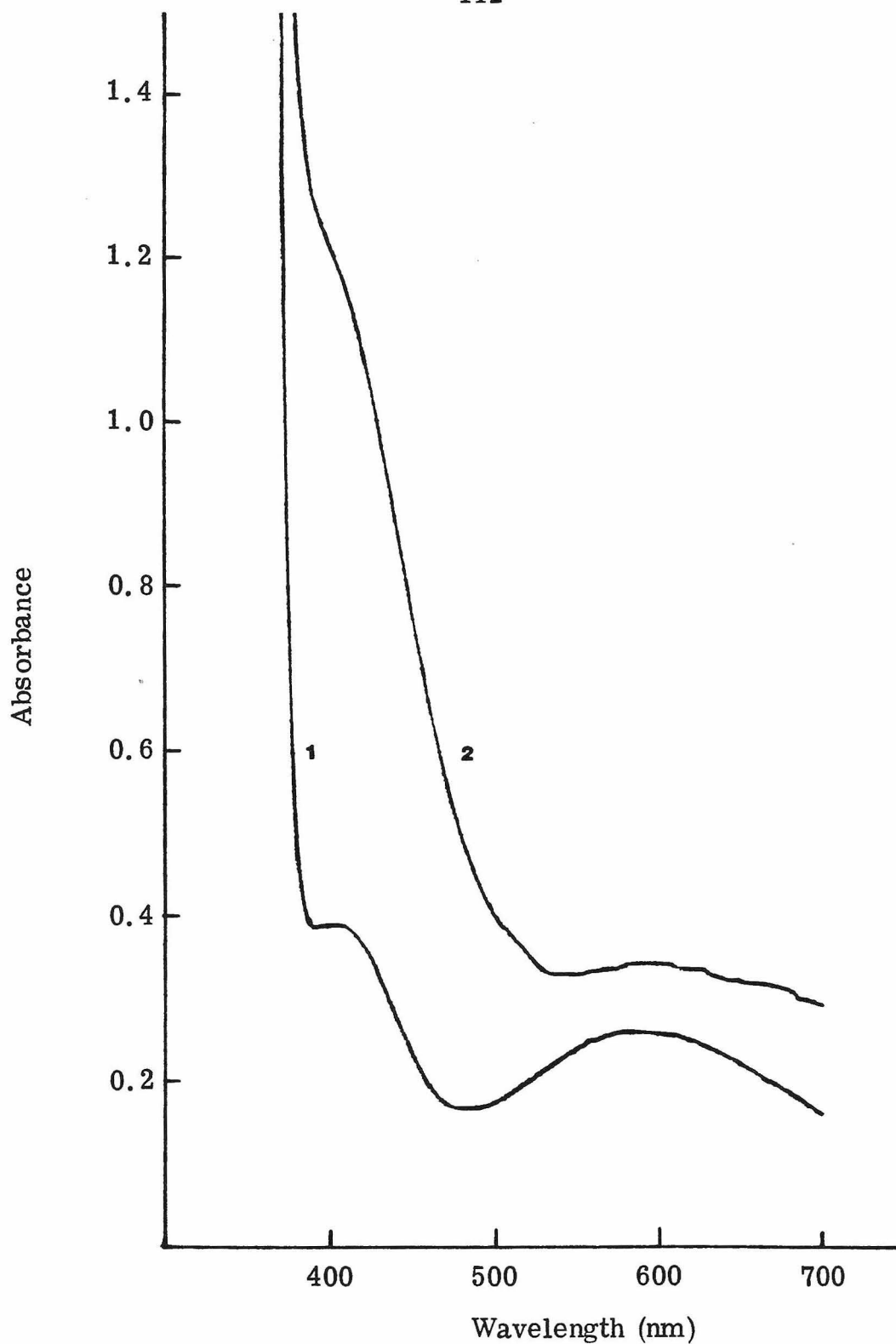
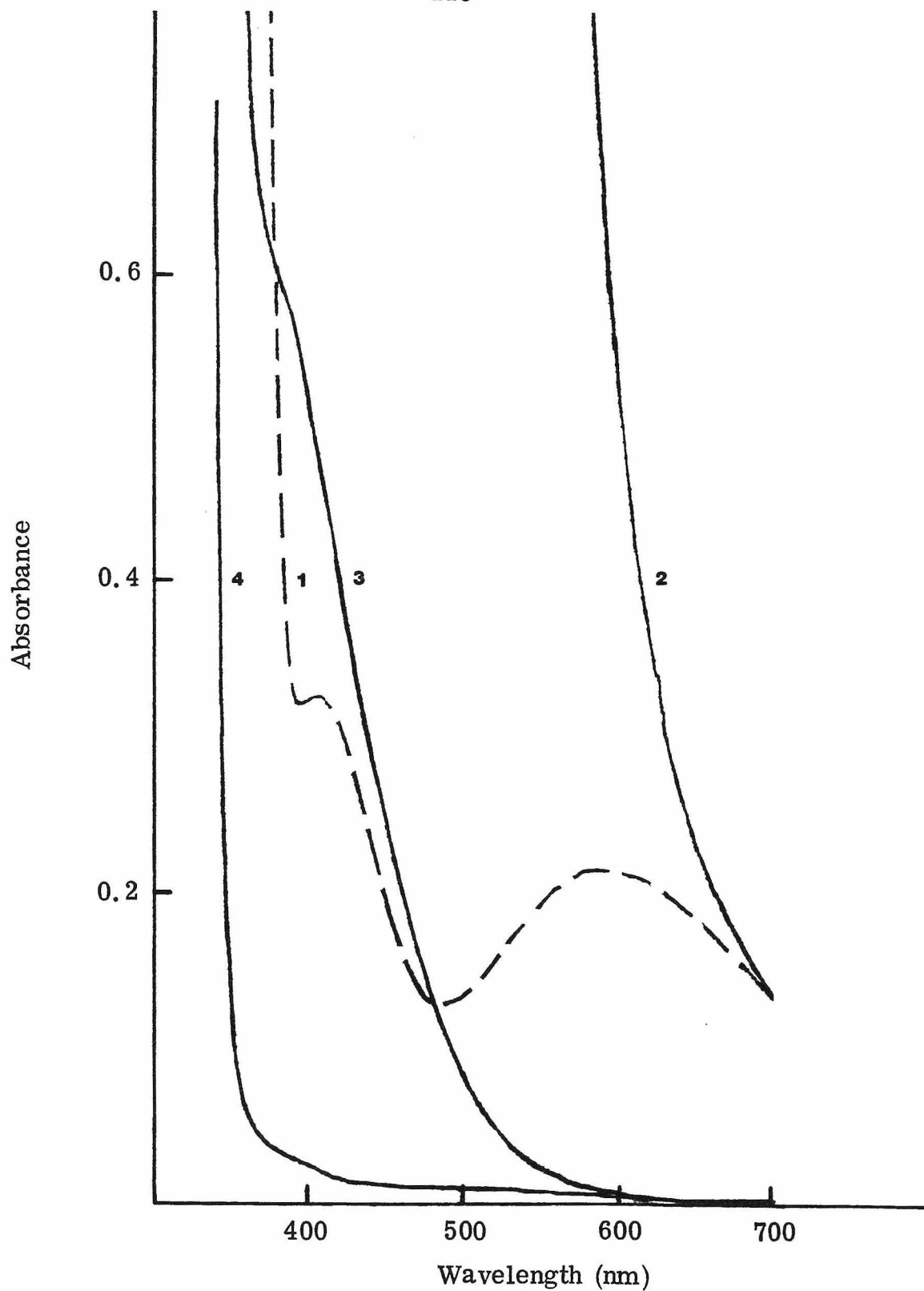


Figure 1. Uv spectrum of transiently colored acetomesitylene reaction mixture at 0° C. a) An 100:1 mixture of 0.34 M benzyl Grignard reagent (curve 1) and acetomesitylene immediately after mixing (curve 2).



b) A stoichiometric reaction mixture of 0.34 M benzyl Grignard reagent (curve 1) immediately after adding acetomesitylene (curve 2), after 135 min (curve 3) and 180 min (curve 4).

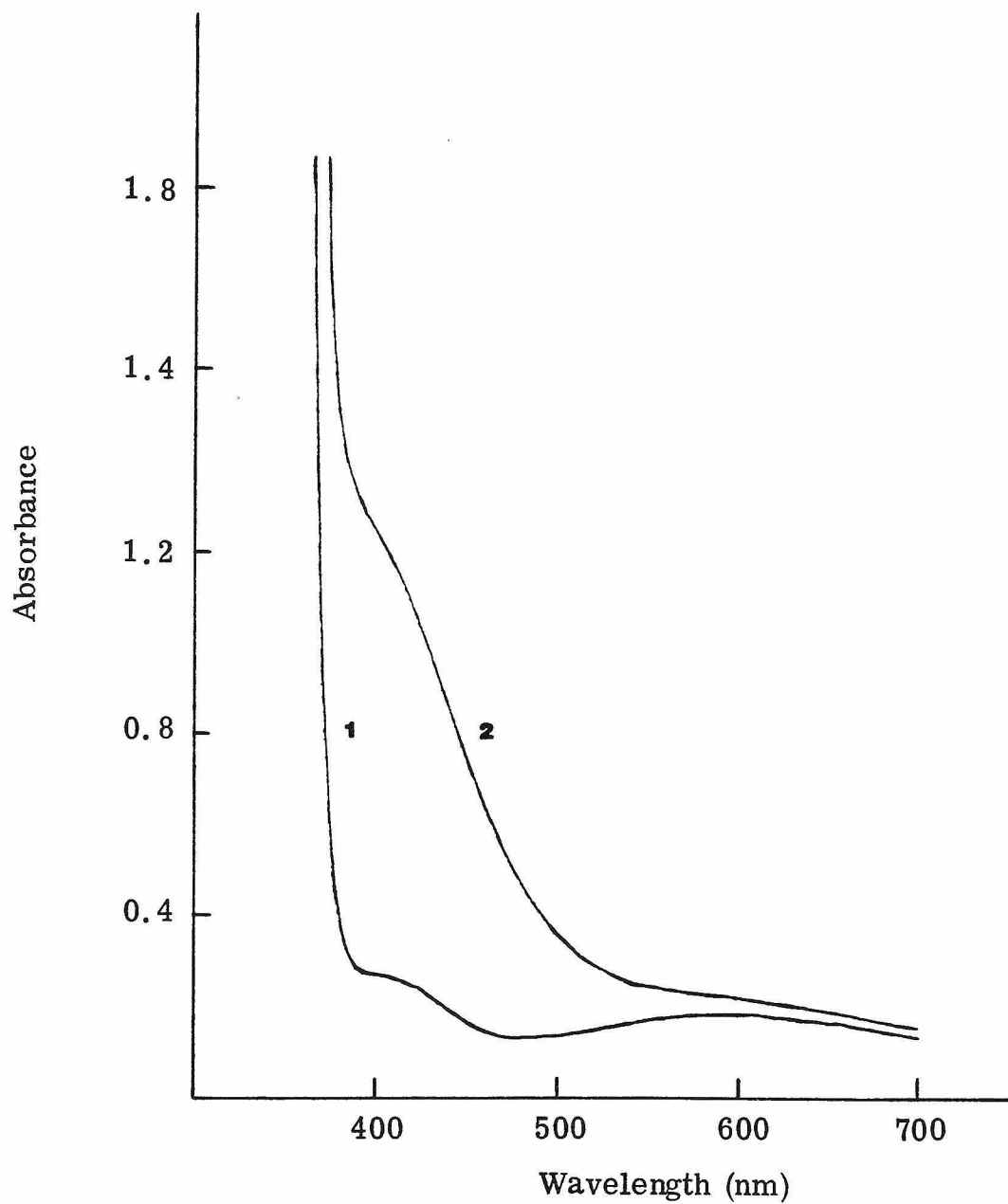


Figure 2. Uv spectrum of the orange pivaloylmesitylene reaction mixture. 0.34 M Benzylmagnesium chloride (curve 1) with added pivaloylmesitylene (curve 2).

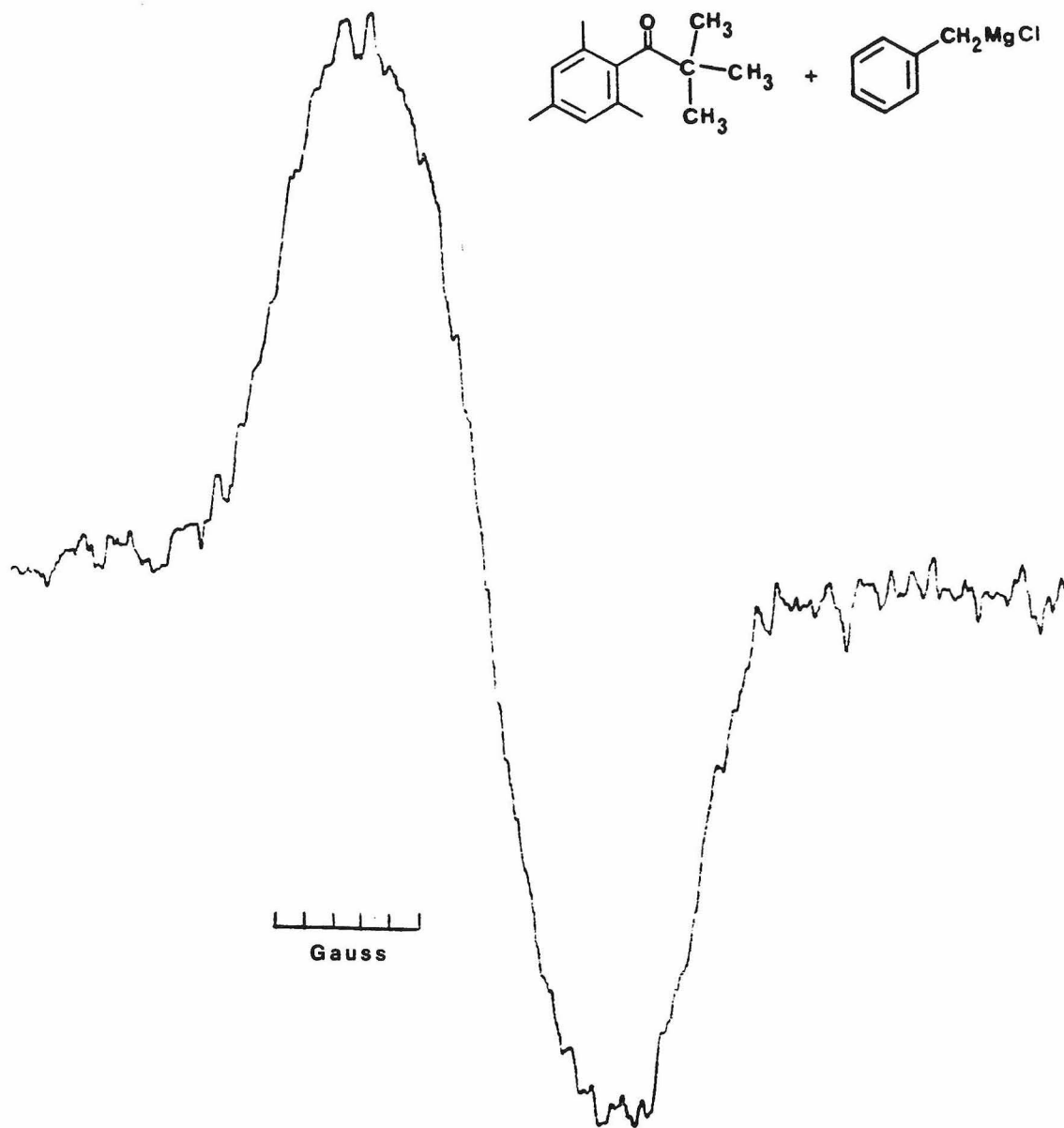


Figure 3. ESR spectrum of the orange reaction mixture from benzyl Grignard reagent and pivaloylmesitylene.

## Experimental

Uv-visible spectra were recorded on a Beckman model 25 spectrophotometer with a thermostated cell holder. Cuvets, sealed with rubber septa, of 1 or 0.1 cm path length were used. Proton NMR spectra were taken on Varian A-56/60A or EM-390 spectrometers. Chemical shifts are reported in parts per million on the  $\delta$  scale relative to tetramethylsilane internal standard. Infrared spectra were recorded on a Perkin Elmer 2 or Beckman IR 4210 spectrometer and are reported in  $\text{cm}^{-1}$ . ESR spectra were recorded on a Varian E-Line EPR spectrometer.

### Preparation of Benzylmagnesium Chloride<sup>36</sup>

A three-necked, 500-ml round-bottomed flask was fitted with a pressure-equalizing dropping funnel, Hershberg stirrer with a rubber seal, and a West condenser under a nitrogen atmosphere. Magnesium turnings (reagent grade; 4.8 g, 0.20 mole) were added to the reaction flask and the apparatus flamed dry. Ether (100 ml freshly distilled from sodium-benzophenone ketyl under nitrogen) was added to the addition funnel and sufficient ether to cover the magnesium was added to the reaction flask. Benzyl chloride (distilled at 70-72°/17 mm; 19.0 g, 0.15 mole) in 100 ml ether was added to the addition funnel and the ether solution mixed. Water flow through the condenser and the stirrer was started and a water bath (15-20°) placed around the flask. The halide was added dropwise over a period of 60 min. The resulting grey suspension (~200 ml) was stirred at room temperature for 15 min and refluxed for 20 min. After the solid had settled,

the Grignard solution was standardized by the method of Watson and Eastham<sup>37</sup> and found to be 0.78 M.

#### Reaction of Benzylmagnesium Chloride and Acetomesitylene

An apparatus similar to that described above in which the addition funnel was calibrated in 50 ml units was assembled and flamed dry. The Grignard reagent described above (100 ml, 0.078 mole) was added to the addition funnel via a glass transfer tube with coarse frit. The resulting grey suspension was added to the reaction flask and the funnel rinsed with several portions of ether. A solution of 8.0 g (0.049 mole) acetomesitylene (Aldrich) in 100 ml of ether was added to the funnel and added dropwise over a 20-minute period under a nitrogen atmosphere. As the addition progressed, the suspended grey solid was replaced with a fluffy white solid. An intense orange color was observed as each drop of ketone solution hit the reaction mixture. At the end of the addition, a yellow mixture resulted which faded to pale yellow after standing at room temperature for 30 min. The reaction was hydrolyzed with ammonium chloride solution as described by Fieser and Fieser.<sup>38</sup> The ethereal solution was dried over anhydrous magnesium sulfate and the ether removed by atmospheric distillation. Additional low boiling material was distilled into a Dry Ice-acetone cooled receiver under reduced pressure (4.4 mm/57° bath tem.). The distillate contained ether and 4 g (0.043 mole) toluene as determined by NMR spectroscopy.

A portion (6.1 g) of the pot residue (10.6 g) was fractionated on a modified Hickman still:

Frac.	Heating block temp., °C	Press., mm	Wt., g	$n_D^{20}$
1	65	0.010-0.008	1.40	1.5502
2	60-65	0.009-0.005	1.28	1.5693
3	60-70	0.009-0.005	1.18	1.5722
Residue (cloudy, viscous green oil)			0.90	

Fractions 2 and 3 and the residue gave rhombohedral crystals on standing. Fractions 1 and 2, by nmr, were 47 and 13 mole % ketone, respectively. Fraction 3 was addition product and the ir of the residue was identical to that of fraction 3. The yield of addition and enolization products from the molecular distillation (based on total ketone added to the Grignard reagent) was 33% and 7%, respectively. For fraction 3: mp 42.0-42.5°; nmr (CDCl<sub>3</sub>) 7.33-6.88 (m, 5H, phenyl), 6.76 (s, 2H, 3,5-H), 3.16 (AB quartet, J 13.5 Hz, 2H, -CH<sub>2</sub>-), 2.36 (s, 6H, 2,6-CH<sub>3</sub>), 2.21 (s, 3H, 4-CH<sub>3</sub>), 1.74 (s, -OH, D<sub>2</sub>O exchangeable), 1.65 (s, 3H, CCH<sub>3</sub>); ir (neat) cm<sup>-1</sup> 3470 (m, broad), 3035 (s), 2975 (s), 2920 (s), 1670 (m), 1495 (s), 1455 (s), 1380 (m), 1090 (m), 857 (m), 702 (s).

#### Preparation of Butenylmagnesium Bromide

The Grignard reagent was prepared by the method described for benzylmagnesium chloride. From 10.8 g (0.44 mole) magnesium turnings and 19.0 g (0.14 mole) crotyl bromide (97-105°) in 200 ml dry ether was obtained 0.6 M solution of butenylmagnesium bromide. Similarly, 6.4 g (0.26 mole) magnesium turnings and 11.3 g

(0.084 mole) crotyl bromide in 200 ml tetrahydrofuran (freshly distilled from sodiumbenzophenone ketyl) gave 0.6 M Grignard reagent.

### Reaction of Butenylmagnesium Bromide and Acetomesitylene<sup>11</sup>

These reactions were run in a manner analogous to the reaction with benzylmagnesium chloride. Products were analyzed on a Hewlett-Packard model 5750 gas chromatograph with flame-ionization detector using a 6'  $\times$   $\frac{1}{8}$ " SE-30 column (inj. 150°, col. 145°, det. 270°). A Varian model 920 chromatograph (thermal conductivity detector) with 5'  $\times$   $\frac{3}{8}$ " 25% DC 550 AW Chrom. P 60/80 (inj. 218°, col. 170°, det. 210°) was used for preparative separations.

Ether: a) Five minutes after the addition of 4.0 g acetomesitylene (0.025 mole) in 30 ml ether to 50 ml (0.03 mole) Grignard reagent the reaction mixture was hydrolyzed. The crude product was fractionally distilled through a 120  $\times$  15 mm vacuum-jacketed Vigreux column and short-path distillation head fitted with a rotating fraction collector.

Frac.	Head temp., °C	Wt., g	% Alcohol*
1	74	0.38	81
2	74-76	2.32	100
3**	75-79	0.95	100
Residue (brown oil)		0.20	

\*By gc. \*\*Holdup distilled through short-path column.

$\alpha$ -Methylallylmesitylmethylcarbinol was obtained in 66% yield; nmr (CDCl<sub>3</sub>), 6.80 (s, 2H, phenyl), 6.30-5.62 (m, 1H, CH=), 5.22-4.88 (m, 2H, =CH<sub>2</sub>), 3.28-2.72 (m, 1H, methine), 2.52 (s, 6H, 2,6-CH<sub>3</sub>), 2.20 (s, 3H, 4-CH<sub>3</sub>), 1.62 (s, 4H, 3° CH<sub>3</sub> and OH), 0.97 (d, J=6.5 Hz, 3H, allylic CH<sub>3</sub>); ir (film) cm<sup>-1</sup> 3560 (m), 3500 (m, broad), 3070 (w), 2970 (s), 2930 (s), 1653 (m), 1615 (m), 1460 (s), 1380 (s), 915 (s), 855 (s).

b) After addition of 4.0 g (0.035 mole) acetomesitylene in 30 ml ether to 50 ml (0.03 mole) Grignard reagent, the reaction mixture was allowed to stand at room temperature for 30 minutes then refluxed 30 minutes. Distillation of the crude product gave 67% yield of  $\alpha$ -methylallylmesitylmethyl carbinol.

Tetrahydrofuran: Acetomesitylene (4.0 g, 0.025 mole) in 30 ml tetrahydrofuran was added to 50 ml Grignard reagent (0.03 mole) and the yellow reaction mixture refluxed for 2.5 hours. The crude product was distilled and the fractions analyzed by gc. The yield of  $\alpha$ -methylallylmesitylmethylcarbinol was 60%. Gc analysis showed that the crude

Frac.	Head temp. °C	Wt., g	% Alcohol	% Diene
1	89	0.62	24	67
2	89-94	1.45	69	22
3*	89-94	1.30	98	2

Residue (brown oil)

\*Holdup distilled through short-path column.

product partially decomposed on distillation (bath temp.  $\sim 170^\circ$ ).

The decomposition product, 2-mesityl-3-methyl-1,4-pentadiene, was isolated from fraction 1 by prep gc: nmr ( $\text{CDCl}_3$ ), 6.86 (s, 2H, 3,5-H), 6.26-5.59 (m, 1H, -CH=), 5.36-4.78 (m, 4H, =CH<sub>2</sub>), 3.17-2.67 (m, 1H, methine), 2.28 and 2.22 (9H, 2,4,6-CH<sub>3</sub>), 1.18 (d, J=7.5 Hz, 3H, allylic CH<sub>3</sub>); ir ( $\text{CHCl}_3$ )  $\text{cm}^{-1}$  3078 (m), 3002 (s), 2962 (s), 2930 (s), 1622 (m), 1602 (m), 1472 (m), 1318 (m), 1065 (m), 992 (m), 910 (s), 847 (s).

#### Reaction of Pivaloylmesitylene with Benzylmagnesium Chloride

In a flame-dried, 3-necked, 25-ml round-bottomed flask equipped with dropping funnel, West condenser, and nitrogen inlet was placed 2 ml of 2.6 M (4.6 mmole) benzylmagnesium chloride and 10 ml ether. Pivaloylmesitylene<sup>39</sup> (1.0 g, 4.9 mmole) in 10 ml ether was added dropwise to the reaction flask and an orange color was seen as the ketone solution entered the reaction mixture. NMR spectra of aliquots withdrawn at 3 and 12 hours indicated the presence of starting materials, and new resonances for toluene were seen as the intensity of the methylene resonance of the Grignard reagent decreased. An aliquot withdrawn for esr spectra indicated the presence of radicals in solution. The orange reaction mixture was hydrolyzed after 24 hrs. After extraction of the aqueous phase and removal of solvent, the ir and NMR spectra of the organic phase were consistent with a mixture of pivaloylmesitylene and toluene.

Grignard Reactions Monitored by Uv-visible or ESR Spectroscopy

The Grignard reagents were prepared by standard methods as previously described and transferred to base-washed, oven-dried bottles with serum caps. Aliquots for standardization were removed with a syringe. A stock solution of 0.34 M benzylmagnesium chloride in ether was used. The Grignard reagent solution was transferred with a syringe into dried, argon-filled uv cuvetts, and after temperature equilibration in the spectrometer, ketone solutions were added with a syringe. Spectra were recorded immediately after mixing the reagents.

The samples for esr spectra were prepared by adding acetomesitylene or isobutyromesitylene<sup>39</sup> to Grignard solutions in 4-mm, dry, argon-filled cuvetts. The contents of the cuvetts were mixed by shaking and the spectra of the orange solutions recorded immediately.

References

1. For a review see E. C. Ashby, Acc. Chem. Res., 7, 272-80 (1974).
2. (a) L. L. Ingraham in M. S. Newman (Ed.), "Steric Effects in Organic Chemistry," Wiley, New York, 1956, pp. 479-522;  
(b) R. E. Ireland, "Organic Synthesis," Prentice-Hall, Inc., Englewood Cliffs, N.J., 1969, pp. 42-43;  
(c) R. T. Conley, "Infrared Spectroscopy," 2nd Ed., Allyn and Bacon, Inc., Boston, 1972, p. 152.
3. A. G. Pinkus and H. C. Custard, Jr., J. Phys. Chem., 74, 1042-49 (1970).
4. (a) G. Montaudo, P. Finchiaro and P. Maravigna, J. Am. Chem. Soc., 93, 4214-17 (1971);  
(b) K. S. Dhami and J. B. Stothers, Can. J. Chem., 43, 479-97, 498-504 (1965).
5. W. M. Shubert and W. A. Sweeney, J. Am. Chem. Soc., 77, 4172-73 (1955).
6. R. H. Saunders, M. J. Murray and F. F. Cleveland, J. Am. Chem. Soc., 63, 3121-23 (1941).
7. E. P. Kohler and R. Baltzly, J. Am. Chem. Soc., 54, 4015-26 (1932).
8. H. Gilman and R. G. Jones, J. Am. Chem. Soc., 63, 1162-63 (1941).
9. E. M. Kaiser, L. E. Solter, R. A. Schwartz, R. D. Beard, and C. R. Hauser, J. Am. Chem. Soc., 93, 4237-42 (1976).

References (continued)

10. A. G. Pinkus, J. G. Lindberg and A.-B. Wu, Chem. Comm., 1969, 1350-51.
11. (a) W. G. Young and J. D. Roberts, J. Am. Chem. Soc., 68, 1472-75 (1946);  
(b) J. D. Roberts, Ph.D. Thesis, University of California at Los Angeles, Los Angeles, California, 1944.
12. As discussed in Ref. 11a and Ref. 11b, pp. 88-90.
13. As summarized in W. G. Young and J. D. Roberts, J. Am. Chem. Soc., 68, 649-52 (1946) and refs. 11.
14. J. D. Roberts, personal communication.
15. (a) T. Holm and I. Crossland, Acta Chem. Scand., 25, 59-69 (1971);  
(b) E. C. Ashby and T. L. Wiesemann, J. Am. Chem. Soc., 100, 189-99 (1978);  
(c) B. Miller, J. Org. Chem., 42, 1402-1408, 1408-15 (1977).
16. (a) M. Dagonneau and J. Vialle, Tetrahedron Lett., 1973, 3017-20;  
(b) P. Beak and J. W. Worley, J. Am. Chem. Soc., 94, 597-604 (1972).
17. N. Hirota in E. T. Kaiser and L. Kevan (Eds.), "Radical Anions," Wiley, New York, 1968, pp. 35-85.
18. (a) R. A. Benkeser and W. E. Broxterman, J. Am. Chem. Soc., 91, 5162-63 (1969);  
(b) R. A. Benkeser and M. P. Siklosi, J. Org. Chem., 41,

References (continued)

- 3212-13 (1976);
- (c) R. A. Benkeser, M. P. Siklosi and E. C. Mozdzen, J. Am. Chem. Soc., 100, 2134-39 (1978).
19. Reviewed in D. S. Matteson, "Organometallic Reaction Mechanisms," Academic Press, New York, 1974, pp. 137-149.
20. I. G. Lopp, J. D. Buhler and E. C. Ashby, J. Am. Chem. Soc., 97, 4966-70 (1975).
21. N. Hirota and S. I. Weissman, J. Am. Chem. Soc., 83, 3533 (1961).
22. M. R. Kulibekov, Azerb. Khim. Zh., 1963, 55-59; C.A., 62, 9038b (1965).
23. R. Ya. Levina, V. N. Kostin, P. A. Gembitskii, S. M. Shostakovskii and E. G. Treshchova, Zh. Obshch. Khim., 32, 1377-82 (1962); C.A., 58, 4442g (1963); English translation: J. Gen. Chem. USSR, 32, 1363-68 (1962).
24. K. Maruyama, Bull. Chem. Soc. Jpn., 37, 897-98 (1964).
25. F. Fauvarque and E. Rouget, C. R. Acad. Sci., Paris, Ser. C, 267, 1355-58 (1968).
26. H. F. Ebel and B. O. Wagner, Chem. Ber., 104, 307-19, 320-32 (1971).
27. (a) G. E. Adams, B. D. Michael and J. T. Richards, Nature, 215, 1248-50 (1967);
- (b) N. Steinberger and G. K. Fraenkel, J. Chem. Phys., 40, 723-29 (1964).

References (continued)

28. E. C. Ashby, J. Laemmle and H. M. Neumann, J. Am. Chem. Soc., 94, 5421-34 (1972).
29. T. Holm, Acta Chem. Scand., 19, 1819-26 (1965).
30. (a) S. G. Smith, Tetrahedron Lett., 1963, 409-414;  
(b) S. G. Smith and J. Billet, J. Am. Chem. Soc., 89, 6948-53 (1967);  
(c) S. G. Smith and J. Billet, J. Am. Chem. Soc., 90, 4108-16 (1968).
31. (a) S. G. Smith and G. Su, J. Am. Chem. Soc., 88, 3995-4000 (1968);  
(b) N. M. Bikales and E. Becker, Can. J. Chem., 41, 1320-43 (1963).
32. H. O. House, D. S. Crumrine, A. Y. Teranishi and H. D. Olmstead, J. Am. Chem. Soc., 95, 3310-24 (1973).
33. (a) V. F. Raaen and J. F. Eastham, J. Am. Chem. Soc., 82, 1349-52 (1960);  
(b) W. J. Bailey and R. Bayloony, J. Org. Chem., 27, 3476-78 (1962).
34. (a) R. C. Fuson, Adv. Organometl. Chem., 1, 221-38 (1964);  
(b) R. C. Fuson and R. Gaertner, J. Org. Chem., 13, 496-501 (1948);  
(c) R. C. Fuson and B. C. McKusick, J. Am. Chem. Soc., 65, 60-64 (1943);  
(d) M. Okubo, Bull. Chem. Soc. Jpn., 50, 2379-84 (1977).
35. I. Crossland and T. Holm, Acta Chem. Scand., 25, 1158-59 (1971).

References (continued)

36. H. Gilman and W. E. Catlin, Org. Syn., Coll. Vol. 1, 471-73 (1941).
37. (a) S. C. Watson and J. F. Eastham, J. Organometal. Chem., 9, 165-68 (1967);  
(b) M. Gall and H. O. House, Org. Syn., 52, 39-52 (1976).
38. L. F. Fieser and M. Fieser, "Reagents for Organic Synthesis," Vol. 1, Wiley, New York, N. Y., 1967, pp. 418-9.
39. (a) P. H. Gore and J. A. Hoskins, J. Chem. Soc. C, 1970, 517-22.  
(b) D. V. Nightingale, R. L. Sublett, R. A. Carpenter, and H. D. Radford, J. Org. Chem., 16, 655-59 (1951).